2014-01-01

Gbetagamma-Microtubule Mediated Mechanism Of Neuronal Differentiation

Jorge Anibal Sierra Fonseca
University of Texas at El Paso, jasierra3@miners.utep.edu

Gβγ-MICROTUBULE MEDIATED MECHANISM OF NEURONAL DIFFERENTIATION

JORGE ANIBAL SIERRA FONSECA

Department of Biological Sciences

APPROVED:

_____
Sukla Roychowdhury, Ph.D., Co-Chair

_____
Siddhartha Das, Ph.D., Co-Chair

_____
Manuel Miranda, Ph.D.

_____
Laura O'Dell, Ph.D.

_____
Marc B. Cox, Ph.D.

_____
Arshad M. Khan, Ph.D.

_____
Benjamin C. Flores, Ph.D.
Dean of the Graduate School

Gβγ-MICROTUBULE MEDIATED MECHANISM OF NEURONAL DIFFERENTIATION

by

JORGE ANIBAL SIERRA FONSECA, B.S.

DISSERTATION

Presented to the Faculty of the Graduate School of

The University of Texas at El Paso

in Partial Fulfillment

of the Requirements

for the Degree of

DOCTOR OF PHILOSOPHY

Department of Biological Sciences

THE UNIVERSITY OF TEXAS AT EL PASO

May 2014

ACKNOWLEDGEMENTS

I would like to thank the University of Texas at El Paso, particularly the Department of Biological Sciences and the Border Biomedical Research Center, for all the help and support provided through my time in the doctoral program.

I would like to express my deepest gratitude to my research mentors, Dr. Sukla Roychowdhury and Dr. Siddhartha Das, for their guidance, support, friendship, and advising, and for welcoming me in their laboratories to conduct this research project.

My sincere acknowledgement goes to the members of my dissertation committee, Dr. Manuel Miranda, Dr. Marc Cox, Dr. Laura O'Dell, and Dr. Arshad Khan, for their time, help, and contributions. Likewise, I would like to sincerely thank my academic advisor and advocate, Dr. Elizabeth Walsh, for her help and guidance during my time in the program.

I also want to thank Dr. Nazarius Lamango, from the Florida A&M University (Tallahassee, Florida), for his interest in collaborating in this research project, and for his kind contribution and suggestions. I also thank Dr. Narasimhan Gautam, from Washington University (St. Louis, Missouri), for his kind donation of constructs.

I would also like to thank past and present members of the Roychowdhury's lab: Jessica Martinez, Omar Najera, Jane Martinez, Amaris Castañon, Martha Flores,

Soledad Lucero, and Melissa Duran. Special thanks go to Dr. Javier Vargas, Dr. Debarshi Roy, Dr. Tavis Mendez, Dr. Susana Barrera, Dr. Atasi De Chatterjee, Dr. Linda Herrera, Dr. Carylinda Serna, Dr. Rituraj Pal, Dr. Vicente Castrejon, Mariana Vargas, Trevor Duarte, Joaquin de Leon, Felipe Lopes, Elisa Robles, Alejandra Villescas, Natalie Alonso, Pedro Jacquez, Parijat Kabiraj, Bryan Lopez, and Matthew Gaynor, for their friendship and help during graduate school.

My sincere and deep gratitude goes to the staff of the Cytometry, Screening, and Imaging core facility, Dr. Armando Varela and Gladys Almodovar, who were always there to help unconditionally.

Special thanks to Dr. Manuel Llano, Dr. Kyle Johnson, Dr. Charles Spencer, Dr. Janelle Salkowitz, Dr. Horacio Gonzalez, and Dr. Larry Jones, for giving me the opportunity to assist them in teaching laboratory courses, and to Cristina Gonzalez, Elizabeth Anaya, and Diana Martinez for their technical support.

My sincere gratitude goes to the ladies of the Pan American Round Table of El Paso, who kindly provided me with financial support in the form of a scholarship for three consecutive years.

Last but not least, I would like to thank my family, my parents and brothers, for their constant support during my graduate studies, and to my wife, for her unconditional encouragement and support.

ABSTRACT

Neurodegeneration, a progressive loss of nerve cells (neurons), occurs in many neurological disorders, including Alzheimer's and Parkinson's diseases, as well as in the aging brain. Disruption of microtubules in neurons and the aggregation of proteins associated with them is the hallmark of neurodegeneration. Nevertheless, the cause of this disorder is largely unknown, and no effective drugs are available to treat the disease processes. Therefore, there is a need to understand the molecular mechanisms that drive the assembly and disassembly of microtubules during neurite outgrowth and differentiation. Evidence suggests that nerve growth factor (NGF) induces neurite outgrowth from PC12 cells by activating the receptor tyrosine kinase (TrkA) and the phosphoinositide-3-kinase (PI3K) pathway. G-protein-coupled receptors (GPCRs), as well as heterotrimeric G proteins, are also involved in regulating neurite outgrowth. However, the possible connection between these pathways and how they might ultimately converge to regulate the assembly and organization of MTs during neurite outgrowth is not well understood. In my dissertation, I tested the hypothesis that $G\beta\gamma$, an important component of the GPCR pathway, is involved in neuronal differentiation by modulating MT assembly, and that the disruption of the interaction between $G\beta\gamma$ and tubulin/MT in neurons will inhibit neurite outgrowth. To test this hypothesis, PC12 cells were used because they respond to NGF with growth arrest and exhibit a typical phenotype of neuronal cells sending out neurites. In addition, primary hippocampal and cerebellar neurons in culture were used for the study. It was found that NGF promoted the interaction of $G\beta\gamma$ with MTs and stimulated MT assembly. In further support for a

role of Gβγ-MT interaction in neuronal differentiation, it was observed that overexpression of Gβγ in PC12 cells induced neurite outgrowth in the absence of added NGF. In addition, by using inhibitors of PI3K, I provide evidence that Gβγ may coordinate with PI3K signaling to regulate MT assembly and neurite outgrowth. I found that Gβγ-sequestering peptide GRK2i inhibited neurite formation, disrupted MTs, and induced axonal damage, indicating the involvement of Gβγ in this process. Because it was shown in earlier studies that prenylation and subsequent methylation/demethylation of γ subunits are required for the Gβγ-MTs interaction *in vitro*, in the current study, small-molecule inhibitors targeting prenylated methylated protein methyl esterase (PMPMEase) were tested, and I found that these inhibitors disrupted Gβγ and MT organization, affected cellular morphology, and inhibited neurite outgrowth. Altogether, this study demonstrates that the interaction of Gβγ with MTs could be a determining factor for MT rearrangement and the induction of neurite outgrowth, and that interfering with this process may trigger an early stage of neurodegeneration. This knowledge will be helpful for designing and developing novel therapies targeting Gβγ-MT mediated pathway that is altered during neurodegeneration.

TABLE OF CONTENTS

LIST OF FIGURES

CHAPTER 1: INTRODUCTION

1.1. Microtubule assembly and dynamics

Microtubules (MTs) are intracellular polymeric structures found in all eukaryotic cells. Along with the intermediate filaments and the actin-based microfilaments, MTs constitute the structural framework of the cell, the cytoskeleton. One of the features that make MTs fascinating objects of study is their remarkable diversity in function. These functions include chromosome movement during cell division, neuronal differentiation, organelle transport within the cell, and the maintenance of cell morphology. These functions of MTs are critically dependent upon their ability to polymerize and depolymerize (Desai and Mitchinson, 1997). MTs in cells exist as dynamic and stable populations, each one called upon to carry out distinct cellular functions (Gelfand and Berchadsky, 1991). For instance, during mitosis, the interphase network of MTs radiating throughout the cell changes into a bipolar spindle that mediates the accurate segregation of chromosomes. The half-life of MTs changes from 5–10 min. to 30 sec.–1 min. during this transition (McNally, 1996). On the other hand, the stability of the MTs increases significantly during neuronal differentiation (Bulinski and Gundersen, 1991).

The major component of MTs is the heterodimeric protein tubulin, consisting of α and β subunits, which are assembled into linear protofilaments. The protofilaments associate laterally to form the microtubule, a 25 nm-wide hollow cylindrical polymeric structure (Desai and Mitchinson, 1997). Due to the asymmetry of the $\alpha\beta$ tubulin

heterodimer, MTs are polar structures with two distinct ends. These ends possess different polymerization rates: a slow growing minus end with an exposed α-tubulin subunit, and a fast growing plus end, at which the β-tubulin subunit is exposed (Jiang and Akhmanova, 2011; Sakakibara et al., 2013). MT assembly occurs in two phases: nucleation, which is facilitated by a third tubulin isoform, γ-tubulin; and elongation, during which αβ-tubulin heterodimers are added to the plus end (Desai and Mitchinson, 1997; Conde and Cáceres, 2009). Tubulin is a unique guanine nucleotide-binding protein containing one exchangeable binding site and one non-exchangeable binding site. GTP at both sites is needed for optimal assembly, and GTP at the exchangeable site is hydrolyzed after assembly (David-Pfeuty et al., 1977; Nogales et al., 1998; Singh et al., 2008). This hydrolysis creates an MT consisting largely of GDP tubulin, but a small region of GTP-bound tubulin, called a "GTP cap," remains at the end. This cap allows MTs to polymerize. The loss of the cap results in a transition from growth to shortening (called a catastrophe), whereas the reacquisition of the GTP cap results in a transition from shortening to growing (called a rescue). This behavior, known as dynamic instability, allows MTs to be remodeled rapidly in order to reach specific targets more effectively (Mitchison and Kirschner, 1984; Carlier et al., 1989; Desai and Mitchinson, 1997; Gundersen et al., 2004). The MT assembly process is depicted in Figure 1 (adopted with permission from Conde and Cáceres, 2009).

MT assembly and stability can be affected by a wide variety of proteins. In this regard, microtubule-associated proteins (MAPs) play a very important role. Members of this group of proteins, such as MAP2 and tau, are known to promote MT assembly and

stabilize MTs *in vivo* and *in vitro* (Murphy and Borisy, 1975; Margolis et al., 1986; Kowalski and Williams, 1993; Gamblin et al., 1996). The phosphorylation of MAPs is critical for their function, since phosphorylated MAPs separate from MTs, causing MTs to become more susceptible to disassembly and destabilization (Ebneth et al., 1999; van der Vaart et al., 2009). Destabilization of MTs can be promoted by a large number of proteins collectively termed catastrophe promoters, as they favor the transition of MTs from elongation to shortening. Examples of these proteins include stathmin/Op18 (a small heat-stable protein that is abundant in many types of cancer cells), katanin, and some kinesin-related motor proteins (Belmont and Mitchison, 1996; Kline-Smith and Walczak, 2002). Also, many drugs are known to alter tubulin polymerization, and they are considered valuable tools in studying the mechanisms of MT assembly. Some of these drugs, such as nocodazole, depolymerize MTs, whereas others, such as taxol, promote MT assembly (McGuire et al., 1988; Vasquez et al., 1997). Even though MTs are composed of α/β tubulin heterodimers in all eukaryotic cells, MTs exhibit great functional diversity. One possible explanation is that both α and β tubulin undergo a series of post-translational modifications that allow MTs to engage in a variety of cellular activities (Hammond et al., 2008). These modifications include tyrosination/detyrosination, acetylation, glutamylation, and phosphorylation (Wloga and Gaertig, 2010). Although much effort has been made in identifying and characterizing the cellular factors that regulate MT assembly and dynamics, the precise spatial and temporal control of the process is not clearly understood.

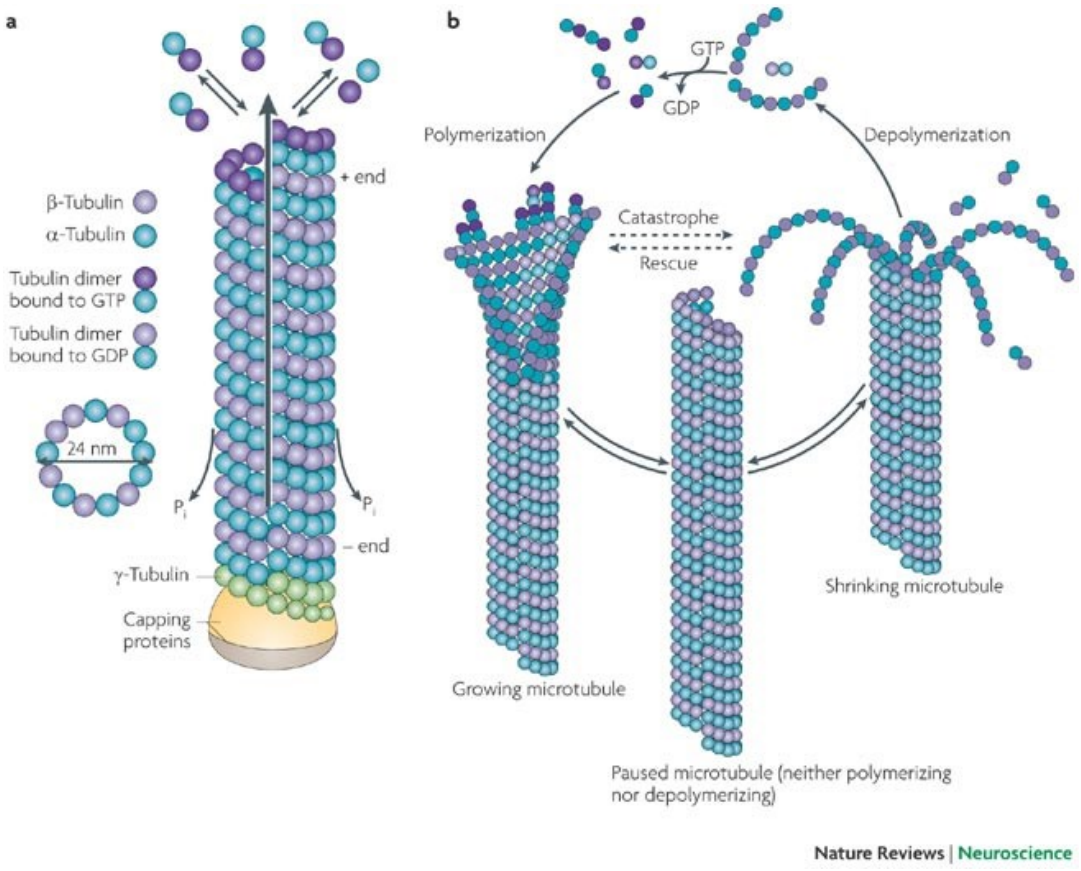

Figure 1. Assembly/disassembly of MTs. MTs are polymerized from heterodimers consisting of α and β tubulin. A third tubulin isoform, γ-tubulin, serves as a template for nucleation. GTP binding to tubulin is necessary for MT assembly to occur. GTP is hydrolyzed to GDP when tubulin is incorporated within MT. In MTs, GDP is bound to tubulin except at the plus (+) end, where tubulin is still in GTP-bound form, establishing a GTP cap. This cap allows MTs to polymerize (assembly). When the cap is lost, tubulin is depolymerized and MTs begin to shrink. Reprinted by permission from Macmillan Publishers Ltd: Nature Reviews Neuroscience, (Conde and Cáceres (2009).

1.2. G protein-mediated signaling

Traditionally, G proteins function as signal transducers in transmembrane signaling pathways that consist of three elements: G protein-coupled receptors (GPCRs), G proteins, and effectors. The GPCR family of proteins is highly diverse. More than 1,000 genes encoding GPCRs are found in the human genome (Fredriksson et al., 2003; Wang et al., 2012). GPCRs participate in the regulation of a wide variety of physiological functions, including neurotransmission, immune system function, cell growth and differentiation, and hormonal signaling. Participation in such a multitude of processes makes GPCRs a very attractive drug target, and approximately 30% of commercially available drugs are designed to target GPCRs (Salon et al., 2011). GPCRs consist of seven transmembrane domains, connected by three extracellular and three intracellular loops. The extracellular region is responsible for agonist binding (neurotransmitters, hormones, and odorants, among others), and the intracellular region is responsible for interacting with heterotrimeric G proteins (Latek et al., 2012).

The G protein heterotrimer is composed of guanine nucleotide-binding α plus $\beta\gamma$ subunits, which forms a tight association under non-denaturing conditions. In humans, there are 21 isoforms of Gα subunits, 6 Gβ isoforms, and 12 isoforms of Gγ (Downes and Gautam, 1999). G protein heterotrimers are typically classified into four classes, depending on the Gα subunit: Gαs (for stimulation of adenylyl cyclase), Gαi (for inhibition of adenylyl cyclase), Gαq (which regulates phospholipase), and Gα12-13, which is involved in the regulation of monomeric G proteins and other molecules, such

as PKC (Simon et al., 1991; Neves et al., 2002). The traditional pathway for GPCR signaling is shown in Figure 2.

The G protein-signaling cascade begins with the agonist-induced activation of a GPCR, which allows GTP to bind to the α subunit of the heterotrimer, and subsequently, the GTP-bound activated Gα changes its association with G$\beta\gamma$ in a manner that permits both subunits to participate in the regulation of intracellular effector molecules. Typical effectors of Gα signaling include adenylyl cyclase, phospholipase C, phospholipase A_2, ion channels, and several kinases and transcription factors. Termination of the signal occurs when GTP bound to the α subunit is hydrolyzed by its intrinsic GTPase activity, which causes its functional dissociation from the effector and reassociation with $\beta\gamma$ (Gilman, 1987; Dohlman et al., 1991; Neves et al., 2002; McCudden et al., 2005). While the signal-transducing ability of heterotrimeric G proteins was once believed to depend fully on the α subunit, it has now become clear that the $\beta\gamma$ subunit is capable of interacting with numerous effector molecules to influence a variety of signaling pathways (Sternweis, 1994; Smrcka, 2008). Among the effector molecules interacting with G$\beta\gamma$ are phospholipases, K^+ and Ca^{2+} channels, GPCR kinases, members of the MAPK signaling pathway, monomeric G proteins, regulators of G protein signaling (RGS proteins), and phosphoinositide-3 kinase (PI3K) (Ueda et al., 1994; Wickman et al., 1994; Faure et al., 1994; Ford et al., 1998; Shi et al., 2001; Smrcka, 2008).

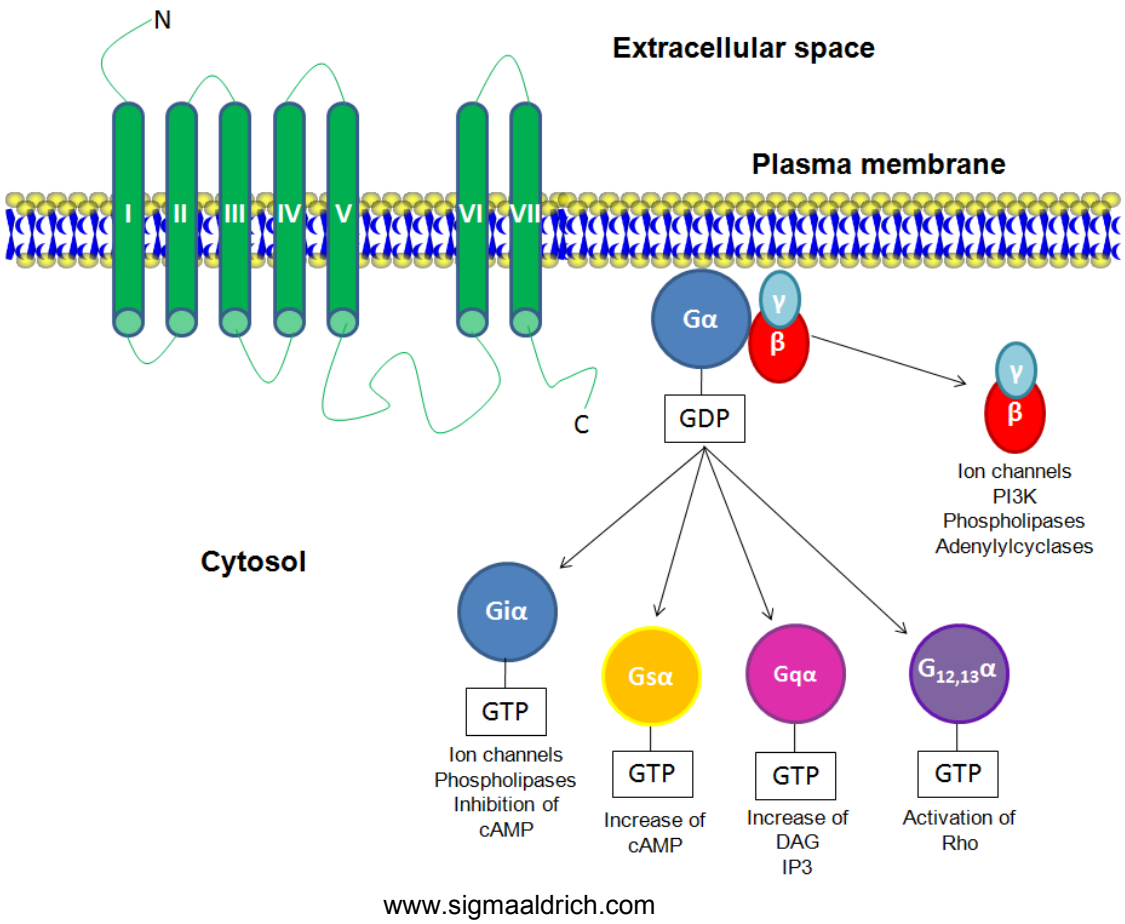

Figure 2. GPCR signaling through heterotrimeric G proteins. Upon agonist activation of the GPCR, the Gα subunit exchanges GDP for GTP, causing the heterotrimer to dissociate and both α and βγ subunits activate a variety of effector molecules. Signal termination occurs when the GTP-bound Gα hydrolyzes the nucleotide, causing the αβγ heterotrimer to reform.

1.3. The interaction of G proteins with microtubules

In addition to their function in the downstream signaling of GPCRs, recent evidences indicate that G proteins associate with several subcellular compartments, including MTs, and participate in both cell division and differentiation (Cote et al., 1997; Willard and Crouch, 2000; Wu et al., 2001; Sarma et al., 2003). For example, G protein β subunit antisense oligonucleotides have been shown to inhibit cell proliferation and to disorganize the mitotic spindle in mammalian cells (Wu et al., 2001). A non-traditional G protein signaling pathway has been shown to be involved in regulating the mitotic spindle for centrosome/chromosome movements in cell division in *C. elegans*, *Drosophila*, and mammals. Components of this pathway include several proteins, such as the Gi class of G proteins, GoLoco domain-containing proteins (such as the mammalian LGN, which contains N-terminal Leu-Gly-Asn repeats), AGS3 (Activator of G protein Signaling 3), and RGS (regulators of G protein signaling) (Gotta and Ahringer, 2001; Schaefer et al., 2001; Kimple et.al., 2002; Fuse et al., 2003; Du and Macara, 2004; Sanada and Tsai, 2005; Siegrist and Doe, 2005). While Giα was shown to regulate MT pulling forces for chromosome movements, Gβγ was found to be involved in spindle positioning and orientation. Several GPCRs capable of triggering neurite outgrowth have been identified. These receptors are coupled to Gi/o, G12/13 or Gs families of G proteins (Reinoso et al., 1996; Lotto et al., 1999; He et al., 2006). Thus, G proteins appear to provide a link between hormones or neurotransmitters and cell division, differentiation, and MTs.

1.4. Regulation of MT assembly by α and βγ subunits of heterotrimeric G proteins *in vitro*

Direct interactions between tubulin and G protein subunits (α and βγ) have been demonstrated earlier and these interactions modulate MT assembly *in vitro* (Figure 3) (Wang et al., 1990; Roychowdhury and Rasenick, 1997; Roychowdhury et al., 1999; Roychowdhury et al., 2006). It was found that Gα inhibits MT assembly and promotes tubulin depolymerization by activating the intrinsic GTPase activity of tubulin (Roychowdhury et al., 1999). Thus, Gα may act as a GAP (GTPase-activating protein) for tubulin and may increase the dynamic behavior of MTs by removing the GTP cap. The Gβγ subunit has the opposite effect on tubulin polymerization, as it was found that Gβγ promotes MT assembly *in vitro*. While β1γ2 stimulated MT assembly, β1γ1 had no effect, suggesting that specificity exists among Gβγ isoforms. Furthermore, a mutant β1γ2, β1γ2 (C68S), which does not undergo prenylation and subsequent carboxy-terminal processing on the γ subunit, does not stimulate the formation of MTs (Roychowdhury and Rasenick, 1997). This result suggests that prenylation of the γ subunit is a major determinant for the observed difference. Reconstituted heterotrimers were shown to be inactive in the modulation of MT assembly (Roychowdhury et al., 2006), suggesting that G protein activation is required for functional coupling between Gα/Gβγ and tubulin/MTs. The result also suggests that G protein coupled receptors (GPCRs) may be involved in the regulation of MT assembly and dynamics *in vivo* by mobilizing G protein subunits to bind to MTs. By doing so, GPCRs may control a variety of cellular activities.

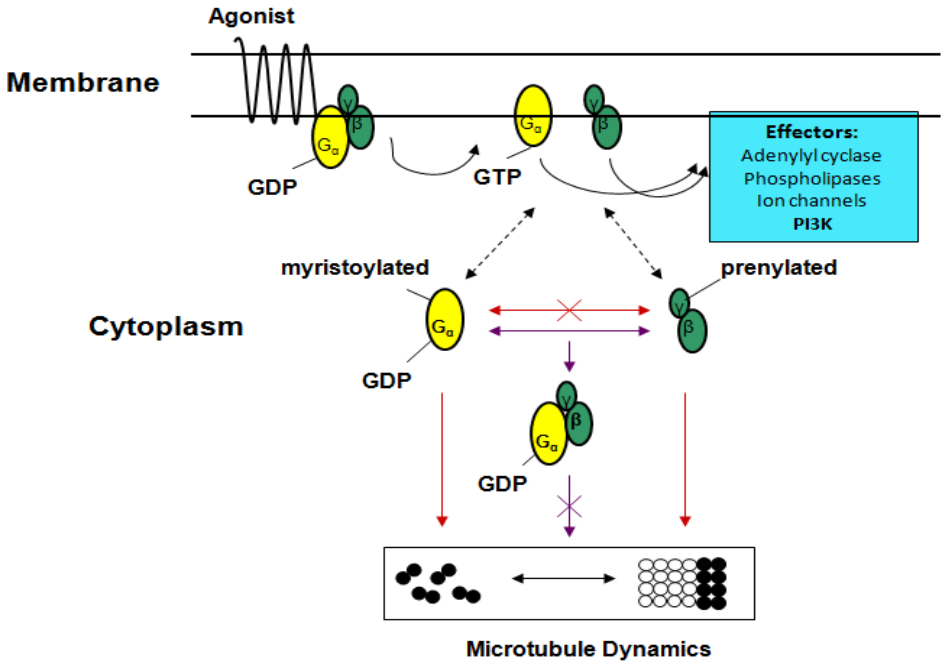

Figure 3. Regulation of MT assembly by G protein-mediated signaling. Based on the *in vitro* results using purified tubulin and G protein subunits (Roychowdhury and Rasenick, 1997; Roychowdhury et al., 1999; Roychowdhury et al., 2006), it is suggested that the Gα inhibits MT assembly and promotes MT disassembly by interacting with tubulin-GTP or the GTP cap of growing MTs and initiating GTP hydrolysis of tubulin. Gβγ, on the other hand, promotes MT assembly. The Gαβγ heterotrimer is functionally inactive, but it can be activated either by agonist-mediated or agonist-independent pathways. Upon activation, Gα dissociates from Gβγ subunits, and both subunits then interact with tubulin/MTs and modulate assembly/dynamics. (Adapted from Roychowdhury and Rasenick, 2008).

1.5. Regulation of MT assembly by Gβγ in cultured cell lines

In recent years, our laboratory has been focusing on understanding the functional consequences of Gβγ-dependent regulation of MT assembly *in vivo*. By using the anti-mitotic agent nocodazole, it has been demonstrated that the assembly/disassembly of MTs alters the tubulin-Gβγ interaction in cultured PC12 and NIH3T3 cells (Montoya et al., 2007). While MT depolymerization by nocodazole inhibited the interactions between tubulin and Gβγ , this inhibition was reversed when MT assembly was restored by the removal of nocodazole. The result suggests that Gβγ might be involved in promoting MT assembly and/or stabilization of MTs *in vivo* as demonstrated *in vitro*. More recently, we found that the activation of GPCRs (β- and α2-adrenergic receptors) stimulated MT assembly in NIH3T3 cells. The stimulation of MT assembly in response to GPCR activation correlated with increased association of Gβγ with polymerized tubulin, suggesting that GPCRs may utilize Gβγ to regulate MT assembly *in vivo* (Gutierrez et al., manuscript under preparation).

1.6. The carboxy-terminal of the G protein-coupled receptor kinase 2 (GRK2) as an inhibitor of Gβγ-mediated signaling

The G protein-coupled receptor kinase 2 (GRK2), also known as β-adrenergic receptor kinase 1 (βARK1), is a member of the GRK family of kinases, a group of proteins involved in the regulation of GPCR desensitization (Kamal et al., 2012). GRK2

is ubiquitously expressed and is found in the cytosol. Upon agonist activation of GPCRs, Gβγ binds to GRK2 and recruits it to the membrane, where it phosphorylates the GPCR, inducing its clathrin-mediated internalization and allowing desensitization (Claing et al., 2002).

GRK2 binds to Gβγ by means of a domain that is located in the carboxy-terminal region of the kinase (Fushman et al., 1996; Kamal et al., 2011). Since the GRK2-Gβγ interaction is highly specific, the carboxy terminus of GRK2 (GRK2ct) has been widely used as a peptide inhibitor of Gβγ-signaling, including β-adrenergic receptor desensitization, adenylate cyclase activity, activation of the mitogen-activated protein kinase pathway, and regulation of PI3K signaling (Koch et al., 1994a; Crespo et al., 1994; Perrino et al., 2005; Smrcka et al., 2008; Kamal et al., 2011). A very important feature of GRK2ct is its ability to inhibit signaling through a variety of Gβγ effector molecules without disrupting normal G protein activation and signaling. This derives from the fact that the presence of GRK2ct inhibits pathways that Gβγ is known to regulate, but has no effect on pathways controlled by Gα subunits (Koch et al., 1994a; Koch et al., 1994b; Inglese et al., 1994; Smrcka, 2008). Although the precise mechanism for the selectivity of GRK2ct remains unclear, the use of the peptide provides a very helpful tool in attempting to understand Gβγ-mediated cellular functions.

1.7. Prenylation of γ subunit of Gβγ is required for its binding to MTs and stimulation of MT assembly

A number of proteins undergo a process of post-translational modification known as prenylation. This consists of the attachment of 15-carbon farnesyl or 20-carbon geranylgeranyl groups to a carboxy-terminal motif termed CAAX, where “C” is a cysteine, “A” is an aliphatic amino acid, and “X” is any amino acid (Gelb et al., 2006). Approximately 2% of eukaryotic proteins are known to undergo prenylation, denoting the importance of this modification (Nalivaeva and Turner, 2001). Prenylation can affect the subcellular localization of proteins, as well as their biological function, and can play a part in mediating protein-protein interactions (Novelli and D’Apice, 2012).

The prenylation pathway (Figure 4) consists of three enzymatic steps, the first of which is the addition of a prenyl group to the cysteine residue of the carboxy-terminal CAAX motif, followed by the cleavage of the tripeptide (AAX). The terminal carboxylic acid group then undergoes methylation, which is then catalyzed by the prenylated protein methyl transferase (PPMTase, also known as isoprenylcysteine carboxyl methyltransferase, or ICMT). PMPMEase readily hydrolyzes ester bonds of the methylated prenylated proteins, thus making the methylation step reversible (Winter-Vann and Casey, 2005; Lamango, 2005; Gelb et al., 2006). For this reason, the last enzymatic step in this series of reactions has become an attractive target for drug development, since defects in protein prenylation have been documented in human

cancers and neurodegenerative diseases (Seabra et al., 1995; Pereira-Leal et al., 2001; Ghobrial and Adjei, 2002).

The γ subunit of Gβγ is known to undergo prenylation and subsequent methylation of the carboxy-terminal cysteine, and this modification is believed to influence protein activity and subcellular localization (Fung et al., 1990; Takida and Wedegaertner, 2003; Marrari et al., 2007). In this regard, prenylation has been found to play an important role in the Gβγ-mediated regulation of MT assembly, since a prenylation-deficient mutant Gβ1γ2 (C68S), which does not undergo prenylation and subsequent carboxy-terminal processing on the γ subunit, fails to bind to MTs and does not stimulate tubulin polymerization (Roychowdhury and Rasenick, 1997; Roychowdhury et al., 2006). Therefore, inhibitors of the prenylation pathway could be a valuable tool to study the functional regulation of MTs through Gβγ.

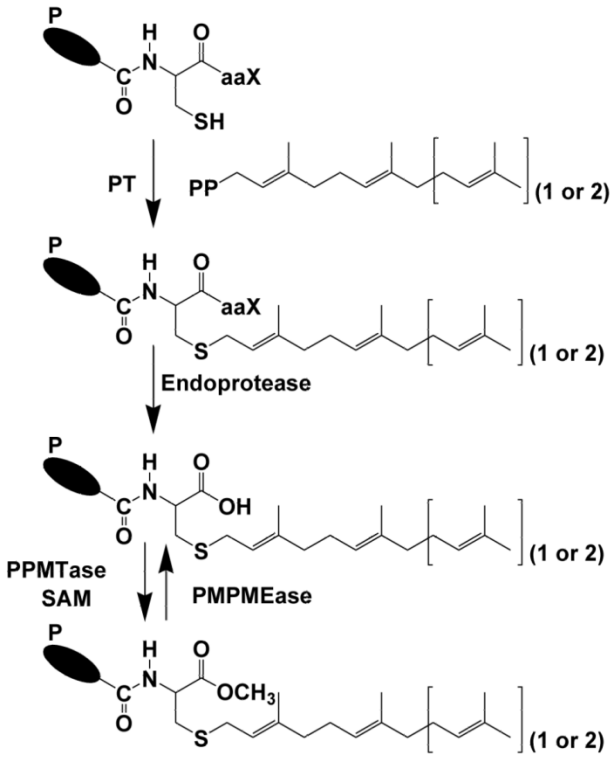

Figure 4. The protein prenylation pathway. Protein prenylation is catalyzed by a series of three enzymatic reactions that culminate with the methylation of the C-terminal prenylated cysteine, which is the only reversible step in the enzymatic pathway. Figure adapted with permission (Amissah et al., 2011).

1.8. Actin filaments or microfilaments

Actin filaments (AFs) are another important component of the cytoskeleton. AFs participate in a variety of cellular processes, such as cell division, differentiation, morphogenesis, intracellular trafficking, and the generation of the motile force of the cells. AFs are capable of generating specialized structures within the cell, such as stress fibers, filopodia, and lamellipodia (Bailly and Condeelis, 2002; Sekino et al., 2007; Cingolani and Goda, 2008). The biochemical basis for actin's versatility to participate in these cellular processes is its ability to transition from globular G-actin (monomeric) to filamentous F-actin (polymerized). Actin polymerization is essentially a condensation reaction, with the initial association of an unstable dimer, followed by the formation of a stable trimer that represents the nucleus of polymerization, and finally, the elongation phase, during which the actin monomers are rapidly assembled (Grazi and Trombetta, 1985; Wang et al., 1989; Dos Remedios et al., 2003). Actin possesses intrinsic ATPase activity, given that ATP hydrolysis plays a critical role in the polymerization process. AFs are polar structures, with polymerization occurring on the barbed end (ATP-bound), and depolymerization occurring preferentially on the pointed end, which consists of ADP-bound actin (Lee and Dominguez, 2010). Actin polymerization is tightly regulated by a number of actin-binding proteins (ABPs). Small GTPases—such as Rho, Cdc42, and Rac—are involved in the regulation of actin dynamics during the formation of filopodia and lamellipodia (Ettienne-Manneville and Hall, 2002). Another well-characterized example of ABPs is the WASP complex, which plays a role in promoting actin polymerization (Takenawa and Tsuetsugu, 2007). On the

other hand, the ABP known as actin-depolymerizing factor, or ADF/cofilin, is involved in the regulation of actin filament severing and depolymerization (Pak et al., 2008).

1.9. Neuronal cytoskeleton

The cytoskeleton plays a key role in inducing neurite outgrowth and maintaining the highly asymmetrical shape and structural polarity of neurons that are essential for neuronal function. Neuronal outgrowth is a complex process in which two distinct domains emerge from the cell body: a long, thin axon that transmits signals, and multiple shorter dendrites, which are specialized primarily for receiving signals. When fully differentiated through axon and dendrite elongation, this unique morphology allows neurons to achieve precise connectivity between appropriate sets of neurons, which is crucial for the proper functioning of the nervous system (Figure 5). While many signals are known to drive neuronal outgrowth, it is the assembly and disassembly of cytoskeletal structures embodied within neurite extension and growth cone formation that are essential for establishing appropriate synaptic connections and signal transmission.

MTs form dense parallel arrays in axons and dendrites that are required for the growth and maintenance of these neurites. Unlike MTs, actin filaments in neurons are enriched in growth cones and organized into long bundles forming filamentous protrusions, or filopodia, or veil-like sheets of branched actin forming lamellipodia. The

interactions between these two cytoskeletal filaments are important for advancement of growth cones and axon guidance (Witte and Bradke, 2008; Geraldo and Gordon-Weeks, 2009). In the axon, MTs are bundled by MAPs, with the plus end oriented toward the nerve terminal. They are also found in the cell body and dendritic processes, where they provide structural support and help to stabilize dendrite branches (Goldstein and Yang, 2000).

During neuronal differentiation, the organization of MTs needs to be remodeled rapidly, and MT stability changes depending on their cellular localization. The stability of neuronal MTs is predominantly regulated by the reversible tyrosination/detyrosination of α tubulin. This process involves the removal of C-terminal tyrosine (Tyr-tubulin) by an enzyme called tubulin carboxypeptidase, thus generating detyrosinated tubulin (glutaminated-tubulin or Glu-tubulin). This modification is reversible, as the enzyme tubulin tyrosine ligase is able to catalyze the addition of tyrosine back onto the C-terminus of Glu-tubulin, thus forming Tyr-tubulin again (Barra et al., 1973; Raybin and Flavin, 1977; Argarana et al., 1978; Schröder et al., 1985; Paturle et al., 1989; Ersfeld et al., 1993; Janke and Kneussel, 2010). The detyrosinated form of tubulin (Glu-tubulin) is generally linked to stable MTs, as long-lived MTs are detyrosinated in different cell types (Schulze et al., 1987; Janke and Kneussel, 2010). Thus, in neurons, the MTs containing detyrosinated tubulin are predominantly found in axons, where highly stable MTs are required (Paturle-Lafanechere et al., 1994). In the growth cones, where highly dynamic MTs are needed to facilitate advancement, MTs are enriched in Tyr-tubulin (Janke and Kneussel, 2010).

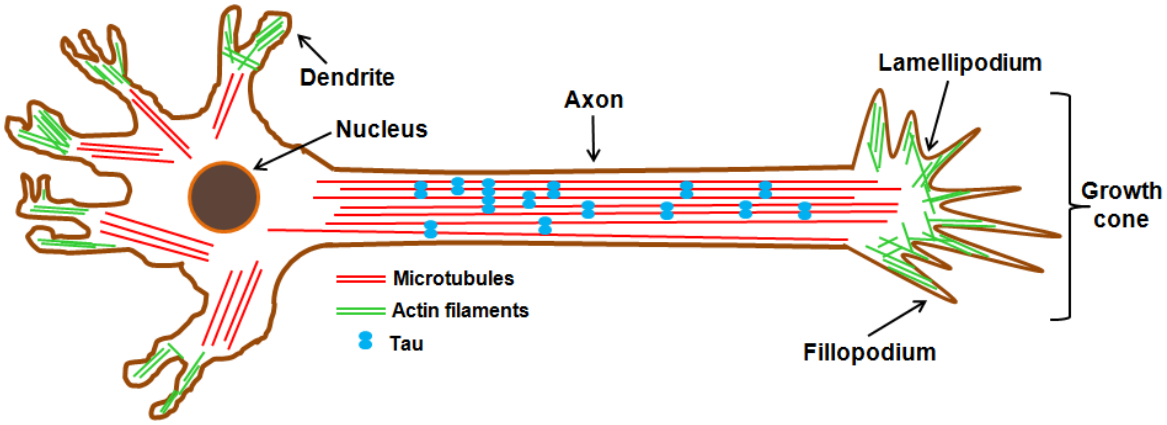

Figure 5. Neuronal cytoskeleton. MTs (red) are shown in the axon, dendrites, and the central domain of the growth cone. Tau (blue), a microtubule-associated protein (MAP), is found in the axon, where it participates in MT bundling. Actin filaments (green) are present in the growth cone and dendrites, where they form specialized structures such as lamellipodia and filopodia.

1.10. Key regulators of MTs/actin cytoskeleton during neurite outgrowth

It is clear that cytoskeletal components are able to detect biochemical signals and respond to them in order to change neuronal cell morphology. However, the precise signaling pathways that lead to this unique organization of the cytoskeleton are not clearly understood (Li and Gundersen, 2008). PC12 cells have been used extensively for these studies, since they respond to nerve growth factor (NGF) with growth arrest and exhibit a typical phenotype of neuronal cells sending out neurites (Greene and Tischler, 1976). The receptor commonly associated with this process is receptor tyrosine kinase (TrkA) by which NGF exerts its effect (Patapoutian and Reichardt, 2001). PI3K appears to be the key molecule in this pathway, and regulates localized assembly of MTs/actin filaments by downstream Akt/GSK3β pathways (Cantley, 2002; Zhou et al., 2004). The Rho and Ras families of small GTPases also emerged as critical players in regulating the actin-MT cytoskeleton by modulating downstream effectors, including serine threonine kinase, p21-activated kinase, ROCK, and mDia (Govek et al., 2005; Hall and Lalli, 2010). GPCRs, as well as α and $\beta\gamma$ subunits of heterotrimeric G proteins, have also been shown to regulate neurite outgrowth (Reinoso et al., 1996; Kwon et al., 1998; Lotto et al., 1999; He et al., 2005; Igarashi et al., 1993; Sarma et al., 2003; Wolfgang et al., 2004; Sachdev et al., 2007; Yu et al., 2009). Earlier studies to understand the role of G proteins in neurite outgrowth were mainly focused on α subunits of G proteins because α subunits were thought to be the physiological mediator of GPCR signaling. More recently, G$\beta\gamma$ has also been shown to regulate neurite outgrowth in primary hippocampal neurons by interacting with Tctex-1, a light-

chain component of the cytoplasmic dynein motor complex. It has been proposed that Gβγ might accomplish this function by linking extracellular signals to localized regulation of MTs and actin filaments through Rho GTPase and downstream MT modulators (Sachdev et al., 2007; Wang and Wong, 2009). PI3K is also a downstream effector of Gβγ in GPCR signaling (Stoyanov et al., 1995; Stephens et al., 1997), and recent results suggest that the activation of PI3K/Akt pathway by NGF is, in part, mediated through the βγ subunit (Wu and Wong, 2005a and 2005b; Wang and Wong, 2009). These studies collectively suggest a role of Gβγ in neuronal differentiation. However, the mechanisms by which Gβγ acts to regulate neurite outgrowth are still poorly understood. The prevailing view is that Gβγ would activate downstream signals and involve MAPs and other MT modulators to regulate MT assembly and neurite outgrowth (Sachdev et al., 2007; Wang and Wong, 2009).

1.11. Aberrant organization of the cytoskeleton in neurodegeneration

Neurodegeneration is a pathological condition in which a loss of neuronal structure and function occurs progressively, ultimately leading to neuronal cell death (Jellinger, 2009). Many alterations in normal cellular processes take place during neurodegeneration, including defects in protein folding, mitochondrial dysfunction, impaired intracellular transport, and increased oxidative stress (Jellinger, 2010). In addition, one of the hallmarks of neurodegeneration is the presence of abnormal protein aggregates in neuronal cells (Cairns et al., 2004). These pathological protein inclusions

are present in many neurodegenerative diseases, such as Alzheimer's and Parkinson's diseases. Importantly, further characterization of these abnormal protein deposits has revealed the presence of cytoskeletal proteins, such as tubulin and MAPs (Goedert et al., 2001; Al-Chalabi and Miller, 2003; Skovronsky et al., 2006; Jellinger, 2010).

Alzheimer's disease (AD) is the most common neurodegenerative disorder, affecting ~10% of people over 70 (Plassman et al., 2007). Amyloid plaques (consisting of extracellular deposits of Aβ peptides) and neurofibrillary tangles (NFT) constitute the two major neuropathological alterations in the brains of AD patients. NFTs are formed of abnormally aggregated, paired helical filaments consisting of the MAP, tau. Under normal conditions, tau binds to MTs, stabilizing neuronal structure and integrity. In AD brain, the MT structure is disrupted, and tau is hyperphosphorylated and does not bind to MTs (Drechsel et al., 1992; Ittner and Gotz, 2010). Figure 6 shows NFT formation and MT disruption in neuronal cells.

Cytoskeletal alterations are also present in Parkinson's disease (PD). α-synuclein is a major component of the cytopathological markers of PD, the Lewy bodies, but cytoskeletal proteins—such as tubulin, MAP1, MAP2, and neurofilaments—are also present (Alonso et al., 2008; Amniai et al., 2008; Gustav et al., 2010). Although α-synuclein-induced neurotoxicity is believed to play a major role in the pathogenesis of PD, recent evidence suggests that disruptions in the microtubule cytoskeleton may also play an important role (Cardoso et al., 2012).

Other neurodegenerative diseases, such as Pick's disease, frontotemporal lobar degeneration, progressive supranuclear palsy, and amyotrophic lateral sclerosis, are also known to include cytoskeletal alterations as part of the underlying disruptions in cellular machinery (Cairns et al., 2004; Brunden et al., 2009). Additionally, aberrant cytoskeletal structure and function is now believed to play a critical role in the development of other neurological disorders, such as schizophrenia and depression, with alterations in the microtubule network as a key feature (Arnold et al., 1991; Gozes, 2011; Wong et al., 2013).

The majority of the research and drug discovery effort in the area of neurodegenerative diseases in the past focused on these pathological markers. However, the cause of these disorders remains largely unknown. Most importantly, no effective drugs are currently available to treat neurodegenerative disorders, suggesting that there is a critical knowledge gap in our understanding of how the disease is triggered and how it progresses. Recent results suggest that MT assembly is severely compromised in AD and PD brains (Cash et al., 2003; Buxton et al., 2010; Cartelli et al., 2010, 2013). This could play a significant role in triggering early phases of the disease, which could be followed by the demise of neurons and neuronal death.

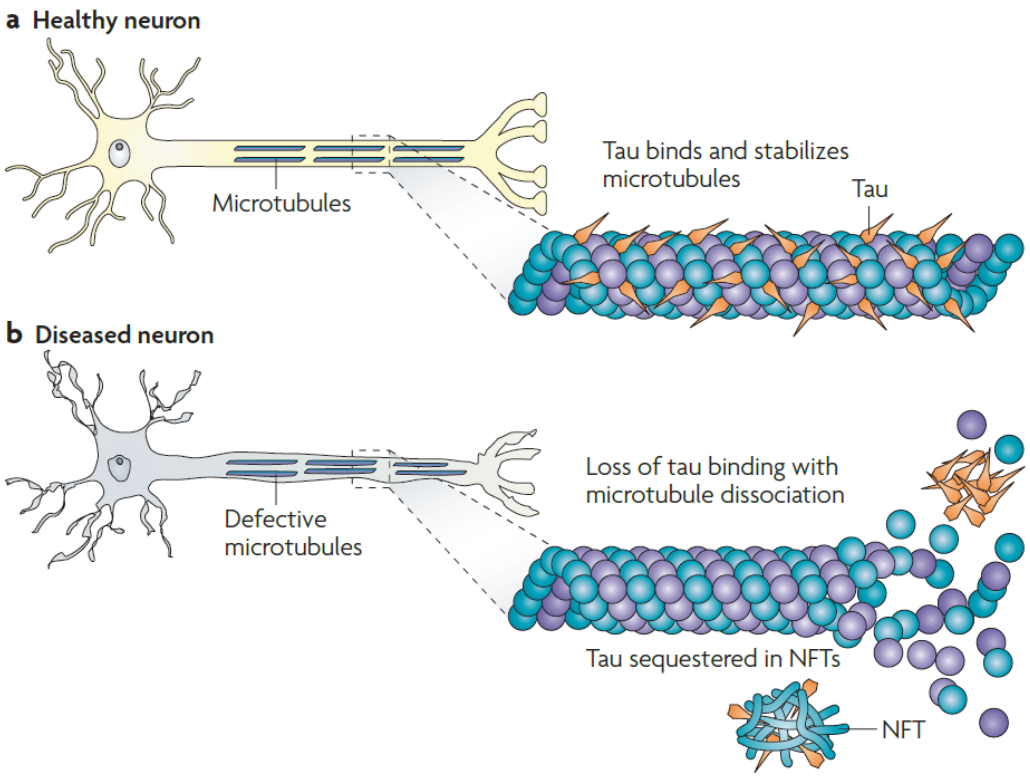

Figure 6. Tau in healthy neuronal cells and formation of NFTs in diseased cells. In normal neurons, tau participates in MT stabilization, helping to preserve neuronal integrity and facilitating neuronal function. During neurodegeneration, tau becomes hyperphosphorylated and does not bind to MTs, forming abnormal aggregates that are deposited in the cells. This leads to impaired MT stability, axonal damage, and overall loss of neuronal integrity. Reprinted by permission from Macmillan Publishers Ltd: Nature Reviews Drug Discovery (Brunden et al., 2009).

1.12. Hypothesis and specific aims

Neuronal differentiation and neurite formation are dependent on a highly specialized organization of the MT/actin cytoskeleton. However, the precise molecular mechanism and the specific cellular signals that drive these cytoskeletal changes are poorly understood. This knowledge is critically important because severe cytoskeletal alterations occur during neurodegeneration. Previous results from our laboratory indicated that the βγ subunit of heterotrimeric G proteins binds to tubulin and stimulates MT assembly *in vitro*. We have also demonstrated that the tubulin-Gβγ interaction is critical for MT assembly/stability in cultured PC12 cells. I hypothesize that Gβγ is involved in neuronal differentiation by modulating MT assembly, and that the disruption of the interaction between Gβγ and tubulin/MT in neurons will disrupt the MT/actin cytoskeleton and inhibit neuritogenesis. This hypothesis was tested by addressing the following specific aims:

Specific Aim 1: Determine if Gβγ and its interaction with MTs is important for neurite outgrowth.

Specific Aim 2: Determine if blocking the interactions between Gβγ and MTs alters MT organization and inhibits neurite outgrowth.

Specific Aim 3: Determine the signaling pathways involved in Gβγ-dependent regulation of MT assembly and neurite outgrowth.

CHAPTER 2: MATERIALS AND METHODS

2.1. Cell culture and NGF treatment

PC12 cells (pheochromocytoma cells derived from the adrenal gland of *Rattus norvegicus*) (ATCC, Manassas, VA), were grown in 75-cm^2 culture flasks at 37 °C in Dulbecco's Modified Eagle's Medium (DMEM, CellGro, Manassas, VA) (4.5 g/L glucose, L-glutamine, without pyruvate), supplemented with 10% bovine calf serum and antibiotics (100 U/mL penicillin and 100 μg/mL streptomycin) in 10% CO_2. For NGF treatment, PC12 cells were treated with 100 ng/mL of NGF (Sigma-Aldrich, St. Louis, MO) dissolved in complete media for three consecutive days. Control cells without NGF were also grown under the same conditions. For quantitative assessment of neurite outgrowth, PC12 cells were only treated with NGF for 2 days instead of 3, given that the density of neurite outgrowth does not allow for proper tracing of neurites belonging to a specific cell body. SH-SY5Y neuroblastoma cells (a kind gift from Dr. M. Narayan's lab, UTEP) were grown in 75-cm^2 flasks in a 1:1 mixture of DMEM and F-12 media (Invitrogen), supplemented with 10% fetal bovine serum and antibiotics (100 U/mL penicillin and 100 μg/mL streptomycin) in 10% CO_2.

2.2. PMPMEase inhibitors and Gβγ-blocking peptide (GRK2i)

Using phenylmethylsulfonyl fluoride (PMSF) as a prototypical molecule, the laboratory of Dr. N. Lamango (Florida A&M University) recently synthesized high-affinity specific inhibitors of PMPMEase (Aguilar et al., 2011). Two such inhibitors, 2-*trans*-geranylthioethanesulfonyl fluoride (L-23) and 2-*trans, trans*-farnesylthioethanesulfonyl

fluoride (L-28) were used in our study. Stock solutions of 20 mM L-23, L-28, or PMSF were prepared in dimethyl sulfoxide (DMSO) and diluted in tissue culture media to final concentrations of 1, 5, or 10 μM, and added to the cells as indicated in the figures. The DMSO concentration in the culture media never exceeded 0.05%. In addition, a control experiment was performed in the presence of a similar concentration of DMSO. The Gβγ-blocking peptide, GRK2i (WKKELRDAYREAQQLVQRVPKMKNKPRS), was obtained from Tocris Bioscience (Bristol, UK), and it consists of the Gβγ-binding domain of the G protein-coupled receptor kinase 2 (GRK2) and acts as a cellular Gβγ antagonist. A stock solution of the peptide (1 mM) was prepared in 10% DMSO, and was added to the cells at final concentrations of 1, 5, or 10 μM as indicated in the figure. The DMSO concentration in the culture media never exceeded 0.1% as indicated above, and the control experiment was also performed in the presence of 0.1% DMSO in the culture media.

2.3. Gallein and PI3K inhibitors

The small molecule inhibitor gallein, which has been shown to bind to Gβγ and inhibit downstream activation of PI3-Kγ (Lehman et al., 2008) was obtained from Tocris Bioscience. In addition, two highly specific and widely validated PI3K inhibitors, wortmannin and LY294002 (Sigma-Aldrich), were employed. Stock solutions of all three inhibitors were prepared in DMSO (20 mM gallein, 10 mM Wortmannin, and 14.5 mM LY294002) and further diluted in culture media right before being added to the cells. Control experiments in the presence of similar concentrations of DMSO were conducted for each inhibitor.

2.4. Extraction of cytoskeletal (CSK) and soluble protein (SOL) fractions

Cells were grown on 100- or 150-mm plates to 70% confluence over 1–2 days as described in section 2.1. The plates were used in duplicates for each condition. Cytoskeletal (CSK; enriched in MTs) and soluble (SOL; enriched in tubulin dimers) fractions were prepared by extracting soluble proteins in a MT stabilizing (MS) buffer as described previously (Montoya et al., 2007) with a minor modification adopted from Marklund et al. (1996). Briefly, cells were rinsed and incubated with 0.5–1 mL of MS buffer (0.1 M PIPES, pH 6.9, 2 M glycerol, 5 mM $MgCl_2$, 2 mM EGTA, 0.5% Triton X-100, 1 mM DTT, and 10 μM GTP) supplemented with protease inhibitor cocktail (Roche Applied Science, Indianapolis, IN) for ~10 min at room temperature. Subsequently, the cells were removed mechanically (using a cell scraper) and centrifuged at 10,000 × g for 10 min. The supernatant constitutes the SOL fraction and the cell pellets represent the CSK fraction that includes the tubulin and actin polymers. Pellets were then washed in PEM buffer (100 mm PIPES, pH 6.9, 2 mM EGTA, 1 mM $MgCl_2$) and resuspended in PEM buffer containing 1 mM DTT, 10 μM GTP, and protease inhibitor cocktail, followed by incubation on ice for 30 min. Protein extraction from the pellets was performed by sonicating the samples on ice for 1 min and clarifying by centrifugation at 10,000 × g for 10 min. The resulting supernatant was saved as CSK fraction. The protein concentration of the samples was determined by a previously described method (Bradford, 1976), using bovine serum albumin (BSA) as standard. The subcellular fractionation procedure yielded highly reproducible results in technically replicated samples used for each condition in a given experiment.

2.5. Preparation of whole cell lysates

PC12 cells were grown under the conditions described in section 2.1. For nocodazole treatment, cells were grown on 150 mm culture dishes until they reached ~80% confluence. Cells were treated with the drug (10 μM) for 4 hours. Whole cell lysates were also prepared. After treatment or transfection, culture media was removed, cells were washed with PBS, and then lysed by incubation in 1 ml lysis buffer (10 mM Tris-HCl, pH 7.9, 1.5 mM MgCl2, 0.3 M sucrose, 0.1% Triton X-100, 1 mM DTT, and 10 μM GTP) supplemented with protease inhibitor cocktail, for 10 min at room temperature. Cells were then scraped and sonicated for 1 min, followed by centrifugation at 10,000 × g for 10 min. The supernatants constituted whole cell lysates, and the protein concentration was determined by the Bradford (1976) assay.

2.6. Electrophoresis and immunoblotting

Samples for immunoblotting were subjected to SDS-polyacrylamide gel (10%) electrophoresis, followed by electrotransfer onto nitrocellulose membranes (Laemmli, 1970; Towbin et al., 1970). The membranes were blocked in 5% nonfat dry milk in TBS (10 mM Tris-HCl and 150 mM NaCl, pH 7.4) for 2 h at room temperature, followed by overnight incubation at 4 °C with mouse monoclonal anti-α-tubulin (DMIA, Sigma-Aldrich, 1:200), rabbit polyclonal anti-Gβ (Santa Cruz Biotechnology, 1:250), goat polyclonal anti-actin (Santa Cruz Biotechnology, 1:250), or rabbit monoclonal anti-Akt and anti-pAkt (Cell Signaling Technology, 1:500) antibodies in TBS containing 0.01% BSA as previously described (Montoya et al., 2007). The membranes were washed three times with 0.05% Tween-20 in TBS (TBST) and incubated with the appropriate

HRP-conjugated secondary antibodies (goat anti-mouse or goat anti-rabbit from Promega, Madison, WI; 1:1000, or donkey anti-goat from Santa Cruz Biotechnology; 1:1000) in TBST containing 0.01% BSA for 1 h. For sensitive detection, the chemiluminescence (ECL) technique (SuperSignal West Pico Chemiluminescent Substrate) was used according to the manufacturer's instructions (Pierce Biotechnology, Rockford, IL). Quantitative analysis of the protein bands was performed with the LabWorks image acquisition and analysis software (UVP Laboratory Products, Upland, CA).

2.7. Immunoprecipitation

For immunoprecipitation experiments, 100 μL aliquots of cellular fractions (~0.25–1 mg/mL of protein) were incubated with or without anti-Gβ antibody (5-10 μl), or non-specific rabbit IgG for 1 h at 4 °C, followed by an overnight incubation (4 °C) with 100 μL of 50% protein A-sepharose (Amersham Biochemical, Piscataway, NJ), as previously described (Montoya et al., 2007). Samples were then centrifuged at 10,000 × g for 10 min, and the supernatants (SUP) were saved. The pellets (immunocomplex) were washed with PBS and eluted with 3% SDS Laemmli sample buffer containing 0.15 M dithiothreitol (DTT) and boiled in a water bath for 5 min. Samples were then clarified by centrifugation. Both IP and SUP fractions were then subjected to immunoblotting using anti-tubulin or anti-actin antibodies as described in section 2.6.

2.8. Overexpression of Gβγ

PC12 cells were transiently co-transfected with yellow fluorescent protein (YFP)-tagged pcDNA3.1 plasmids encoding for Gβ1 and Gγ2 subunits. The expression plasmids were generously provided by Dr. N. Gautam (Washington University, St. Louis, MO). A plasmid encoding only YFP (pcDNA3-YFP, Addgene, Cambridge, MA) was used as a control, and the plasmids were transfected separately (Gβ1 and Gγ2) or co-transfected to generate the Gβ1γ2 combination. Cells were transfected with the plasmids using the Lipofectamine LTX PLUS reagent (Invitrogen, Carlsbad, CA) according to the manufacturer's instructions. Briefly, PC12 cells were seeded on glass coverslips using 12-well plates at a density of 50,000 cells /well, and incubated overnight under normal growth conditions. The following day, the cells were transfected with a mixture of Lipofectamine LTX PLUS containing 2 µg of each plasmid (dissolved in antibiotic-free media) and incubated overnight in normal growth media. Cells were monitored for protein expression (YFP fluorescence) and morphological changes using differential interference contrast (DIC) images at different time points (24, 48, and 72 h), with a Zeiss Axiovert 200 fluorescence microscope equipped with a GFP filter. For confocal microscopic analysis, the cells were fixed and processed as described in section 2.8.

2.9. Immunofluorescence and confocal microscopy

For confocal microscopic analysis, cells were allowed to attach to immunocytochemistry slides (Lab-TEK II mounted on glass slides, Thermo Fisher Scientific, Rochester, NY) or seeded on glass coverslips using 12-well plates, and were grown overnight as described in section 2.1. Cells were then treated with or without NGF and/or inhibitors

as indicated and subsequently fixed by the addition of ice-cold 100% methanol (previously cooled to -20 °C) and incubated at -20 °C for 6 min as described (Montoya et al., 2007). The cells were then rinsed three times in PBS, blocked for 1 h at room temperature in 5% normal goat serum (NGS) (Sigma-Aldrich) in PBS, followed by overnight incubation at 4 °C with primary antibodies (anti-α-tubulin, anti-Gβ, and anti-actin; 1:100 dilution) in 1% NGS in PBS. Detailed description of these antibodies is provided in section 2.6. The slides were rinsed as before and incubated with the appropriate secondary antibodies (tetramethyl rhodamine (TMR)-conjugated goat anti-mouse IgG, fluorescein isothiocyanate (FITC)-conjugated goat anti-rabbit IgG, Alexa Fluor 350-conjugated donkey anti-goat IgG; Molecular Probes-Invitrogen, Carlsbad, CA, or TMR congujated bovine anti-goat, Santa Cruz Biotechnology) for 2 h at room temperature and in the dark to diminish photo-bleaching effects. The slides were then mounted with DAKO mounting media (DAKO Corporation, Carpenteria, CA), or with ProLong Gold anti-fade reagent with DAPI (Invitrogen, for nuclear staining), and covered with coverslip. High-resolution, digital, fluorescent images were captured by employing inverted, confocal laser-scanning microscopy (model LSM 700; Zeiss, Thornwood, NY), utilizing a Plan-Apochromat 63x/1.40 immersion-oil DIC objective and assisted with 2009 ZEN software (Zeiss, Thornwood, NY). DAPI and Alexa Fluor 350 (blue), FITC (green), and TMR (red) were excited with laser emissions of 405-, 488-, and 555-nm wavelengths, respectively. Gβγ-transfected cells were only labeled with anti-α-tubulin and TMR antibodies.

2.10. Co-localization analysis

To quantitatively assess the degree of co-localization between Gβγ and MTs, regions of interest (ROIs) were delimited within cells to decrease the background fluorescence contribution. Co-localization was calculated using a squared Manders' overlap coefficient of the defined signals, performed on a pixel-by-pixel basis, which represents an accurate degree of co-localization. The Manders' overlap coefficient provides values within the range from 0 to 1; a value of 0 means that there are no pixels within the selected ROI with overlapped signals, whereas a value of 1 represents perfectly co-localized pixels (Manders et al., 1993). The values for selected ROIs were acquired from images taken from 10–12 cells from different microscope fields, using the ZEN 2009 software. In order to rule out bleed-through of the fluorescent labels, control coverslips were prepared with a single fluorophore and were further imaged under the same microscope settings used with the double-labeled coverslips. In addition, the same microscope settings were applied when imaging the cells for co-localization analysis.

2.11. 3-D image analysis

Image stacks were imported into Volocity 3-D Image Analysis Software (Version 6.0; Perkin Elmer Corporation, Waltham, MA) operating on a Macintosh Pro computer. In Volocity's Restoration module, a point-spread function was calculated to deconvolve the native image stack using iterative restoration (80%, 20 iterations max). In Volocity's Visualization module, a joystick control aided in free flight through the newly rendered 3-D image for selection of proper viewing approaches alongside labeled neuronal

processes of the cell. These instances within the moving sequence were bookmarked, and the bookmarks were dropped into the software's movie-making interface. The final sequence was exported as a QuickTime movie (see Supplementary Movie 1), and still frames from this movie sequence were selected to generate Figure 12.

2.12. Neurite outgrowth assessment

For neurite outgrowth measurement, cells were fixed and processed for confocal microscopy using a mouse monoclonal anti-tubulin antibody and a rabbit polyclonal Gβ antibody, followed by labeling with rhodamine- and FITC-conjugated secondary antibodies. Due to the fast photo-bleaching of the FITC fluorophore, the cells were only imaged using rhodamine staining for the purpose of neurite outgrowth assessment. Cells were viewed using the 40x objective with a Zeiss LSM 700 confocal microscope. The coverslips were scanned from left to right, and 8–10 microscope fields were randomly selected. For each field, neurites were traced and measured using the 2009 ZEN software (Zeiss), and at least 100 cells from three independent experiments were scored for each condition. A cell was considered as neurite-bearing if it contained at least one neuronal process that was longer than the cell body.

2.13. Neuronal primary cultures from rat-brain cerebellum and hippocampus

Primary cultures of cerebellum and hippocampus neurons were prepared from brains of postnatal day (1–2) Sprague Dawley rats as previously described (Goslin et al., 1998; Gomez et al., 2002). The cerebellum and hippocampus were dissected from the brain and dissociated by papain digestion for 1 h at room temperature, followed by

mechanical disaggregation with a Pasteur pipette. Cells were then counted using a hemocytometer and subsequently seeded on glass coverslips using 12-well plates at a density of 250,000 cells/well (for confocal microscopy), or on 100-mm culture dishes at a density of $1x10^7$ cells/plate (for subcellular fractionation experiments). Both glass coverslips and culture dishes were pre-coated with 0.01% poly-D-lysine and 10 µg/mL laminin dissolved in PBS. Neuronal cultures were maintained in Neurobasal A media containing B27 supplement (Invitrogen), Glutamax, antibiotics (100 U/mL penicillin, and 100 µg/mL streptomycin), and mitotic inhibitors (10 µM uridine and 10 µM fluoro-deoxyuridine). Cultures were fed every other day by replacing half of the media with fresh, complete media (including mitotic inhibitors). Neuronal primary cultures were used for confocal microscopy and subcellular fractionation experiments after they became fully differentiated (at least seven days in culture).

2.14. Differential nuclear staining (DNS) assay for cytotoxicity

To determine the levels of cytotoxicity caused by the experimental compounds (L-28, L-23, PMSF, GRK2i) a previously described DNS assay adapted for high-throughput screening was used (Lema et al., 2011). This assay uses two fluorescent nucleic acid intercalators, Hoechst 33342 (Hoechst) and propidium iodide (PI). Briefly, PC12 cells were seeded in a 96-well plate format and incubated with NGF and inhibitors. One hour before image capturing, a staining mixture of Hoechst and PI at a final concentration of 1 µg/mL for each dye was added to the cells. Subsequently, cells were imaged in live-cell mode using a BD Pathway 855 Bioimager system (BD Biosciences, Rockville, MD). Montages (2x2) from four adjacent image fields were captured per well in order to

acquire an adequate number of cells for statistical analysis, utilizing a 10x objective. To determine the percentage of dead cells from each individual well, both image acquisition and data analysis were performed using the BD AttoVision v1.6.2 software (BD Biosciences), and each experimental condition was assessed in triplicate.

2.15. Knockdown of Gβ1

In order to knockdown the expression of Gβ1 in PC12 cells, we employed small interfering (siRNA) technology. A pool of 4 predesigned siRNAs (ON-TARGET plus Smart Pool) targeting the gene encoding for rat Gβ1 (GNB1) was obtained from Dharmacon (Thermo Fisher Scientific, Pittsburgh, PA). The siRNAs were resuspended in RNase-free water at a stock concentration of 100 μM. PC12 cells were transfected with DharmaFECT transfection reagent (Dharmacon), following the manufacturer's instructions. Briefly, PC12 cells were seeded on 6-well plates at a density of 150,000 cells/well and grown overnight on antibiotic-free media with serum. The following day, cells were transfected with a mixture of DharmaFECT transfection reagent and different concentrations of Gβ1 siRNA (50 and 100 nM). Cells were incubated overnight under normal conditions, and the antibiotic free media was replaced with fresh complete media. The following day, a second transfection was performed, using the conditions described above. Three conditions were employed as negative controls: PC12 cells without any treatment, cells treated with transfection reagent only, and finally, a pool of siRNAs that do not target any gene in rat cells was employed (non-targeting siRNA, Dharmacon).

2.16. Statistical analysis

All statistical analyses were performed using Sigma Plot 11 software (Systat Software, Chicago, IL, USA). In the case of Western blot quantitative analysis, the differences between controls and treatments were assessed by means of the Student's paired t-test. In the case of neurite outgrowth analysis, the differences in various conditions were assessed by means of one-way ANOVA followed by Holm-Sidak testing (multiple comparisons vs. control). For comparisons between two groups, the Student's paired t-test was employed, and in all cases, a value of $p < 0.05$ was considered to be statistically significant.

CHAPTER 3: RESULTS

3.1. Specific Aim 1: Determine if Gβγ and its interaction with MTs is important for neurite outgrowth

3.1.1. Objective and Overview

Dynamic rearrangements of MTs and actin filaments are critical for growth cone motility and neurite outgrowth. Previous studies from our laboratory have shown that the βγ subunit of signal-transducing G proteins promotes MT assembly (Roychowdhury and Rasenick, 1997; Roychowdhury et al., 2006; Montoya et al., 2007), which may provide a mechanism for development of axonal processes and neurite outgrowth. Therefore, in Specific Aim 1, we explored the interaction between Gβγ and MTs and its possible role in neuronal outgrowth and differentiation. PC12 cells as a model cell line and rat brain primary neurons in culture were used to conduct the study. Overexpression of Gβγ was employed to address whether Gβγ is involved in regulating MT assembly. In addition, the role of Gβγ in coordinating MT-actin interactions during neuronal differentiation was also investigated.

3.1.2. NGF-induced neuronal differentiation of PC12 cells promotes the interaction of Gβγ with MTs and stimulates MT assembly

Assembly and disassembly of MTs is critical for neurite outgrowth and differentiation. Previously we have shown that Gβγ binds to tubulin and promotes MT assembly *in vitro*, and Gβ immunoreactivity was found exclusively in the MT fraction after assembly in the presence of β1γ2, suggesting a preferential association with MTs rather than soluble tubulin (Roychowdhury and Rasenick, 1997). In PC12 cells, we found that Gβγ interacts with MTs and is involved in regulating MT assembly (Montoya et al., 2007).

Because NGF is known to induce neuronal differentiation, we thought that one of the mechanisms by which NGF induces neuronal differentiation could be via Gβγ-MT interactions and changes in MT assembly. To address this, PC12 cells were treated with NGF over the course of three days to allow for neuronal differentiation. Cytoskeletal (CSK, enriched in MTs) and soluble protein fractions (SOL, enriched in dimeric tubulin) were extracted using MS buffer as indicated in the methods. CSK pellets were resuspended in PEM buffer, followed by sonication and centrifugation as discussed in methods. The interaction of Gβγ with MTs and tubulin was analyzed by co-immunoprecipitation using a Gβ-specific antibody (rabbit polyclonal anti-Gβ) and by determining tubulin immunoreactivity (using a mouse monoclonal anti-α tubulin) in immunoprecipitated (IP) and unbound supernatant fractions (SUP). As indicated in Figure 7A, Gβγ was bound preferentially to MTs (CSK fraction) rather than to dimeric

tubulin (SOL fraction), which is consistent with our previous studies (Roychowdhury and Rasenick, 1997; Roychowdhury et al., 2006; Montoya et al., 2007). The results show that the interaction of Gβγ with MTs was increased significantly (150%) in NGF-treated cells (Figure 7A). When immunoprecipitation was performed (control PC12 cells) in the absence of primary antibody ("No ab") or non-specific rabbit IgG ("IgG"), tubulin immunoreactivity was not detected in the immunocomplex (Figure 7B). This validates the co-immunoprecipitation analysis we have developed to examine tubulin-Gβγ interactions. The result also confirms that the immunoprecipitation experiment can be performed reliably using the CSK fraction employed in our study. The MT assembly was assessed by determining tubulin immunoreactivity in CSK and SOL fractions and measuring the ratio of tubulin incorporated in the MTs vs. free tubulin as a direct measure of MT assembly. We found that MT assembly was stimulated significantly (from 45.3 ± 4.8% to 70.1 ± 3.6%) in NGF-differentiated PC12 cells (Figure 7C). Previously, using the anti-microtubule drug nocodazole we have shown that the interaction of Gβγ with MTs is an important determinant for MT assembly. While microtubule depolymerization by nocodazole inhibited the interactions between MTs and Gβγ, this inhibition was reversed when microtubule assembly was restored by the removal of nocodazole (Montoya et al., 2007). Therefore, the increased interactions of Gβγ with MTs in response to NGF could account for the stimulation of MT assembly observed in the presence of NGF (Figure 7A–C). Although it can be argued that MT structure is no longer intact in CSK fraction subsequent to sonication and low-speed centrifugation, we have shown earlier that the tubulin dimer binds to Gβγ, and that the tubulin-Gβγ complex preferentially associates with MTs (Roychowdhury and Rasenick,

1997; Roychowdhury et al., 2006). Therefore, the tubulin-Gβγ complex is expected to be present in the CSK fraction prepared in this study. The absence of any interactions between Gβγ and tubulin in SOL fraction despite their presence in SOL fraction further supports this result (Figure 7A). Furthermore, tubulin oligomers are expected to be present in the CSK fraction, and the possibility exists that Gβγ preferentially binds the oligomeric structures (Roychowdhury and Rasenick, 1997). The increased interactions of Gβγ with MTs and the stimulation of MT assembly observed in the presence of NGF could allow for a rearrangement of MTs during neuronal differentiation.

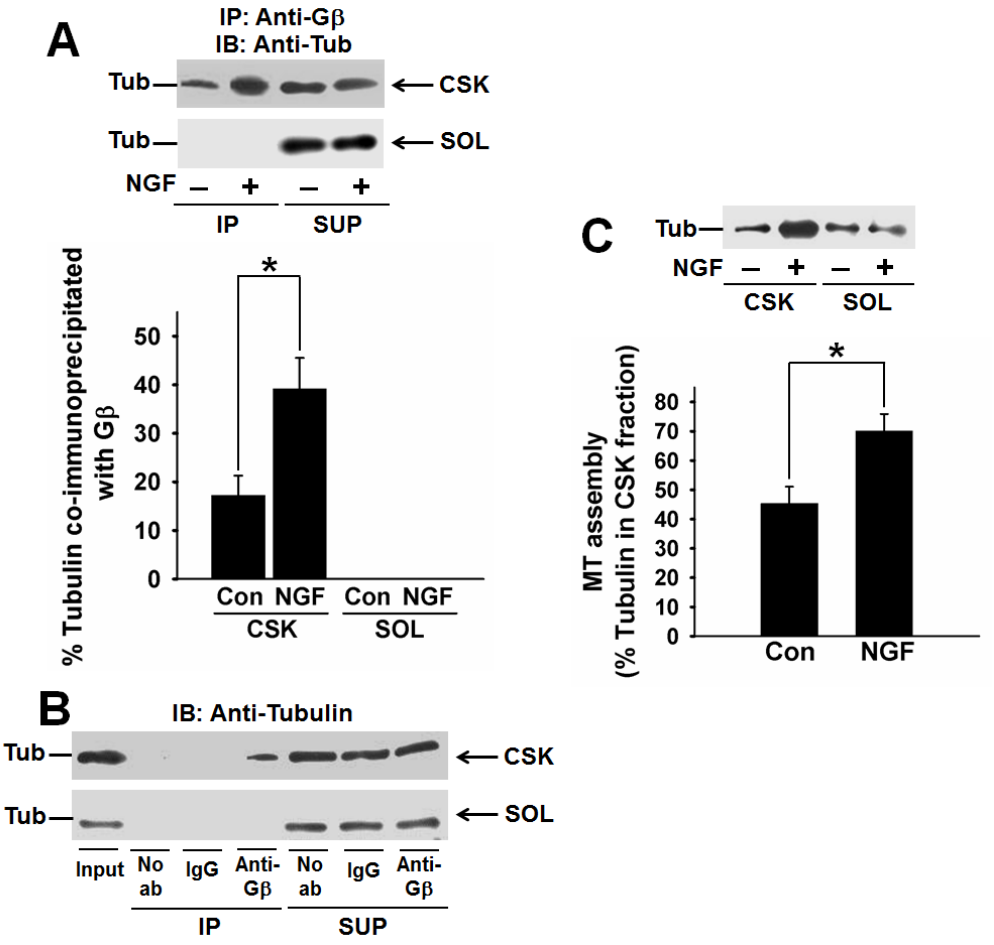

Figure 7. NGF promotes the interaction of Gβγ with MTs and stimulates MT assembly. PC12 cells were treated with 100 ng/mL of NGF for three consecutive days. Cytoskeletal (CSK) and soluble protein (SOL) fractions were prepared as described in the methods. Equal amounts of proteins from each fraction were subjected to immunoblot analysis using anti-tubulin antibody as indicated (C, top panel) or immunoprecipitation using anti-Gβ antibody followed by immunoblot analysis of immunoprecipitates (IP) and supernatants (SUP) using anti-α-tubulin antibody (A, top panel). Protein bands were detected using the ECL-plus reagent, quantitated, and expressed as a percent tubulin co-immunoprecipitated with Gβγ (A, bottom panel) or as a percent of tubulin in the CSK fraction (MT assembly) (A, bottom panel). Immunoprecipitation was also performed (in CSK and SOL from control PC12 cells) in the absence of a primary antibody (No ab), non-specific rabbit IgG (IgG), or anti-Gβ antibody followed by immunoblotting with anti-tubulin (B). A representative experiment is shown. Values shown in the histograms represent mean ± standard error of three independent experiments done in duplicates. *p values < 0.05.

The interaction of Gβγ with MTs in NGF-differentiated cells was also assessed by immunofluorescence microscopy. PC12 cells that were treated with or without NGF were examined for Gβ and tubulin immunostaining by confocal microscopy. Tubulin was detected with a monoclonal anti-tubulin (primary antibody) followed by a secondary antibody (goat-anti-mouse) that was labeled with tetramethyl rhodamine (TMR). Similarly, Gβγ was identified with rabbit polyclonal anti-Gβ followed by FITC-conjugated secondary antibody (goat-anti-rabbit), and their cellular localizations and co-localizations were recorded by laser-scanning confocal microscopy. In control cells (in the absence of NGF), Gβγ co-localized with MTs mainly in the perinuclear region (Figure 8A, a–c; see also enlargement in c'). After NGF treatment, the majority of the cells displayed neurite formation (Figure 8A, d–f). Gβγ was detected in the neurites (solid arrow, yellow) and in cell bodies (broken arrow, yellow), where they co-localized with MTs. Interestingly, Gβγ was also localized at the tips of the growth cones (Figure 8A, f), where very little tubulin immunoreactivity was observed (green arrowhead). The enlarged image of the white box in f (Figure 8A, f') indicates co-localization of Gβγ with MTs/tubulin along the neuronal process and in the central portion of the growth cone, but not at the tip of the growth cones.

In order to quantitatively assess the overall degree of co-localization between Gβγ and MTs/tubulin along the neuronal processes, an entire neuronal process was delineated as a region of interest (ROI) using a white contour (Figure 8B), and the co-localization scattergram (using ZEN 2009 software) is shown in Figure 8C, where green (Gβγ) and red (tubulin) signals were assigned to the *x* and *y* axes, respectively. Each

pixel is presented as a dot, and pixels with well co-localized signals appear as a scatter diagonal line. The average Manders' overlap coefficient (0.91 ± 0.014) suggests a robust interaction between Gβγ and tubulin along the neuronal process. The specificities of the antibodies are demonstrated in Figure 8D, where the monoclonal anti-α tubulin and the polyclonal anti-Gβ antibodies used for the immunofluorescence studies do not show any cross reactivity with other proteins in PC12 cells.

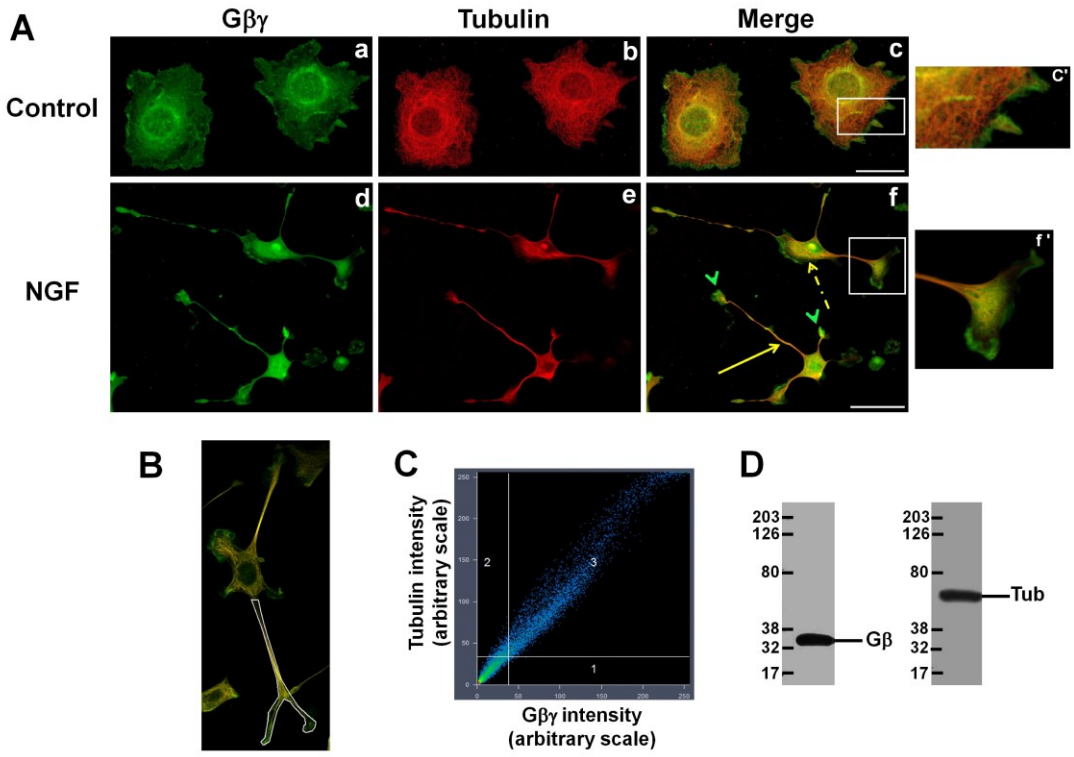

Fig. 8. Gβγ co-localizes with MTs in the neuronal processes in NGF-differentiated PC12 cells. PC12 cells were treated with and without NGF (control). (A) The cells were then fixed and double labeled with anti-tubulin (red) and anti-Gβ (green) antibodies as indicated in the methods. Areas of overlay appear yellow. The enlarged image of the white box (c) shows co-localization of Gβγ with MTs in the perinuclear region (c'). The white box on the lower panel (f') shows the enlarged growth cone, with Gβγ co-localizing with tubulin along the neuronal process and in the central portion of the growth cone, while the neuronal tips show predominant Gβγ immunostaining. The solid yellow arrow indicates neuronal processes, and the broken yellow arrow indicates cell body. The scale bars in “a–c” and “d–f” are 20 μm and 50 μm, respectively. (B) Co-localization of Gβγ with MTs in the neuronal processes was quantitatively assessed using Zeiss ZEN software. A representative image of a region of interest (neuronal process) of an NGF-differentiated PC12 cell is shown. (C) A representative scattergram depicting co-localization of Gβγ with MTs along the neuronal process is shown. (D) Representative Western blots (using PC12 whole-cell lysates) showing the specificity of the anti-Gβ (left) and anti-tubulin (right) antibodies that were used for immunofluorescence.

3.1.3. Overexpression of Gβγ in PC12 cells induces neurite outgrowth in the absence of NGF

In order to further delineate the role of Gβγ during neurite outgrowth, Gβγ was overexpressed in PC12 cells. Since previous studies indicated that Gβ1γ2 promoted MT assembly *in vitro* (Roychowdhury and Rasenick, 1997), PC12 cells were co-transfected with YFP-tagged β1 and γ2 constructs. Cells were either co-transfected with β1 and γ2, or transfected as individual constructs (Gβ1 and Gγ2). A plasmid encoding only YFP was used as control. Transfected cells were monitored for protein expression and possible neurite formation at different time points (24 h, 48 h, and 72 h), and both DIC and fluorescence images of the live cells are shown in Figure 9. We found that within 24 hours of transfection, β1γ2-transfected PC12 cells overexpressed the proteins as demonstrated by fluorescent (YFP) labeling (Figure 9A, b). DIC images indicated no changes in morphology (Figure 9A, a). At 48 h of transfection, YFP-β1γ2-transfected cells displayed neurite formation (in the absence of added NGF) (Figure 9B). Overexpressed protein (YFP-Gβ1γ2) was localized in the neurite processes (long arrows, white), growth cones (arrowhead, red), and cell bodies (short arrow, white), as shown by fluorescent (YFP) labeling (Figure 9B, d, f, h). In some cells, clear cytoskeletal labeling (arrowhead, yellow) was also observed (Figure 9A, h), which suggested localization of the protein with cytoskeletal filaments. Interestingly, we found that many of the β1γ2-overexpressing cells had a tendency to divide into two equal halves at the tips of the neurites (short arrow, yellow) (Figure 9B, g–h). After 72 h, some cells displayed complex neurite formation (Figure. 9C, i–j, long white arrows), but in many

cells the tips became enlarged (Figure 9C, k–l, dashed arrows, white), or they showed multiple, short processes (Figure 9C, m–n, short arrows, red). Control cells overexpressing only YFP did not induce neurite formation after 48 or 72 h of transfection (Figure 9D, q–t). The addition of NGF (100 ng/mL) did not have any additional effect on neurite formation in Gβγ-overexpressed cells.

Because both Gβ and Gγ constructs used in the current study were YFP-tagged, it was not possible to evaluate whether cells that displayed neurites were transfected with both subunits or not. Therefore, PC12 cells were transfected with individual constructs (Gβ1 or Gγ2, Figure10). We found that the cells transfected with either Gβ1 or Gγ2 induced neurite outgrowth (figure not shown), although the neurites appeared to be less defined and the fluorescence intensity (YFP) was found to be lower than that observed in Gβ1γ2 transfected cells (using the same microscope settings). As indicated in Figure 11, the average neurite length was also less than that observed in the presence of Gβ1γ2 overexpression.

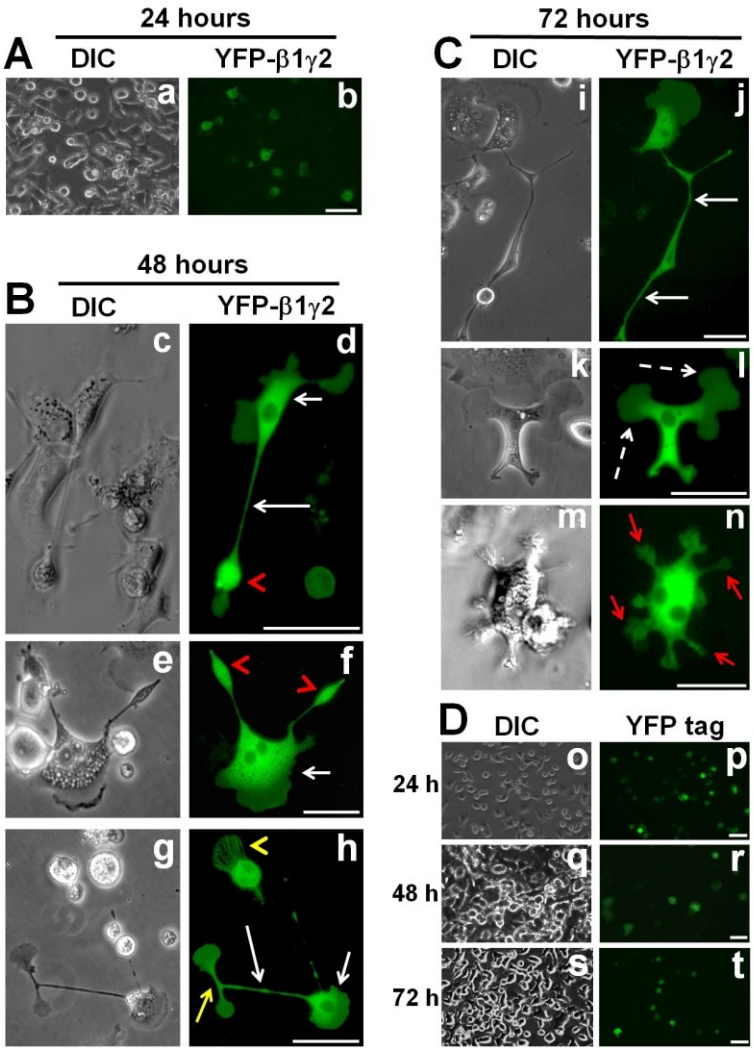

Fig. 9. Overexpression of Gβγ induces neurite outgrowth in PC12 cells. PC12 cells were co-transfected with YFP-tagged constructs encoding Gβ1 and Gγ2 (β1γ2) in the absence of NGF, using Lipofectamine LTX PLUS reagent according to manufacturer instructions. Cells overexpressing fluorescent proteins were monitored at different time points for protein expression and morphological changes using a fluorescence microscope: 24 h (A), 48 h (B), and 72 h (C). PC12 cells transfected with a plasmid-encoding YFP only was used as control (D) and were observed through the same time points. Images taken with DIC and YFP filters are shown. Neuronal processes, long white arrows; cell bodies, short white arrows; growth cones, red arrowheads; axonal branching, short yellow arrow; cytoskeletal labeling, yellow arrowhead; enlarged and bulky neurites, dashed white arrows; and multiple short processes, short red arrows. Scale bars: 50 μm in b, j, l, n, p, r, t; and 40 μm in d, f, h.

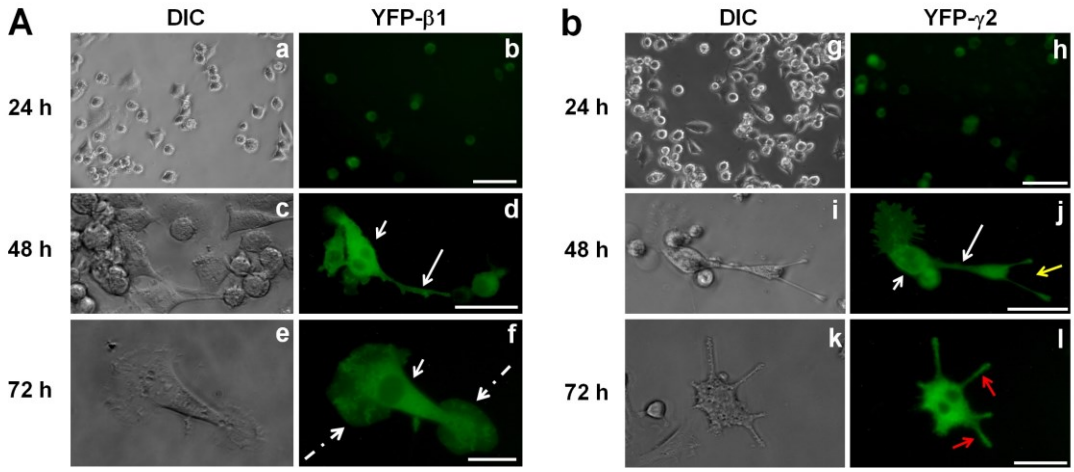

Figure 10. Transfection of PC12 cells with individual constructs (Gβ1 or Gγ2). PC12 cells were transfected with individual YFP-tagged constructs encoding Gβ1 (A) or Gγ2 (B). Cells were then monitored for protein expression and changes in morphology at different time points as indicated in the figure. DIC and YFP images are shown. Scale bars: 50 μm. Neuronal processes, long white arrows; cell bodies, short white arrows; axonal branching, short yellow arrow; enlarged and bulky neurites, dashed white arrows; multiple short processes, short red arrows.

Measurement of the number and length of neurites provides a quantitative assessment of neuronal differentiation (Harrill and Mundy, 2011). Therefore, in order to assess the effect of Gβγ overexpression on neuronal differentiation of PC12 cells, a quantitative assessment of neurite outgrowth was conducted by measuring two different parameters, average neurite length, as well as the percentage of cells bearing neurites, in Gβ1-, Gγ2-, or Gβ1γ2-overexpressing cells (Figure 11A and B). Cells co-transfected with Gβ1 and Gγ2 (42.8 ± 2.1 μm) displayed neurites that were, on average, significantly longer than those of control cells (18.4 ± 0.6 μm) and those of cells overexpressing only Gβ1 or only Gγ2 subunits (Figure 11A). Although the average neurite length in Gβγ-overexpressing cells (42.8 ± 2.1 μm) was slightly lower than that observed in NGF-differentiated PC12 cells (53.6 ± 1.8 μm), the result clearly indicates the effectiveness of Gβγ in inducing neurite outgrowth. We also evaluated the percentage of cells bearing at least one neurite in each condition. We found that ~25% of the Gβ1γ2-overexpressing cells induced at least one neurite (Figure 11B). A cell was considered neurite-bearing if it contained at least one neuronal process that was longer than the cell body (15.6 ± 0.5 μm in diameter).

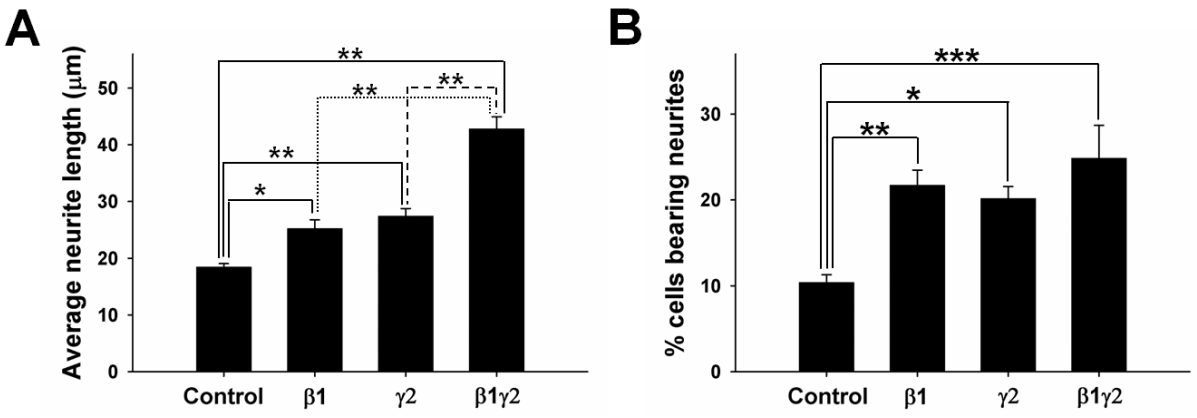

Figure 11. Quantitative assessment of neurite outgrowth in PC12 cells overexpressing of Gβ1, Gγ2, or Gβ1γ2. PC12 cells overexpressing Gβγ were fixed and processed for confocal microscopy using anti-tubulin antibody. (A) The average neurite length of Gβ1-, Gγ2-, or Gβ1γ2-overexpressing PC12 cells is shown. **p* value < 0.05; ***p value* < 0.001. (B) The percentage of cells bearing neurites in transfected cells was also estimated. **p* value < 0.05; ***p value* < 0.005; ****p value* < 0.001.

3.1.4. 3D image analysis of PC12 cells overexpressing Gβγ shows co-localization of overexpressed protein with MTs

To test the localization and association of overexpressed Gβγ (YFP-Gβ1γ2) with MTs, cells overexpressing Gβγ (48 h) were fixed and processed for confocal microscopy (Fig. 12), as was done previously with NGF-differentiated cells. Tubulin was detected with a monoclonal mouse anti-tubulin antibody followed by a secondary antibody (goat anti-mouse) that was labeled with tetramethyl rhodamine. Gβγ and MTs were visualized with high-resolution 3-D reconstructions of confocal image stacks using Volocity 3-D Image Analysis Software. Rotations performed on the deconvolved 3-D reconstruction within the software's graphical user interface allowed the transfected PC12 cells to be viewed from any direction for a more complete picture of the neuronal processes. The localization of Gβγ in neuronal processes and its association with MTs were clearly visible by panning, zooming into, and rotating the 3-D images. Bookmarking the time points at which we performed these translations of the reconstruction allowed for capture within a motion picture format (Movie 1, Supplementary Material), and for still frames from this movie to be extracted (Figure 12). MT filaments (red; Figure 12A, left panel, and Figure 12B, Frame 819) and Gβγ (green; Figure 12A, middle panel, and Figure 12B, Frame 819) interact throughout the neuronal process, as evidenced by clear yellow labeling (Figure 12B, Frame 866). Gβγ labeling (green) was also observed from all directions to be alongside yellow labeling throughout the neuronal process (Figure 12B, Frames 499, 669, 786, 819, and 866). In some areas, red labeling was also clearly visible. This labeling pattern appears to support our *in vitro* results, which

indicate that Gβγ binds on the microtubule wall when promoting MT assembly (Roychowdhury and Rasenick, 1997). These results are consistent with the possibilities that the yellow labeling we observe in neurites marks domains on Gβγ that interact with MT filaments and that the green labeling represents Gβγ domains that are not interacting directly with MTs but are projecting from MT walls. These possibilities notwithstanding, it is reasonable to suggest on the basis of this unique labeling pattern as well as previous *in vitro* results (Roychowdhury and Rasenick, 1997) that Gβγ induces neurite outgrowth through its ability to interact with tubulin/MTs and stimulate MT assembly.

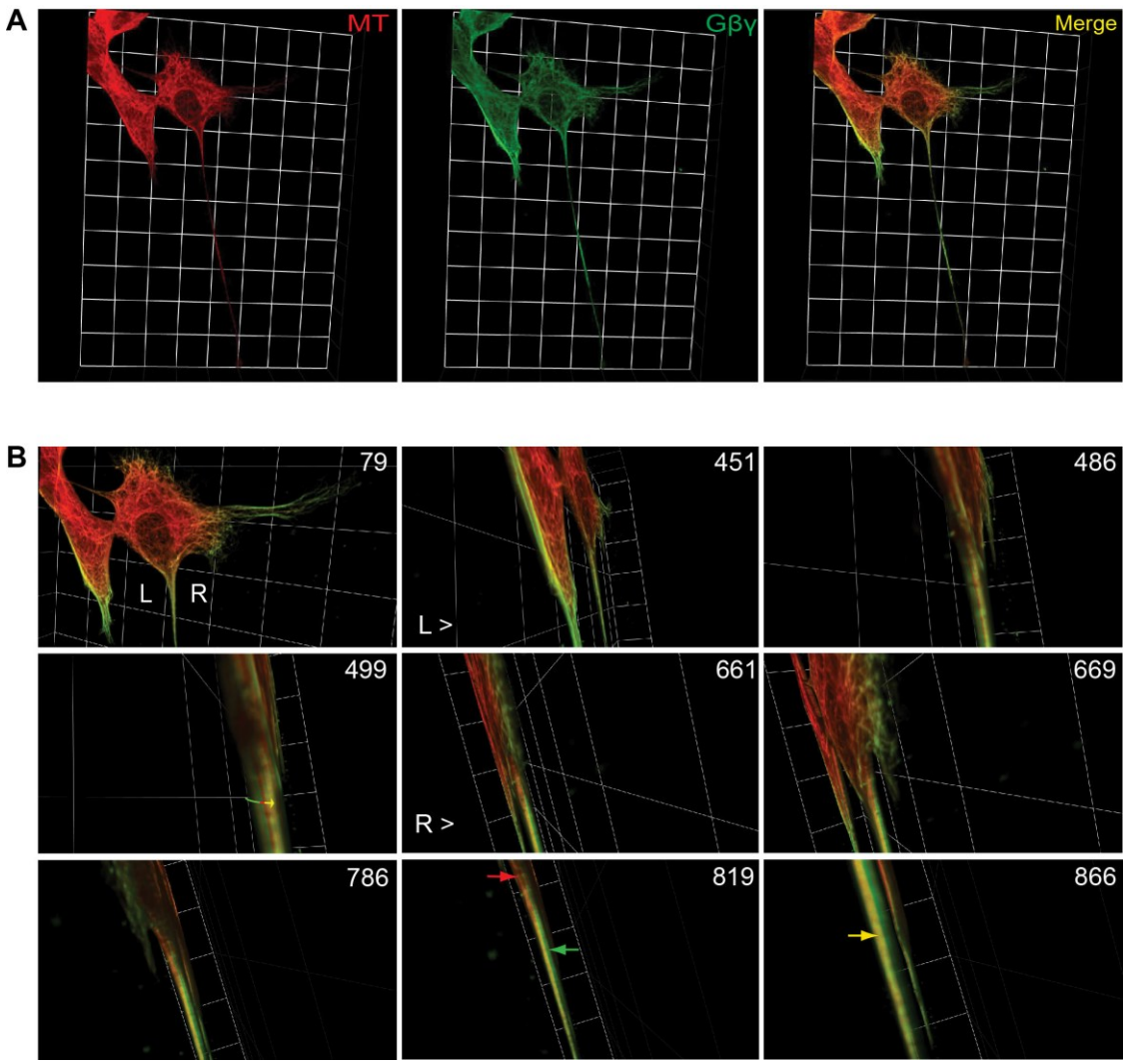

Figure 12. 3-D view of co-localization of Gβγ and microtubules (MTs). Co-localization of overexpressed Gβγ (green) with MTs (red) as visualized by high-resolution 3-D confocal images using Volocity software (see Methods). The images shown in this assembly are still frames from Supplementary movie 1 (Supplementary materials). (A) A still frame from the movie separated into its component channels: MT (red) and Gβγ (green) expression are each confined discretely to similar subcellular locations as shown in the merged panel (yellow). (B) Representative still frames were selected to summarize the content of the movie. The numbers on the top right of each still image denote the frame numbers within the movie. Arrows in frame 819 correspond to MT expression (red, top arrow) and Gβγ (green, bottom arrow) expression. The arrow in frame 866 points to co-localization of MT and Gβγ (yellow). The edges of each individual square in the background grid for each image are 19.21 μm in length.

3.1.5. Gβγ interacts with MTs in hippocampal and cerebellum neurons in cultures from rat brain

Although PC12 cells have been used extensively to study the mechanism of neuronal outgrowth and differentiation, neurons are more complex and give rise to a “dendritic tree” and an axon that may branch hundreds of times before it terminates. The axon terminal contains synapses, which are specialized structures that release neurotransmitters in order to communicate with target neurons. Thus, neurons are capable of interacting with one another to form the complex neuronal networks necessary for the processing and transmission of cellular signals. To precisely identify the role of Gβγ-MTs interactions in neuronal morphology and functioning, it is important to demonstrate whether or not this interaction occurs in neurons. Therefore, as a first step we established neuronal primary cultures from newborn rat brains, specifically from the cerebellum and hippocampus. These brain regions were selected because they have been extensively validated as cell-culture models for studying the role of the cytoskeleton in neuronal polarity and axonal development (Dotti et al., 1988; Powell et al., 1997; Tahirovic and Bradke, 2009). In addition, these two brain regions are associated with different functions. While the hippocampus is involved in memory formation and neural plasticity, the cerebellum is primarily responsible for motor control, posture, and balance (Purves et al., 2008; Koehl and Abrous, 2011).

As described for PC12 cells, confocal microscopy, subcellular fractionation, and co-immunoprecipitation analysis were performed to determine the co-

localization/interactions of Gβγ with MTs in hippocampal and cerebellar neurons. We found that Gβγ co-localizes very intensely with MTs in the neuronal processes in hippocampal neurons (Figure 13A, panels c and c'). Co-immunoprecipitation analysis using CSK and SOL fractions indicates that Gβγ interacts with both MTs and soluble tubulin (Figure. 13B). In cerebellar neurons, both confocal microscopy (Figure 13C) and co-immunoprecipitation analyses (Figure 13D) indicate a weak association of Gβγ with MTs. Since Gβγ appears to interact with MTs/tubulin preferentially in hippocampal neurons, it is possible that Gβγ could be involved in regulating neurite outgrowth and synapse formation by modulating MT assembly in hippocampal neurons.

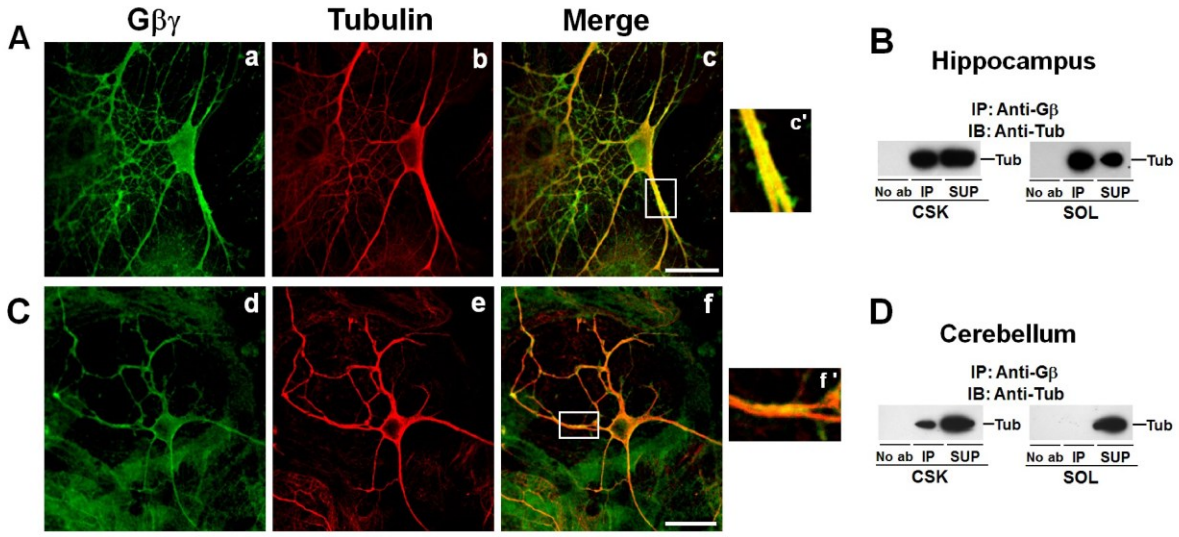

Figure 13. Gβγ interacts with MTs in primary hippocampal and cerebellar neurons. Neuronal primary cultures from rat brain hippocampus and cerebellum were prepared as described in section 2.13. Hippocampal and cerebellar neurons were then either processed for confocal microscopy (A, C) or subcellular fractionation followed by co-immunoprecipitation analysis (B, D). The enlarged view of the white boxes (c', f') depicts Gβγ-tubulin co-localization in the neuronal process in hippocampal and cerebellar neurons. The scale bar is 20 μm. CSK and SOL fractions from hippocampal and cerebellum neurons were subjected to co-immunoprecipitation using anti-Gβ antibody or no antibody (No ab) followed by immunoblotting using anti-tubulin (B, D) antibody.

3.1.6. Gβγ interacts with actin filaments, and this interaction increases during neuronal differentiation

In addition to MTs, neuronal outgrowth is also dependent on actin filaments. Interactions between these two cytoskeletal filaments are also important for growth-cone motility and neurite outgrowth (Griffith and Pollard, 1982; Witte and Bradke, 2008; Geraldo and Gordon-Weeks, 2009). Moreover, axon branching, which requires the interactions between MTs and actin filaments (Griffith and Pollard, 1982), was observed in Gβγ-overexpressing PC12 cells (Figure 9, g-h), suggesting a possible involvement of Gβγ in MT-actin filaments coupling. Therefore, we investigated whether Gβγ, in addition to MTs, also interacts with actin filaments.

The experimental strategy was similar to that employed to study the interaction of Gβγ with MTs, using confocal microscopy, co-immunoprecipitation, and immunoblotting. Our results indicate Gβγ was localized at the tips of neuronal processes/growth cones in both Gβγ-overexpressing and NGF-differentiated PC12 cells (Figure 8c' and 8f'), where actin filaments are also known to be localized and form filopodia and lamellipodia. Using triple immunofluorescence labeling and confocal microscopy, we assessed the co-localization among Gβγ, MTs, and actin filaments (Figure 14A, a–f). Tubulin and Gβγ were labeled as previously indicated, and actin was labeled with goat polyclonal anti-actin followed by an Alexa Fluor 350-conjugated donkey anti-goat secondary antibody. We found that in NGF-treated cells, Gβγ (green, a) was found in cellular processes induced by NGF (white arrows), where it co-localized with tubulin (red, b) and actin-

containing structures (blue, c). However, as anticipated, at the tips of these processes, Gβγ (green arrowheads), as well as actin labeling (blue) was observed where they co-localized (e). The co-localization is clearly visible in the enlarged images of the white box (Figure 14A, d', e', and f').

We also investigated whether Gβγ interacts with actin filaments using co-immunoprecipitation analysis. CSK and SOL fractions were isolated, as shown in Figure 14. Unlike tubulin, Gβγ was found to interact with both AFs (CSK) and actin monomers (SOL) (Figure 14B). However, the interaction of Gβγ with AFs (but not actin monomers) increased by ~100%, from 25 ± 3.3% in control cells, to 52.4 ± 10.1% after NGF treatment (Figure 14C). Actin polymerization was not affected significantly after NGF treatment (figure not shown). The possibility that Gβγ interacts with actin filaments through MTs was ruled out by the observation that the interactions of Gβγ with AFs were not inhibited by the MT depolymerizing drug, nocodazole (Figure 14D). In fact, Gβγ interactions with AFs increased from ~25% to 35% in the presence of 10-μM nocodazole.

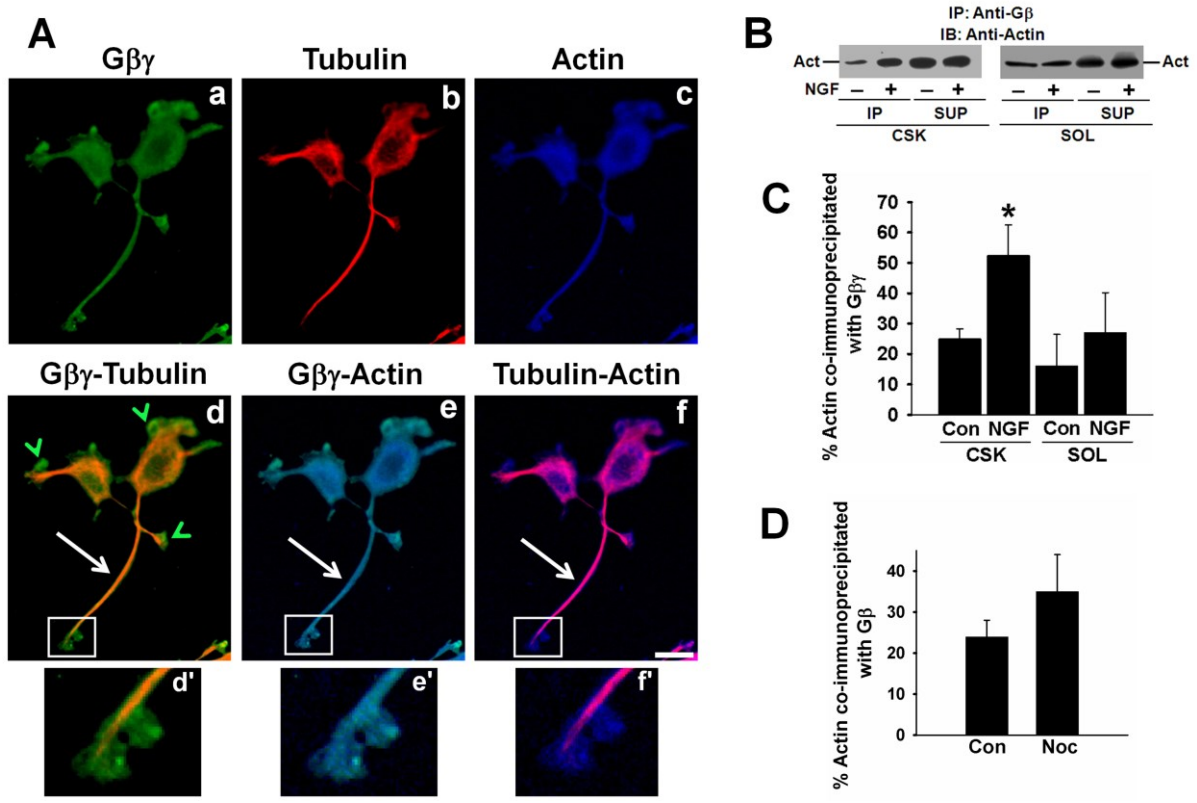

Figure 14. Gβγ interacts with actin filaments in NGF-differentiated PC12 cells. A) NGF-treated PC12 cells were labeled with anti-Gβ (green), anti-tubulin (red), and anti-actin (blue) primary antibodies (A, upper panel, a-c) as previously described. Co-localization patterns are shown in the lower panel (d-e). Insets in the lower panel show co-localization patterns at the tip of neuronal process (d'-f)'. B) PC12 cells were treated with NGF for 3 days and subjected to fractionation (CSK and SOL), followed by immunoprecipitation with anti-Gβ antibody and immunoblotting against actin. C) The interaction of Gβγ with actin is shown in the graphic and it is expressed as percent actin co-immunoprecipitated with Gβγ in the presence and absence of NGF. *p value < 0.05. D) PC12 cells were treated with 10 μM nocodazole for 4 hours, and whole cell lysates were prepared and subjected to co-immunoprecipitation using Gβ antibody. The histogram shows percent actin co-immunoprecipitated with Gβγ in the presence and absence of nocodazole.

3.1.7. Gβγ interacts with actin filaments in neuronal primary cultures of rat brain hippocampus and cerebellum

The interaction of Gβγ with AFs in primary cultures from hippocampal and cerebellar neurons was also studied, using subcellular fractionation, co-immunoprecipitation, and confocal microscopy. Confocal microscopic analysis indicated co-localization of Gβγ with actin filaments in cell bodies and neuronal processes both in hippocampal and cerebellar neurons (Figure 15E and G). In hippocampal neurons, Gβγ was found to interact with actin in the CSK fraction, while no Gβγ-actin interaction was detected in the SOL fraction, suggesting a preferential association of Gβγ with polymerized actin. In cerebellar neurons, Gβγ was found to interact with both AF and actin monomers (Figure 15H).

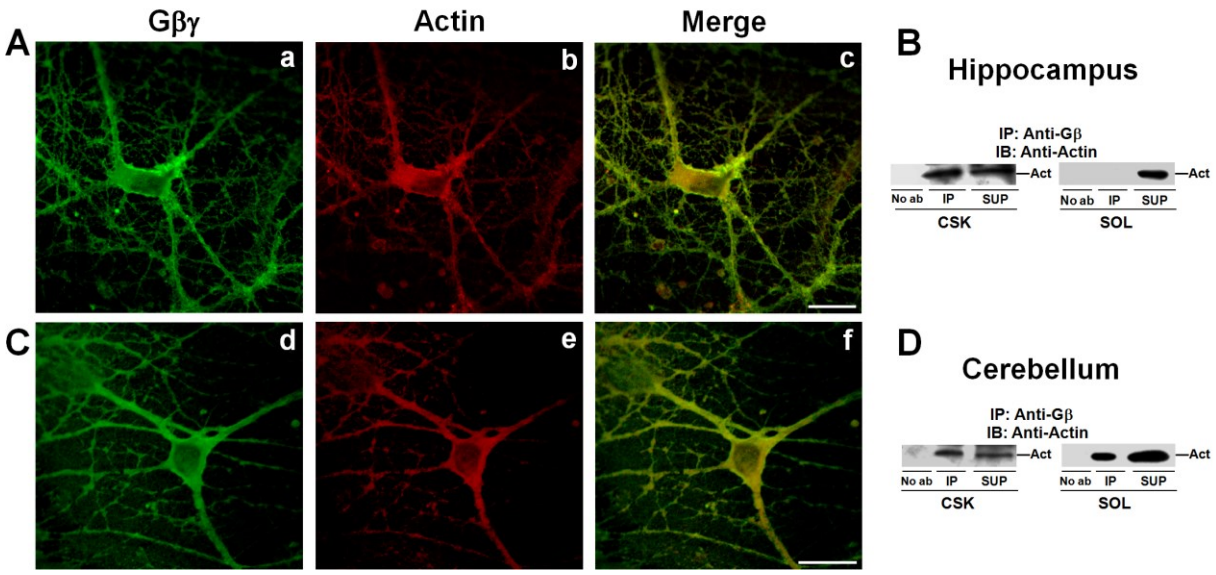

Figure 15. Gβγ interacts with actin filaments in hippocampal and cerebellar neurons. Neuronal primary cultures from rat brain hippocampus and cerebellum were prepared as described in section 2.13. Hippocampal and cerebellar neurons were then either processed for confocal microscopy (A, C) or subcellular fractionation followed by co-immunoprecipitation analysis (B, D). The scale bar is 20 μm. CSK and SOL fractions from hippocampal and cerebellum neurons were subjected to co-immunoprecipitation using anti-Gβ antibody or no antibody (No ab) followed by immunoblotting using anti-actin (A, C) antibody.

3.2. Specific Aim 2: Determine if blocking the interactions between Gβγ and MTs alters MT organization and inhibits neurite outgrowth

3.2.1. Objective and Overview

Since the molecular pathways leading to neurodegeneration are not well understood, and given that no effective drugs against neurodegenerative diseases are currently available, the goal of this aim was to understand whether blocking the Gβγ-MT interaction can disrupt neuronal differentiation and trigger an early stage of neurodegeneration by altering MT assembly in neuronal cells. Two experimental strategies were used to address this specific aim. First, we used a Gβγ-sequestering peptide (GRK2i), in order to shut down Gβγ-mediated signaling. Second, we employed PMPMEase inhibitors developed by our collaborator (Dr. N. Lamango, Florida A&M University). PMPMEase is a critical enzyme in the protein prenylation pathway, and these inhibitors were used in an attempt to target the prenylation and further carboxy-terminal processing by methylation of the γ subunit of Gβγ, since this modification has previously been shown to be critical for its interaction with MTs. PC12 cells, hippocampal neurons in culture, and SH-SY5Y cells were used as cell models for our studies.

3.2.2. GRK2i, a Gβγ-sequestering peptide, disrupts MT organization and inhibits neurite outgrowth

In an attempt to block the Gβγ-MT interaction, and to better understand the role of Gβγ in MT organization and neurite outgrowth, we used a synthetic G protein-coupled receptor kinase 2 (GRK2) inhibitory peptide, known as GRK2i. Gβγ is known to modulate the activity of several signal-transducing effector molecules, including GRK2 (Claing et al., 2002). GRK2i corresponds to the Gβγ-binding domain of GRK2 and selectively prevents Gβγ-mediated signaling and has therefore been used as a valuable tool for understanding Gβγ-dependent functions (Koch et al., 1994; Lodowski et al., 2003). As indicated in Figure 16A (e–h), in the presence of 5 μM GRK2i, neurite damage (enlarged images f', g', and h'), as well as MTs and Gβγ aggregation (enlarged images f'', g'', h''), was observed. In addition, cellular aggregation was also frequently observed in the presence of GRK2i. Images shown here were taken after 60 min of incubation with GRK2i. GRK2i at 1 μM did not have any significant effect on neuronal differentiation (images not shown).

The effect of GRK2i on neuronal differentiation, neurite outgrowth was quantitatively assessed by measuring average neurite lengths as well as the percentage of cells bearing neurites (Figure 16B and C). A cell was considered as neurite-bearing if it contained at least one neuronal process that was longer than the cell body (13.7 ± 0.5 μm in diameter). As indicated in Figure 16B and C, the percentage of cells bearing neurites was reduced significantly, from 38.1 ± 3.1% in control cells to 22.8 ± 3.1% after

30 min of incubation with GRK2i, and did not reduce further after 60 min of incubation. The average neurite length of surviving neurites decreased modestly in the presence of GRK2i and increasing the incubation time from 10 min to 60 min did not have any additional effect, suggesting that NGF-induced neurites are not equally susceptible to $G\beta\gamma$ sequestration.

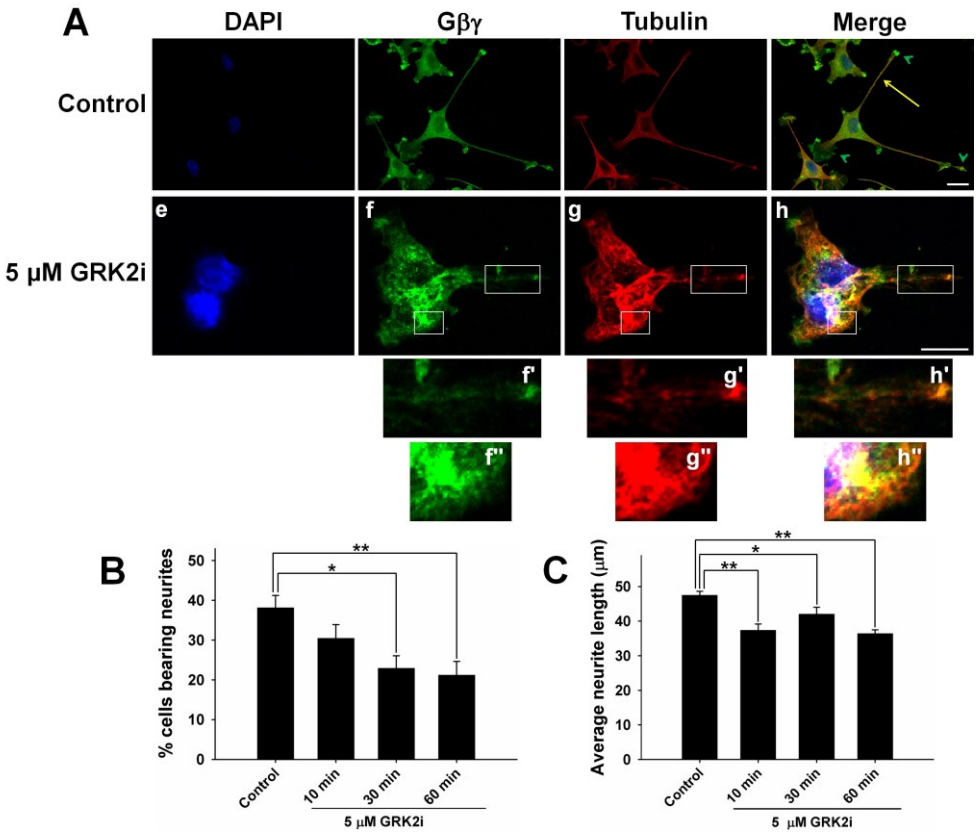

Figure 16. GRK2i, a Gβγ-blocking peptide, disrupts MT and Gβγ organization and inhibits neurite outgrowth. PC12 cells were treated with 100 ng/mL of NGF for two consecutive days. Subsequently, 5 μM GRK2i was added to the media, and the cells were incubated for 10, 30, and 60 min. The cells were then fixed and double labeled with anti-tubulin (red) and anti-Gβ (green) antibodies, and processed for confocal microscopy. DAPI was used for nuclear staining (blue). (A) Control cells exhibit typical morphology, displaying multiple long neurites. Gβγ is shown to co-localize with tubulin/MTs along the neurites (solid yellow arrow) but not at the tip of the neurites (green arrowheads), where Gβγ immunostaining is predominant. Inhibition of Gβγ signaling by incubation with GRK2i causes neurite damage, microtubule disruption, and alters the Gβγ-tubulin co-localization pattern, as shown in the enlarged images in the white boxes (f'–h', and f''–h''). Scale bars are 20 μm. (B–C) PC12 cells were treated with NGF and GRK2i as described above, followed by fixing and processing for confocal microscopy as described previously. Using Zeiss ZEN software, neurites were traced and measured, and average neurite length and percent of cells bearing neurites were determined. Differences between experimental conditions were assessed by one-way ANOVA. *$p < 0.05$; **$p < 0.01$.

3.2.3. Inhibitors of PMPMEase disrupt MTs and Gβγ organization and inhibit neurite outgrowth of NGF-differentiated PC12 cells

In order to determine whether PMPMEase may play a regulatory role in the Gβγ-dependent regulation of MTs and neurite outgrowth, we used two PMPMEase inhibitors (L-23 and L-28) in this study to determine whether this enzyme may play a regulatory role in the Gβγ-dependent regulation of MTs and neurite outgrowth. PC12 cells were treated with the PMPMEase inhibitors (L-23, L-28, or the prototypical molecule PMSF), and then allowed to differentiate in the presence of NGF for two consecutive days. At 1-μM concentration, the inhibitors did not have any noticeable effect on neurite outgrowth, while both 5- and 10-μM inhibitors did affect neurite outgrowth (Figure 17). As indicated in the figure, while neuronal outgrowth was not affected by PMSF (10 μM) (Figure 17A, a–d), both L-23 and L-28 had significant effects on neuronal differentiation, as indicated by axonal damage (Figure 17A, e–h; see the enlarged image in the box), and on inhibition of neurite outgrowth (Figure 17A, i–l), which altered the MTs and Gβγ organization. Cellular aggregation was also evident in the presence of 10 μM L-23 and L-28. As indicated in Figure 17A, m–p, Gβγ was concentrated in the cell-cell contact region (clearly visible in the enlarged box) in the presence of 10 μM L-28 and could be responsible for mediating cellular aggregation.

The effects of L-23 and L-28 on neuronal outgrowth were also assessed quantitatively by measuring average neurite lengths as well as the percentage of cells bearing neurites as was done previously in the presence of GRK2i. As indicated in

Figure 17B and C, the percentage of cells bearing neurites was reduced significantly in the presence of 5 or 10 μM L-23 and L-28, with L-28 at 10 μM being the most potent. The average neurite length of surviving neurites was also modestly decreased in the presence of L-23 and L-28. Once again, L-28 at 10 μM appeared to be the most potent in inhibiting neurite outgrowth. The result indicates that a population of NGF-differentiated cells is not affected by PMPMEase inhibitors.

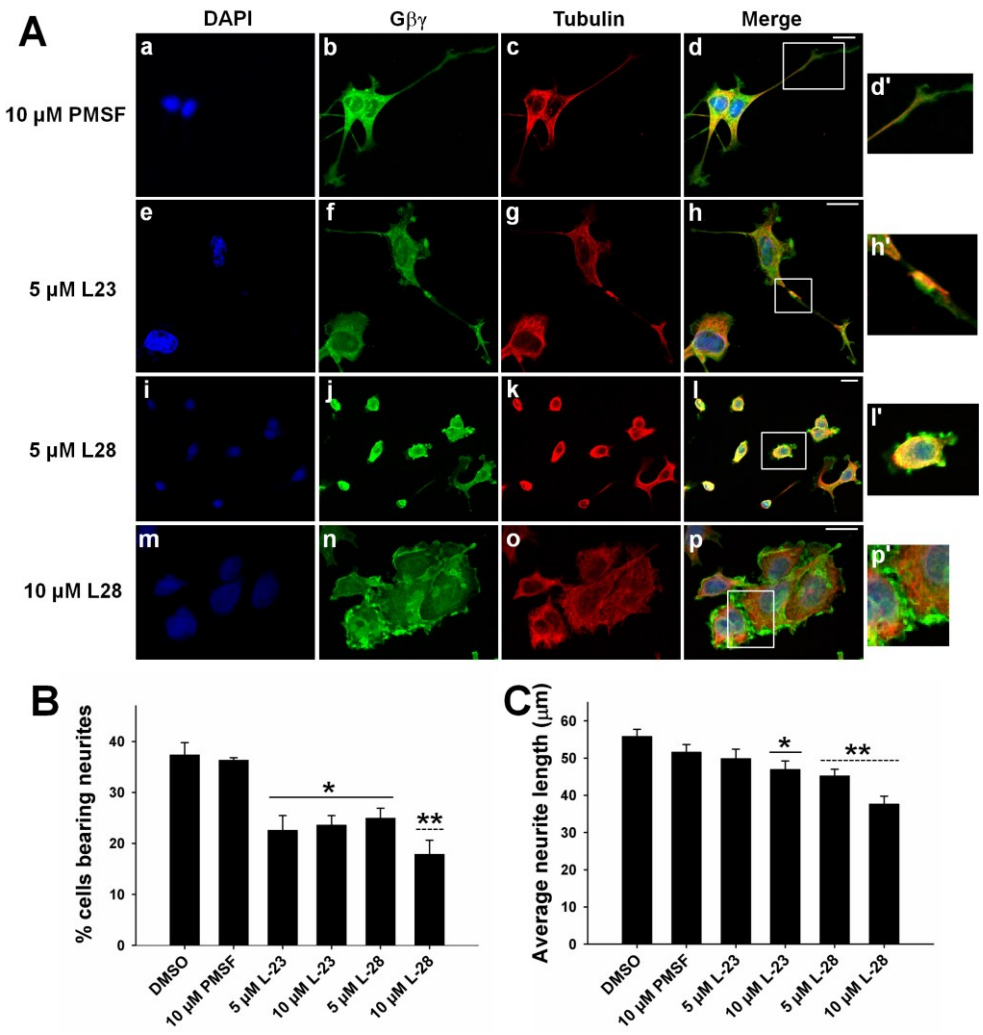

Figure 17. PMPMEase inhibitors disrupt neurite outgrowth of NGF-differentiated PC12 cells. PC12 cells were treated with PMPMEase inhibitors, L-23 (5 μM), and L-28 (5 μM, and 10 μM), or the prototypical molecule PMSF (10 μM) and allowed to differentiate in the presence of 100 ng/mL of NGF for two consecutive days. (A) Cells were then fixed and double labeled with anti-tubulin (red) and anti-Gβ (green) antibodies, and DAPI was used for nuclear staining (blue). Co-localization patterns are also shown in the merged images. PMSF did not seem to have any significant effects on neuronal morphology (a–d). PMPMEase inhibitors inhibited neurite outgrowth of NGF-treated PC12 cells, causing axonal damage (e–h, enlarged image shown in h'), neurite shortening (i–l, enlarged image shown in l'), and cellular aggregation (m–p). Scale bars are 20 μm (B–C). Using Zeiss ZEN software, neurites were traced and measured, and the average neurite length and percent of cells bearing neurites were estimated. The differences between experimental conditions were assessed by one-way ANOVA. *$p < 0.05$; **$p < 0.01$.

3.2.4. Inhibitors of PMPMEase and GRK2i peptide do not cause cell death in PC12 cells

To determine if the GRK2i peptide or PMPMEase inhibitors L-23 or L-28 induced neuronal cell death at the concentrations used, a previously described differential nuclear staining (DNS) assay (Lema et al., 2011) was performed as described in section 2.14. Briefly, PC12 cells were grown on 96-well plates and incubated with NGF and inhibitors as indicated, followed by 1 h incubation with a mixture of Hoechst/propidium iodide (PI). Hoechst has the ability to cross cell membranes of both healthy and dead cells and to stain nuclear DNA, thus providing the total number of cells, whereas PI is only able to stain cells having a loss of plasma-membrane integrity, thus denoting the number of dead cells. Subsequently, cells were imaged in live mode using a BD Pathway 855 Bioimager system as described in the methods section. Representative images corresponding to the same section of 2 x 2 image montages from several conditions (a–l) are shown (Figure 18A). The percentage of dead cells in the presence of inhibitors was determined by using the BD AttoVision v1.6.2 software (BD Biosciences), and the result was plotted as shown in Fig. 18B and C. As indicated in the figure, GRK2i did not cause cytotoxicity on NGF-differentiated PC12 cells. In the case of the PMPMEase inhibitors L-23 and L28, no significant cell death was detected at the tested concentrations. The prototypical compound, PMSF, was also assayed and not found to be cytotoxic. Hydrogen peroxide (100 μM) was used as a positive control.

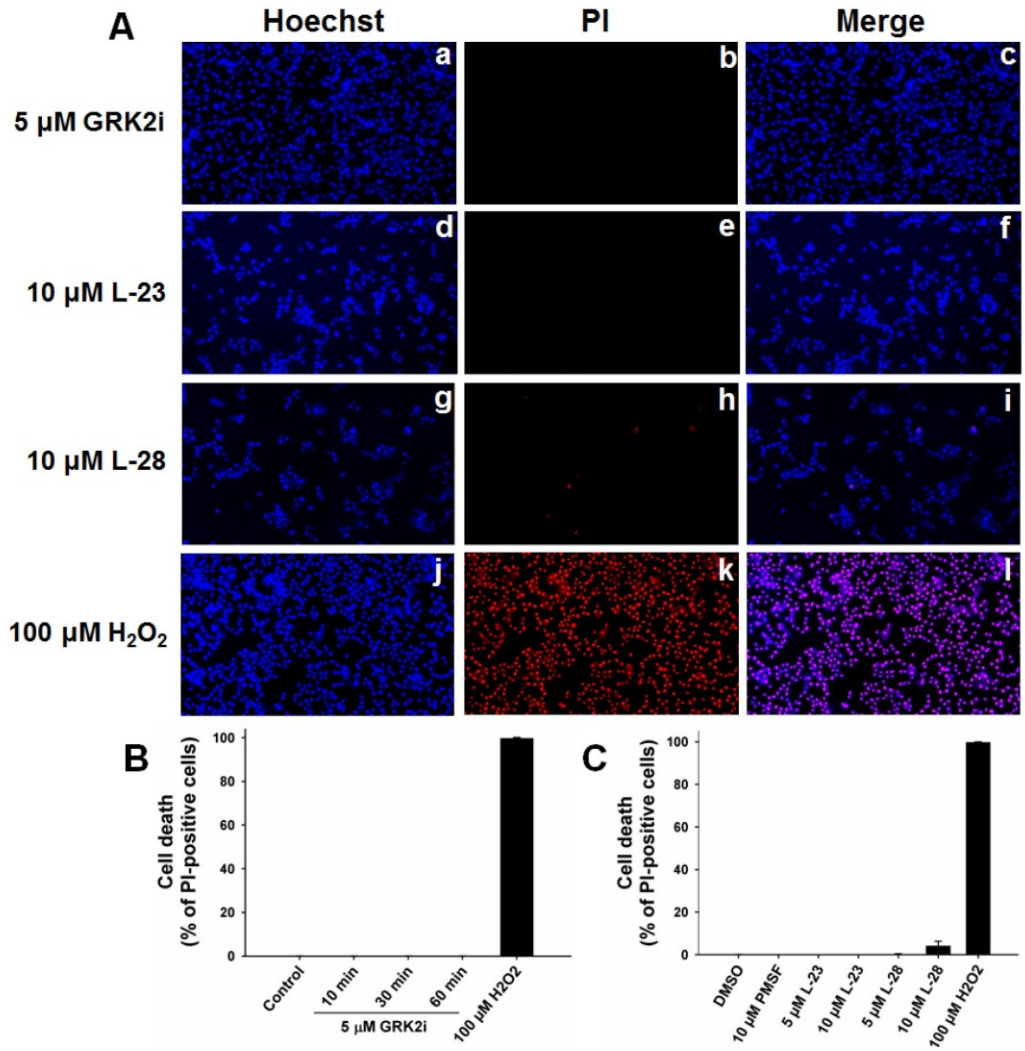

Figure 18. Inhibitors of PMPMEase and GRK2i do not induce neuronal cell death. PC12 cells were grown on 96-well plates and treated with NGF and inhibitors as indicated in methods. Subsequently, cells were incubated with a Hoechst/PI mixture for DNS cytotoxicity assay. The images were captured in live-cell-image mode using the confocal automated microscope BD Pathway Bioimager system and a 10x objective, assisted with AttoVision software. (A) Representative images corresponding to the same section of 2 x 2 image montages from several conditions (a–l) are shown. H_2O_2 (100 μM) was used as a positive control. Cell nuclei stained with Hoechst provided the total number of cells; cell nuclei stained with PI indicate the number of dead cells; merged Hoechst and PI images indicate the number of dead cells in the image. (B-C) Cell death was plotted as the percent of PI-positive cells, denoting the total number of dead cells for each condition.

3.2.5. Inhibition of PMPMEase blocks the interaction of Gβγ with MTs and induces degeneration of SH-SY5Y neuroblastoma cells

The effect of inhibitors of PMPMEase was also tested in human neuroblastoma SH-SY5Y cells, a cell line that has been used as a model to study neuronal differentiation and function (Xie et al., 2010). Both confocal microscopic analysis and co-immunoprecipitation was performed to conduct the study.

For confocal microscopic analysis, SH-SY5Y cells were attached to chambered slide and treated with DMSO, PMSF (100 μM), L-23 (100 μM), or L-28 (10 μM) for 24 hours. The slides were then fixed and processed for confocal microscopy as described before. Cells were immunolabeled for MTs (red) and Gβ (green), and DAPI was used for nuclear staining. As shown on Figure 19A (a-d), control cells (treated with DMSO) displayed typical morphology, with many cells forming neurites (white arrows), and depicting Gβγ co-localizing with MTs along these processes. The prototypical molecule, PMSF (100 μM), does not seem have dramatic effects on cell morphology, as cells still display neurites (Figure 19A, white arrows, e-h). Cells treated with 100 μM L-23 did not seem to cause significant effects, although cells appear to be more aggregated than control and PMSF-treated cells (Figure 19A, i-l). In the presence of L-28 (10 μM), significant cellular damage was evident. Cellular aggregation was very prominent, and neurites seem to be completely disrupted. Localization and co-localization of Gβγ and MTs was also affected (Figure 19A, m-p).

To test whether inhibition of PMPMEase activity alters the interaction of Gβγ with MTs, SH-SY5Y cells were treated with 5 μM L-28 for 24 h followed by subcellular fractionation. We found that L-28 completely abolished the interaction of Gβγ with MTs (CSK fraction), as demonstrated by co-immunoprecipitation analysis (Figure 19B and C). As found earlier, Gβγ did not form a complex with tubulin dimer (SOL fraction), and L-28 did not alter this (figure not shown). Thus, it appears that blocking the prenylation and carboxy-methylation of Gβγ in SH-SY5Y cells disrupted the Gβγ-MT interaction, supporting a critical role of Gβγ prenylation in the regulation of MT assembly, as previously suggested by *in vitro* findings (Roychowdhury and Rasenick, 1997). Taken together, the biochemical and confocal microscopy results indicate that inhibition of PMPMEase blocks the interaction of Gβγ with MTs, disrupting cellular morphology and inducing neurodegeneration of SH-SY5Y cells.

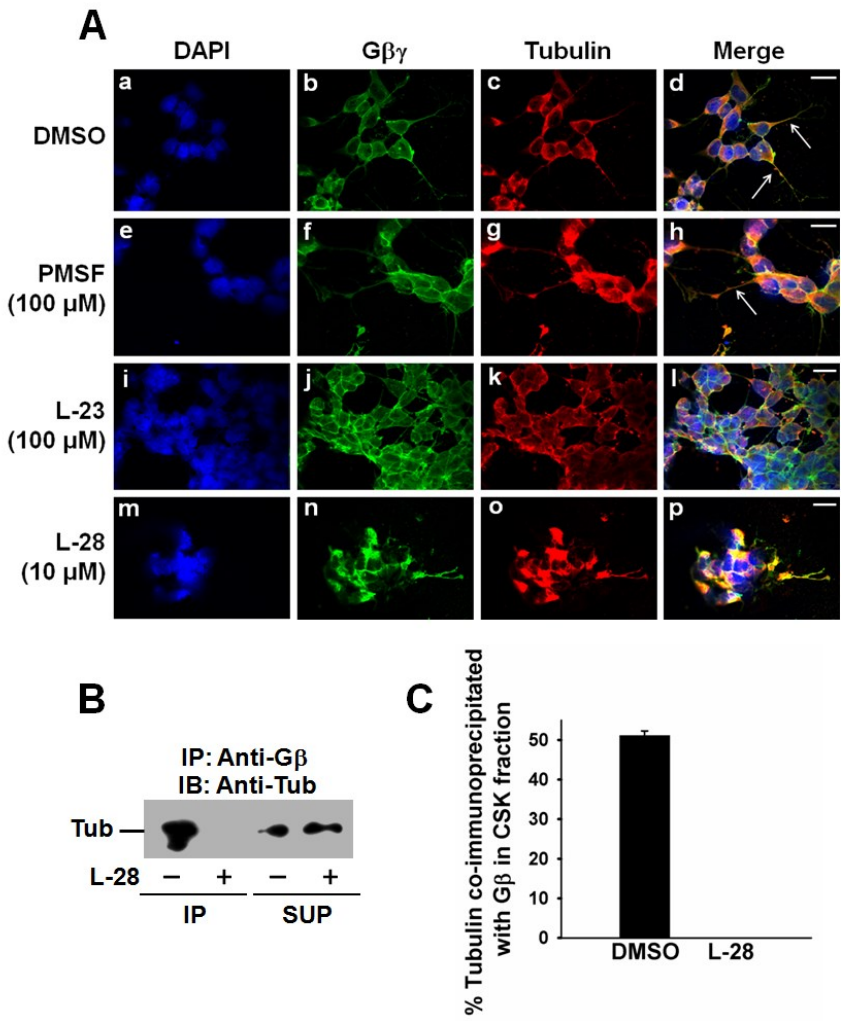

Figure 19. Inhibitors of PMPMEase block the interaction of Gβγ with MTs and cause Gβγ and MT disruption, and cellular aggregation of SHSY5Y neuroblastoma cells. (A) SH-SY5Y cells were treated with PMPMEase inhibitors as indicated, and fixed and processed for confocal microscopy. Gβγ and MTs were detected with FITC (green) and TMR (red) secondary antibodies, and DAPI was employed for nuclear staining. Co-localization patterns are shown in the merged images. Arrows indicate the presence of neurites. Scale bars in d, h, l, and p are 20 μm. (B-C) SH-SY5Y cells were treated with L-28 (5 μM for 24 h), and CSK and SOL fractions were prepared. CSK fractions were subjected to co-immunoprecipitation using anti-Gβ antibody, followed by immunoblotting of IP and SUP samples with anti-tubulin antibody (left panel). The interaction of Gβγ with MTs is expressed as percent tubulin co-immunoprecipitated with Gβ in the CSK fraction (right panel).

3.2.6. PMPMEase inhibitors cause neurite damage and alter the Gβγ/MT organization in hippocampal neurons

While PC12 and SH-SY5Y cells are two widely used and validated models to study neuronal differentiation, function, and degeneration, these cells do not possess the entire set of features that characterize neuronal cells. Thus, the effect of PMPMEase inhibitors was tested primary cultures from rat brain hippocampus. Fully differentiated hippocampal primary neurons (7 days in culture) were treated with inhibitors (L-23 and L-28) and subjected to immunoflorescence labeling and confocal microscopic examination. Control cells display typical neuronal morphology, with long axonal processes extending from the cell body (Figure 20, a-c). Gβγ localizes both in the cell body and neurites, where it co-localizes with MTs (see enlarged box, c'). In L-23 and L-28 treated cells, the overall cellular integrity was affected (Figure 20, d-i). Damage to the neurites was evident, and alteration of the Gβγ/MTs co-localization was observed. Cells treated with L-23 and L-28 (see enlarged boxes, f' and i') exhibited aggregation of proteins along the neurites, suggesting cytoskeletal damage, which could also be an indicator of degeneration of hippocampal neurons.

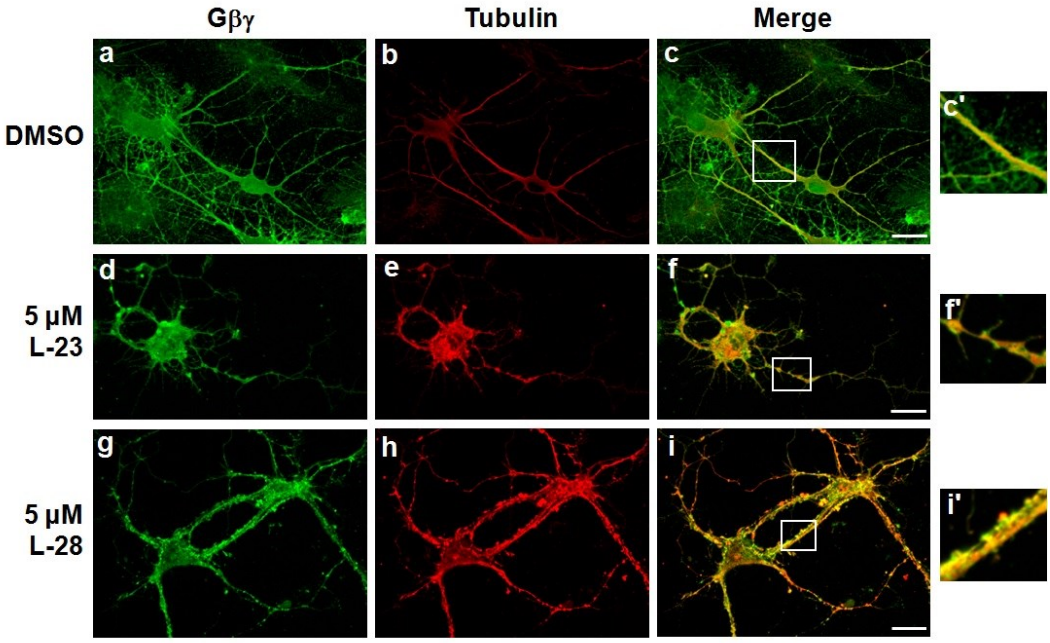

Figure 20. L-23 and L-28 disrupt neuronal cell morphology and alter MTs/Gβγ localization/co-localization in hippocampal primary neurons. Primary cultures of hippocampal neurons were prepared from brains of postnatal day (1-2) Sprague Dawley rats. Neurons were seeded on pre-coated glass coverslips and used for immunofluorescence labeling and confocal microscopy. The localization of microtubules (mouse monoclonal anti-α tubulin, red) and Gβγ (rabbit polyclonal anti-Gβ, green) was visualized by confocal microscopy. Primary neurons were kept in culture for 7 days (to allow full neuronal differentiation) and then treated for 24 hours with either DMSO (controls), 5 μM L23, and 5 μM L28.

3.2.7. Knockdown of Gβ1 using siRNA appears to affect the cellular levels of tubulin

In a further attempt to disrupt the Gβγ-MT interaction, we used siRNA technology to knockdown the expression of Gβ PC12 cells. Since previous studies from our laboratory demonstrated that Gβ1γ2 binds to MTs and promotes MT assembly, we targeted the specific Gβ1 isoform for knockdown. Given that PC12 cells are derived from rat, the siRNAs were specifically designed to target rat Gβ1. Cells were transfected with a pre-designed pool of siRNAs, and the knockdown was assessed by immunoblotting.

The results show that two concentrations of siRNA (50 and 100 nM) were effective in completely abolishing Gβ1 expression (Figure 21). When the total levels of Gβ were assessed, no significant decrease in protein expression was detected. Interestingly, the levels of tubulin appear to be affected by the knockdown of Gβ, since we found that tubulin expression seems to decrease after transfection of PC12 cells with 100 nM Gβ1 siRNA. This result further supports the notion that Gβγ is a critical player in the regulation of the MT cytoskeleton. The levels of actin, another cytoskeletal protein, do not appear to be affected by knockdown of Gβ1. The cytosolic protein glyceraldehyde 3-phosphate dehydrogenase (GAPDH) was used as a control to verify sample loading. A non-targeting pool of siRNAs was employed as a negative control, and it does not have any effect on protein expression, thus validating the knockdown experiment.

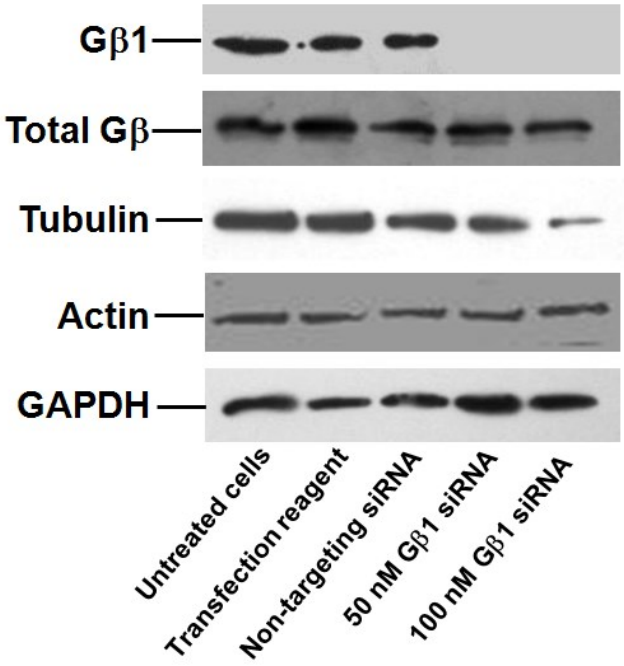

Figure 21. Knockdown of Gβ1 using siRNA in PC12 cells. PC12 cells were transfected with two concentration of a pool of siRNAs targeting the rat Gβ1. Negative controls were included (untreated cells, transfection reagent, and non-targeting siRNA) to validate the knockdown of Gβ1. Cells were subsequently lysed and subjected to imunoblotting against different antibodies as indicated.

3.3. Specific Aim 3: Determine the signaling pathways involved in Gβγ-dependent regulation of MT assembly and neurite outgrowth

3.3.1. Objective and Overview

The goal of this aim was to identify the signaling pathway by which Gβγ regulates the MT cytoskeleton and neurite outgrowth. Both receptor tyrosine kinase TrkA and G protein-coupled receptor (GPCR) pathways appear to play key roles in this process. However, the mechanism by which these two pathways coordinate to regulate assembly/organization of MTs during neurite outgrowth is not well understood. PI3K signaling emerged as an important pathway downstream to TrkA that regulates cytoskeletal rearrangement in neurons (Cantley, 2002; Zhou et al., 2004). Since PI3K is also a downstream effector of Gβγ in GPCR signaling, and recent results suggest that the activation of PI3K/Akt pathway by NGF is in part mediated through the βγ subunit (Wu and Wong, 2005; Wang and Wong, 2009), we hypothesized that Gβγ, in association with PI3K, coordinates the signals from TrkA and GPCR to regulate MT cytoskeleton and neurite outgrowth.

Therefore, in Specific Aim 3, we investigated the dynamic interactions between Gβγ and PI3K signaling, and their roles in regulating MT assembly and neurite outgrowth. Both PC12 cells and neuronal primary cultures from rat brains were used for these studies.

3.3.2. Gallein, as well as PI3K inhibitors, promotes neurite outgrowth of NGF-differentiated PC12 cells, but does not alter levels of MT assembly

To understand the role of PI3K in modulating Gβγ-dependent regulation of MT assembly and neurite outgrowth, we used gallein, a small molecule known to bind to Gβγ and inhibit Gβγ-dependent activation of PI3K-γ (Lehmann et al., 2008). In addition to gallein, we also used two well-established PI3K inhibitors, wortmannin and LY294002. Both confocal microscopic analysis and subcellular fractionation were carried out to determine if PI3K is involved in Gβγ-dependent regulation of MT assembly and neurite outgrowth. For confocal microscopic analysis, PC12 cells were seeded in immunocytochemistry chamber slides and allowed to differentiate in the presence of NGF (three consecutive days), followed by treatment with 10 μM gallein (30 min.), 0.2 μM wortmannin (1 h), or 100 μM LY294002 (1 h). The concentrations and time of incubation with the inhibitors were chosen based on their use in the literature. Subsequently, cells were fixed and processed for confocal microscopy, using Gβ and tubulin specific antibodies, and FITC- and TMR-conjugated secondary antibodies. We used laser-scanning confocal microscopy to examine the cells. Control cells were found to display typical morphology with neurites extending from the cell body. Gβγ-tubulin co-localization can be observed along the neurites, except at the neuronal tips, where predominant Gβγ immunostaining is found (Figure 22A, a-c). Cells treated with inhibitors (Figure 22A, d-l) do not seem to display significant changes in morphology and the co-localization patterns between Gβγ and MTs were similar to those observed in control cells. However, neurites appeared to be longer in the presence of all three inhibitors.

Therefore, we used the 2009 Zen software to trace and measure the neurites in order to obtain a quantitative assessment of neurite length after treatment with inhibitors. We found that the average neurite length was increased from 47.7 ± 2.7 μm in control cells, to 61.9 ± 3.1 μm, 63.2 ± 4.7 μm, and 59.5 ± 4.6 μm in gallein-, wortmannin-, and LY294002-treated cells, respectively. The percent of cells bearing neurites was also determined (Fig. 22C), but no significant differences were observed between controls and cells treated with inhibitors. The result suggests that the inhibition of PI3K activity favors Gβγ-MT interactions and neurite outgrowth. Since gallein binds to Gβγ and blocks Gβγ-dependent activation of PI3K-γ, the data also suggests that Gβγ and PI3K may work in concert to regulate neuronal outgrowth and differentiation.

To assess the possible changes in MT assembly after inhibition of PI3K, PC12 cells were seeded in 100 mm plates and allowed to differentiate in the presence of NGF, followed by treatment with inhibitors as indicated in the figure (Figure 23). Subsequently, cells were fractionated into CSK and SOL fractions as indicated in the methods, and MT assembly was assessed by determining tubulin immunoreactivity in both fractions. We found that gallein or PI3K inhibitors did not alter the level of MT assembly in NGF-differentiated PC12 cells (Figure 23A). Although average neurite length increased modestly in the presence of gallein or PI3K inhibitors, this effect may not be sufficient to alter MT/ST equilibrium in cells. In addition, NGF has been shown to increase the levels of MT assembly by ~70% (Section 3.1.2, Figure 7C), therefore making it difficult to assess any differences in MT assembly that may have been caused by the inhibitors.

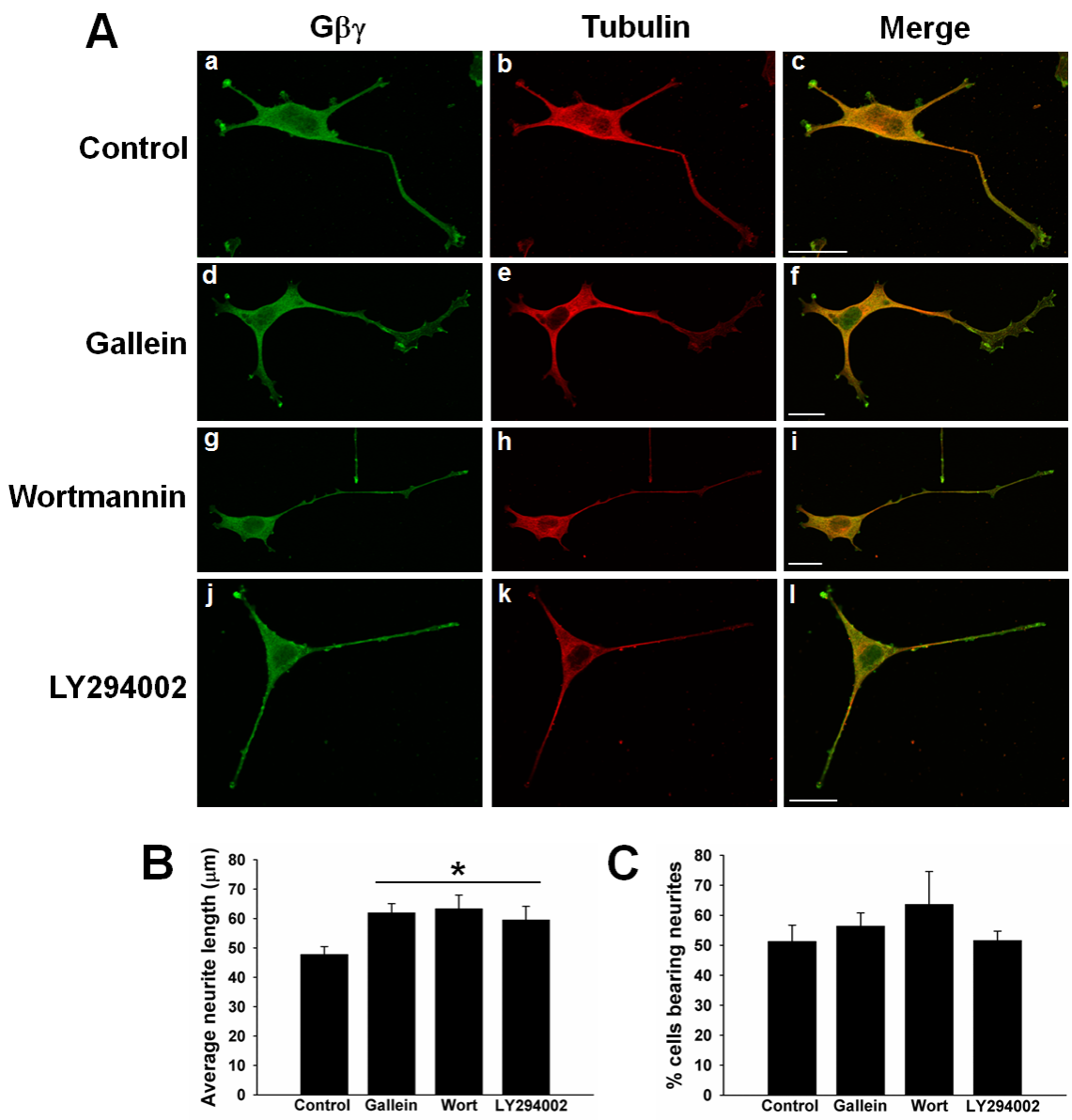

Figure 22. Gallein and PI3K inhibitors promote neurite outgrowth of NGF-differentiated PC12 cells. PC12 cells were induced to differentiate by treatment with NGF for three consecutive days. Cells were then treated with or without gallein (10 μM for 30 min.), wortmannin (0.2 μM for 1 h), and LY294002 (100 μM for 1 h). A) Cells were fixed and processed for confocal microscopy. Gβγ was detected with FITC (green), and tubulin/MTs was detected with TMR (red). Scale bars are 20 μm. B) Using the Zen software, neurites were traced and measured, and average neurite length was calculated. *p value < 0.05. C) Percent cells bearing neurites was also determined.

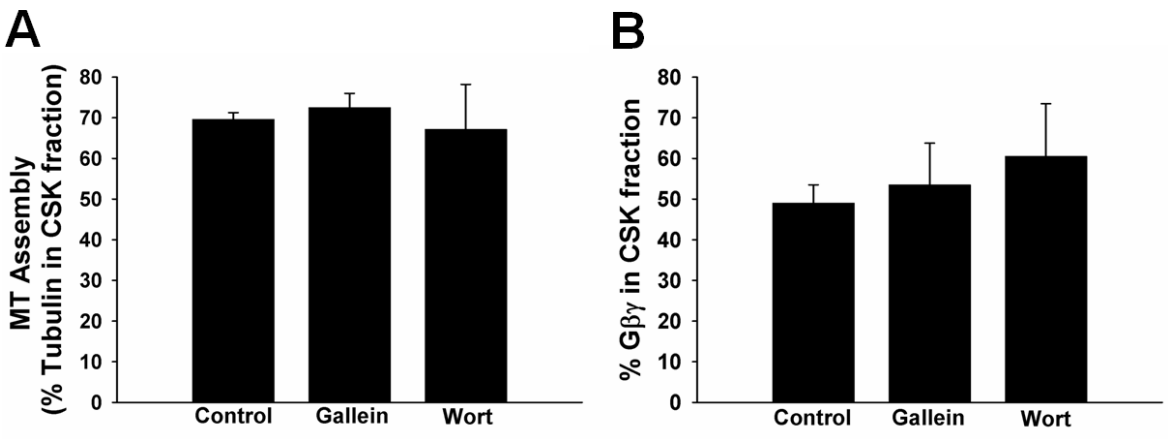

Figure 23. PI3K inhibitors do not affect MT assembly in NGF-differentiated PC12 cells. PC12 cells were induced to differentiate by incubation with NGF for three consecutive days. This was followed by treatment with or without gallein (10 μM for 30 min.), wortmannin (0.2 μM for 1 h), and LY294002 (100 μM for 1 h). CSK and SOL fractions were then prepared and subjected to the following: (A) CSK fractions were subjected to western blotting using an anti-tubulin antibody as indicated in the methods. MT assembly was determined by assessing tubulin immunoreactivity in both fractions, and it is expressed as percent tubulin in CSK fraction; and (B) immunoblotting using Gβ antibody to determine the percent Gβγ in CSK fraction.

3.3.3. Gallein and PI3K inhibitors stimulate MT assembly and promote the interactions of Gβγ with MTs in undifferentiated PC12 cells (without NGF)

Since we were unable to detect any differences in MT assembly in NGF-differentiated PC12 cells in the presence of gallein or PI3K inhibitors, we decided to use undifferentiated PC12 cells, given that the basal levels of MT assembly are lower in PC12 cells in the absence of NGF and therefore could allow us to observe changes in MT assembly in the presence of the inhibitors. In addition to MT assembly, the effect of inhibitors on MT-Gβγ interaction was also determined.

We found that MT assembly was significantly increased in PC12 cells after treatment with all three molecules under study (Figure 24A). Treatment with gallein increased MT assembly from 17.5 ± 2.5% to 32.1 ± 0.89%. However, more significant increases in MT assembly were seen in the presence of wortmannin and LY294002, as we found that they stimulated MT assembly to 63.08 ± 1.97% and 65.6 ± 2.36%, respectively. We also found that treatment with PI3K inhibitors significantly promoted the interaction of Gβγ with MTs (CSK fraction) by ~100%, as demonstrated by co-immunoprecipitation analysis (Figure 24B and C). As found before (Section 3.1.2, Figure 7A) tubulin did not form a complex with Gβγ in the SOL fraction, and the PI3K inhibitors did not alter this (figure not shown). The observation that two well-characterized PI3K inhibitors (wortmannin and LY294002) stimulated MT assembly and promoted the interaction of Gβγ with MTs (Figure 24A) supports the notion that inhibition of PI3K activity in cells stimulates MT assembly by promoting the interaction of Gβγ with

MTs. This is further supported by the fact that gallein (which binds to Gβγ and inhibits Gβγ-dependent activation of PI3Kγ) also stimulated MT assembly and increased the interaction of Gβγ with MTs. Thus, it appears that Gβγ and PI3K work in concert to regulate MT assembly in PC12 cells. Although gallein and PI3K inhibitors did not affect the levels of MT assembly in NGF-differentiated PC12 cells, average neurite lengths were significantly increased in the presence of all three inhibitors, and it is reasonable to suggest that Gβγ and PI3K worked together to regulate neurite outgrowth in PC12 cells.

We also tested whether gallein or PI3K inhibitors alter cell morphology and localization/co-localization of Gβγ and MTs using immunofluorescence microscopy (Figure 25A). As indicated in the figure, PC12 cell morphology was not altered in the presence of gallein, wortmannin, or LY294002. However, an increase in the size of the cells in the presence of all three inhibitors became apparent, and we used the 2009 Zen software to assess these differences by measuring cell area in several microscopic fields. The analysis showed that treatment of PC12 cells with PI3K inhibitors significantly affected cell size, as demonstrated by an increase in cell area (Figure 25B). The changes in cell size could be attributed to the increase in MT assembly as observed in the presence of these inhibitors. We found that inhibitors did not alter the patterns of localization/co-localization of Gβγ and MTs. In sum, our biochemical and microscopic results suggest that Gβγ may coordinate with PI3K to modulate MT assembly, which in turn may alter cell size.

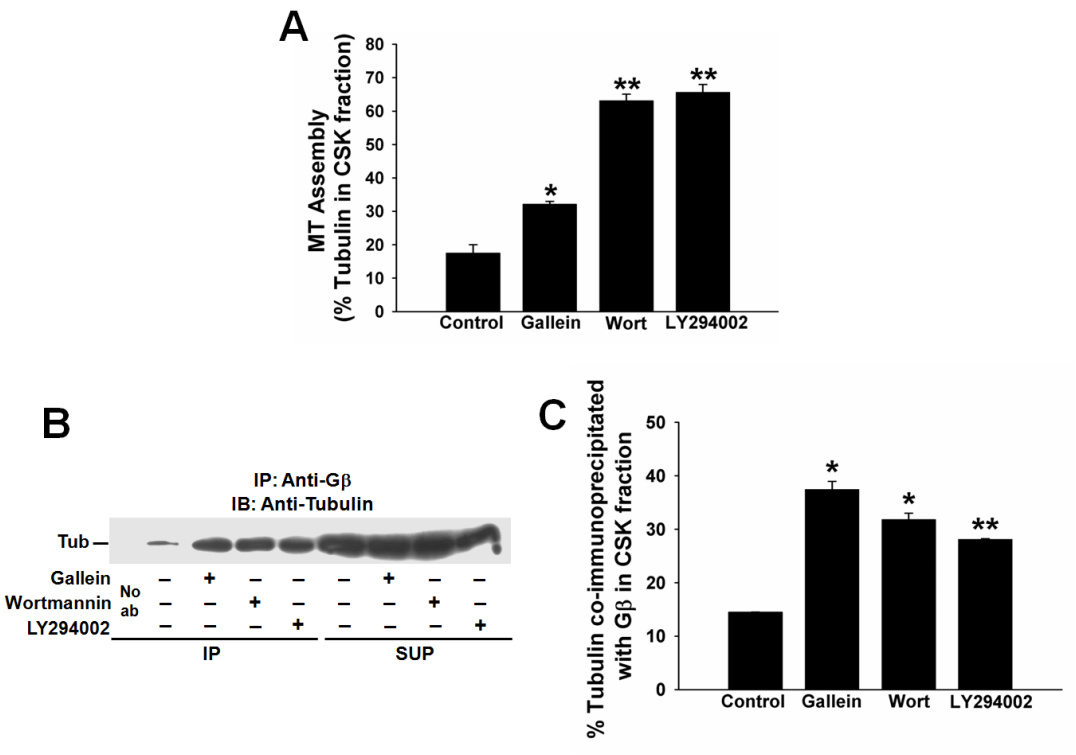

Figure 24. Inhibition of PI3K activity stimulates MT assembly and promotes the Gβγ-MT interaction in undifferentiated PC12 cells. PC12 cells were treated with or without gallein (10 μM for 30 min.), wortmannin (0.2 μM for 1 h), and LY294002 (100 μM for 1 h). CSK and SOL fractions were then prepared and subjected to the following: (A) Western blot using anti-tubulin antibody as indicated in the method. MT assembly was determined by assessing tubulin immunoreactivity in both fractions, and it is expressed as percent tubulin in CSK fraction; (B) CSK fractions were subjected to co-immunoprecipitation with Gβ antibody, followed by western blotting using anti-tubulin (tubulin immunoreactivity in both immunoprecipitated (IP) and supernatant (SUP) fractions are shown; and (C) the interaction of Gβγ with tubulin is expressed in the graphic as percent tubulin co-immunoprecipitated with Gβ. *p values < 0.05. **p values < 0.005.

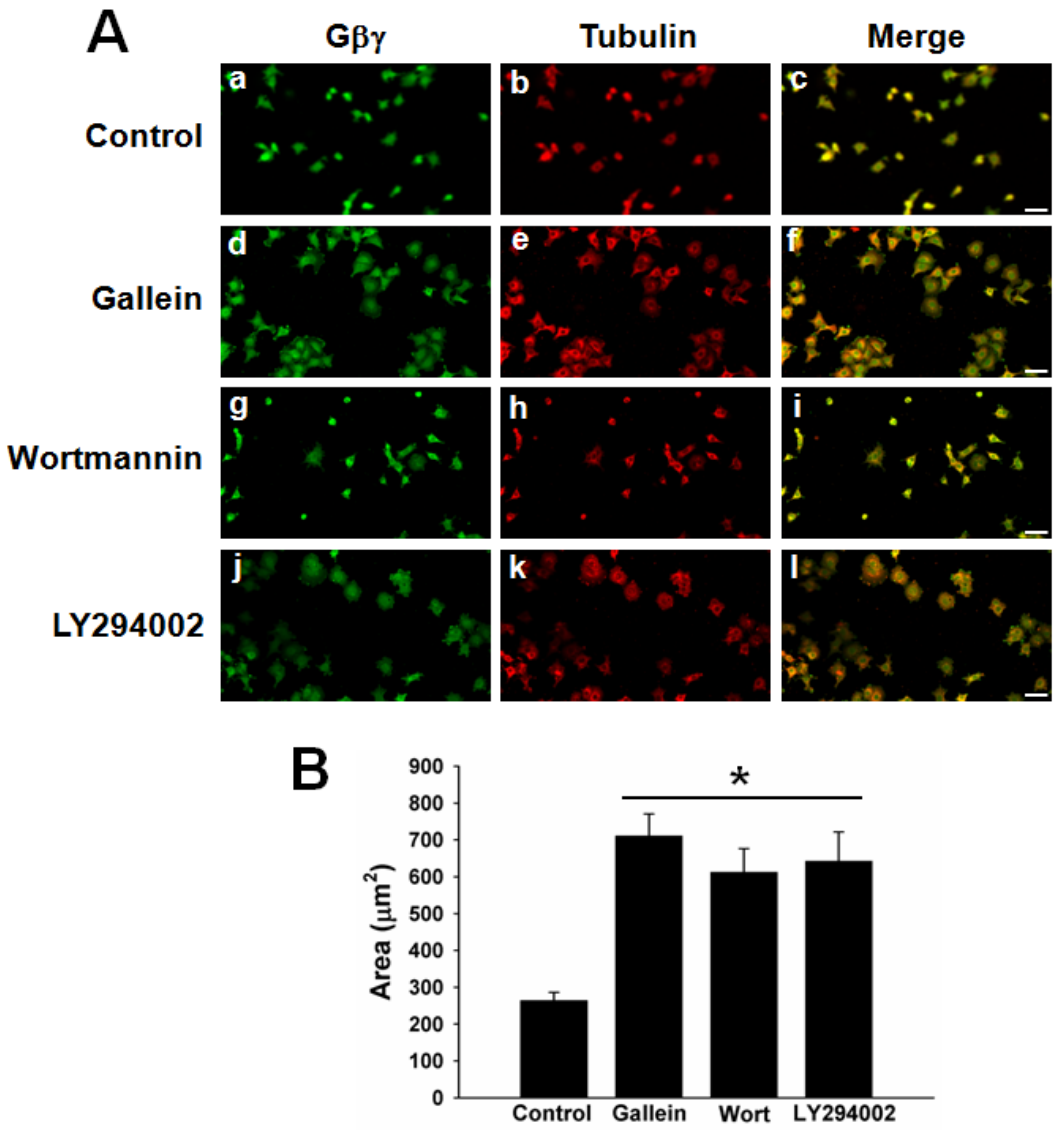

Figure 25. PI3K inhibitors cause changes in cell size of undifferentiated PC12 cells. PC12 cells were treated with or without gallein (10 μM for 30 min.), wortmannin (100 μM for 1 h), and LY294002 (0.2 μM for 1 h). A) Cells were fixed and processed for confocal microscopy. Gβγ was detected with FITC (green), and tubulin/MTs was detected with TMR (red). Scale bars are 100 μm. B) PC12 cells were images using confocal microscopy, and individual cells were delineated using the Zen software to obtain area values (μm^2). *p value < 0.001.

3.3.4. Inhibition of PI3K promotes the interaction of Gβγ with MTs and affects MT assembly in neuronal primary cultures

Since gallein, wortmannin, and LY294002 affected MT assembly and Gβγ-MT interactions in PC12 cells, and increased neurite outgrowth was observed in NGF-differentiated PC12 cells, we tested the effect of these molecules in neuronal primary cultures derived from rat brain cerebellum and hippocampus. Given the limited availability of brain tissue, only two inhibitors (gallein and wortmannin) were tested during biochemical experiments, but all three inhibitors were tested in confocal microscopy experiments.

As indicated in Figure 26A and B, gallein and wortmannin promoted the Gβγ-MTs interaction from 17.9 ± 0.9% (control cells) to 25.1 ± 2.3% and 29.8 ± 0.8%, respectively. No interaction between Gβγ and tubulin was observed in the SOL fraction, in either the presence or absence of inhibitors (figure not shown). Furthermore, the effect of the PI3K inhibitors was also tested on MT assembly. However, the results seem to differ from the findings obtained in undifferentiated PC12 cells, since gallein and wortmannin were found to decrease MT assembly modestly in primary cultures (Figure 26C). At this point, we are not able to explain this finding. It should be noted, however, that PC12 cells (undifferentiated) and primary neurons are different in nature, and future experiments will be needed to address this issue.

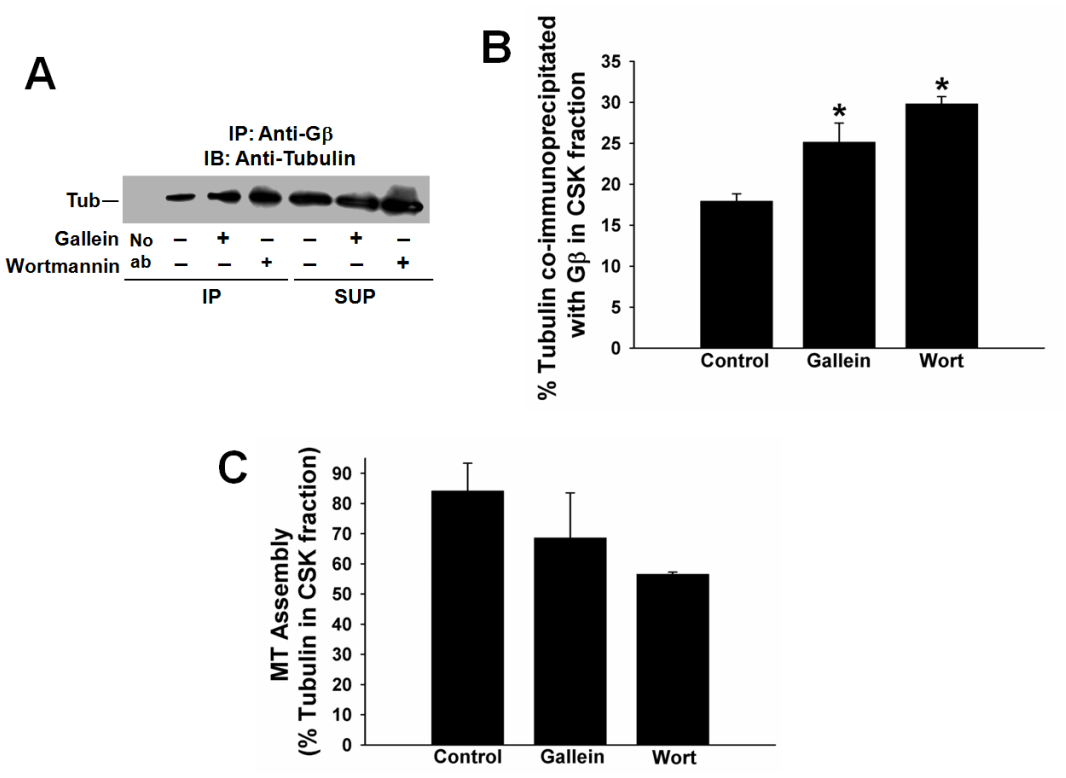

Figure 26. Inhibition of PI3K signaling alters MT assembly and promotes the interaction between Gβγ and MTs in cerebellar neurons. (A) Cerebellum primary cultures were treated with PI3K inhibitors as previously described, and CSK/SOL fractions were extracted. CSK fractions were subjected to co-immunoprecipitation using anti-Gβ followed by immunoblotting using an anti-tubulin antibody. (B) The Gβγ-tubulin interaction is expressed in the graphic as percent tubulin co-immunoprecipitated with Gβ in CSK fraction (bottom panel). (C) CSK and soluble fractions were immunoblotted using an anti-tubulin antibody. Percent tubulin in CSK fraction (MT assembly) and percent Gβγ in CSK fraction are expressed in the histograms. **p* values < 0.05. ***p* values < 0.005.

The effect of gallein, and PI3K inhibitors on neuronal primary cultures was also assessed using immunofluorescence labeling and confocal microscopy. Primary cultures were established on glass coverslips, and were allowed to differentiate fully. Cultures were then treated with or without inhibitors, followed by fixing and processing for confocal microscopy. Cells were labeled for Gβγ (green) and tubulin (red) and were examined by confocal microscopy.

In cerebellum primary cultures, control neurons displayed typical morphology, with cells forming two long neurites that extended from both sides of the cell body, a characteristic of cerebellar neurons in culture (Powell et al., 1997). Gβγ-MT co-localization along these processes can also be observed (Figure 27, a-c). After treatment with 10 μM gallein for 30 min, cells still showed neuronal processes (Figure 27, d-f), although some areas in the observed slides were found to have clusters of neurons. The PI3K inhibitors wortmannin and LY294002 did not alter neuronal morphology (Figure 27, g-l). However, the neuronal processes appeared to be much longer than those observed in the control cells.

Hippocampal primary cultures were also employed to study the effect of gallein and PI3K inhibitors on Gβγ-MT co-localization and neuronal morphology. Normal morphology was observed in control hippocampal neurons (Figure. 28, a-c), with cells displaying a very long process (usually the axon), and several shorter neurites (which have the characteristics of dendrites). This morphology is typical of hippocampal neurons in culture (Dotti et al., 1988). Treatment with gallein does not appear to affect

neuronal morphology, as cells still display the features described above (Figure 28, d-f). However, treatment with the PI3K inhibitors wortmannin and LY294002 seems to alter hippocampal neuron morphology dramatically (Figure 28, g-l). Cells treated with these compounds seemed to have longer neurites, and the presence of a neuronal process longer than the others (a typical feature of these neurons in culture) was not detected. In addition, tubulin labeling in the neurites appeared to be decreased (Figure 28, h, k), suggesting that cytoskeletal reorganization occurs in response to the inhibition of PI3K signaling.

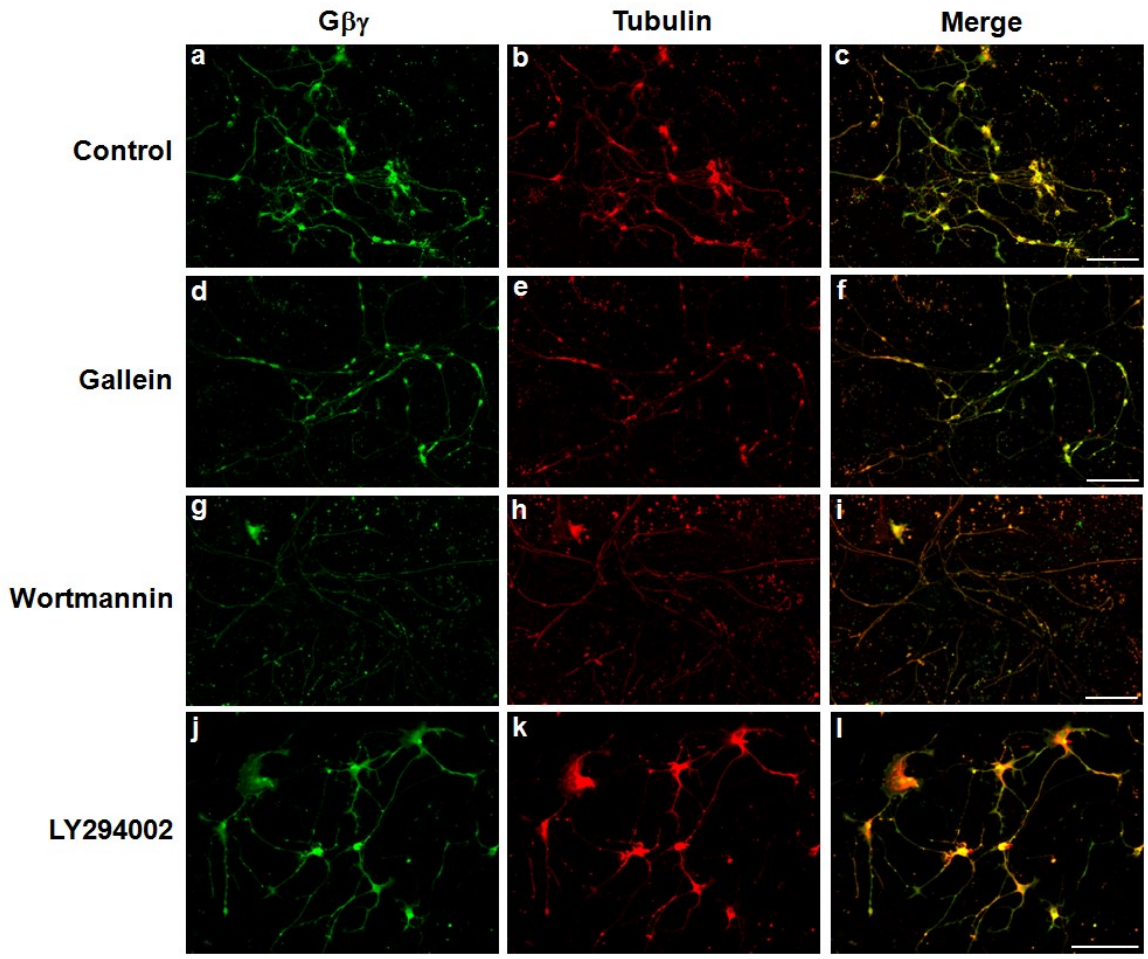

Figure 27. PI3K inhibitors alter neurite development in cerebellar cultures. Cerebellum primary cultures were established on pre-coated glass coverslips. The cultures were then treated with or without gallein (10 μM for 30 min.), wortmannin (0.2 μM for 1 h), and LY294002 (100 μM for 1 h), and cultures were fixed and processed for confocal microscopy. Gβγ is shown in green (FITC labeling), and tubulin is shown in red (TMR labeling). Colocalization patterns are shown in the merged images. Scale bars are 100 μm.

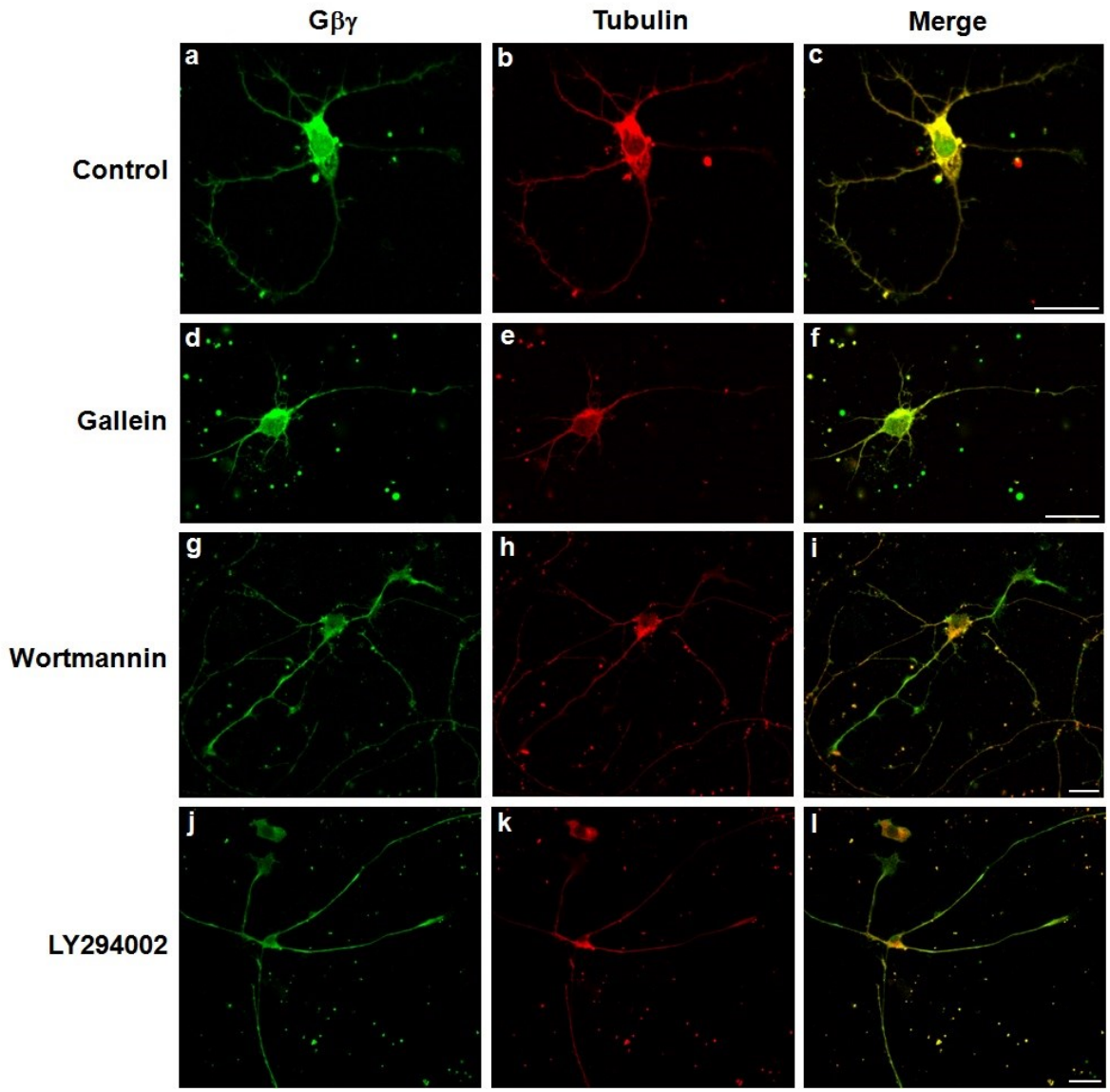

Figure 28. PI3K inhibitors affect neurite outgrowth in hippocampal primary neurons from rat brains. Hippocampal primary cultures were established on pre-coated glass coverslips. The cultures were then treated with or without gallein (10 μM for 30 min.), wortmannin (0.2 μM for 1 h), and LY294002 (100 μM for 1 h), and cultures were fixed and processed for confocal microscopy. Gβγ is shown in green (FITC labeling), and tubulin is shown in red (TMR labeling). Colocalization patterns are shown in the merged images. Scale bars are 20 μm.

3.3.5. PI3K inhibitor wortmannin inhibits the association of pAkt with the CSK fraction in primary neurons from rat brain cerebellum

Phosphorylation of Akt is known to occur due to upstream PI3K activity. PI3K/Akt signaling pathway plays a critical role in the regulation of MT stability in directed cell migration in NIH3T3 fibroblast cells, as well as during neurite outgrowth of PC12 cells (Cantley, 2002; Zhou et al., 2004). Therefore, we investigated whether inhibition of PI3K signaling affects the association of Akt/pAkt with MTs in cerebellar primary neurons. CSK and SOL fractions from cerebellar cultures treated with wortmannin, and gallein and subjected to immunoblotting using anti-Akt and anti-pAkt antibodies.

The results show that the association of total Akt with the CSK fraction appears to increase, albeit not significantly in the presence of gallein or wortmannin (Figure 29A). Gallein, which is known to specifically inhibit G$\beta\gamma$-mediated activation of PI3K-γ, did not affect the association of pAkt in the CSK fraction. However, treatment of cerebellar neurons with wortmannin, a general PI3K inhibitor, completely abolished the association of phosphorylated Akt with MTs (Figure 29B). The result suggests that while overall inhibition of the PI3K/Akt/pAkt signaling pathway appears to favor the G$\beta\gamma$-MT mediated pathway, as demonstrated by stimulation of MT-G$\beta\gamma$ interactions, MT assembly, and neurite outgrowth (Figures 22-28), gallein (which binds to G$\beta\gamma$) does not interfere with downstream signaling of PI3K (Akt/pAkt).

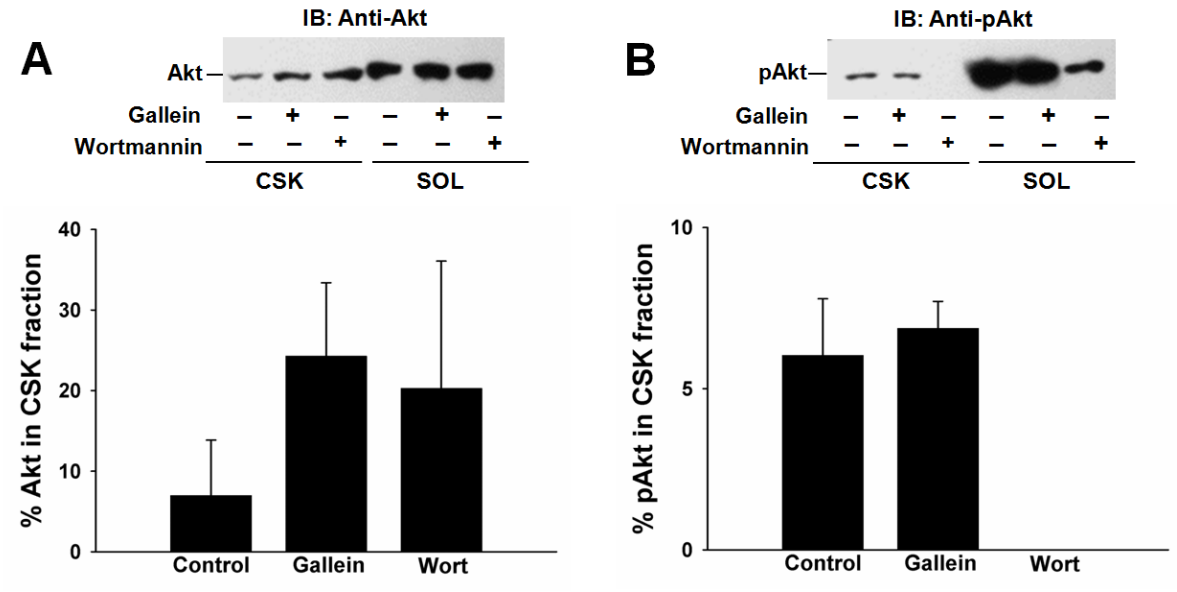

Figure 29. Inhibition of PI3K with wortmannin abolishes the association of pAkt with the CSK fraction in PC12 cells. Cerebellum primary cultures were treated with PI3K inhibitors as described previously, and CSK/SOL fractions were extracted. CSK fractions were subjected to immunoblotting using anti-Akt (A, top panel), and anti-pAkt (B, top panel) antibodies. The histograms (A, B, bottom panels) show percent Akt (A) or pAkt (B) in the CSK fraction.

CHAPTER 4: DISCUSSION

Neuronal outgrowth and plasticity is a complex phenomenon that requires the coordination of different cellular mechanisms. While many signals are known to drive the process, it is the assembly and disassembly of cytoskeletal structures that take the form of neurite extension and synapse formation that is essential to establish appropriate synaptic connections and for the brain's ability to store and process signals. Dynamic rearrangement of MTs and AFs is critical for growth cone motility and neurite outgrowth. Although several signaling pathways involving a large number of proteins and lipids in regulating neurite outgrowth have been identified, the linkage between these pathways and how they ultimately converge to regulate assembly and disassembly of MTs and AFs is not well understood (Tahirovic and Bradke, 2009; Wang and Wong, 2009). The results presented here demonstrate that the regulated interaction of $G\beta\gamma$ with MTs may be critical for neurite outgrowth and differentiation, and that NGF could facilitate the process by promoting this interaction. Thus, $G\beta\gamma$ may play a key role during neuronal differentiation by linking extracellular signals to the cytoskeletal filaments, exerting the changes that are required for neurite outgrowth.

Although $G\beta\gamma$ has been shown to bind to tubulin and to promote MT assembly *in vitro* and in cultured PC12 and NIH3T3 cells (Roychowdhury and Rasenick, 1997; Roychowdhury et al., 2006; Montoya et al., 2007; Roychowdhury and Rasenick, 2008), the functional implication of this interaction has not been demonstrated. Reports from several laboratories have indicated the involvement of $G\beta\gamma$ in neuronal development

and differentiation (Sanada and Tsai, 2005; Sachdev et al., 2007). Gβ1-deficient mice have been shown to have neural tube defects (Okae and Iwakura, 2010), and Gβ5-knockout mice have been shown to display abnormal behavior and develop multiple brain abnormalities (Zhang et al., 2011). Earlier, it was shown that impaired Gβγ signaling promoted neurogenesis in the developing neocortex and increased neuronal differentiation of progenitor cells (Sanada and Tsai, 2005). Although the mechanism by which Gβγ controls this process is not yet understood, the possibility that Gβγ may act on MTs has been suggested. Sachdev et al. (2007) have also suggested that Gβγ-Tctex-1 complex plays a key role in regulating neurite outgrowth in primary hippocampal neurons, most likely by modulating MTs and actin filaments. These studies suggested a connection between Gβγ signaling and the modulation of MTs during neurite outgrowth and development. The data presented here clearly suggest that the interaction of Gβγ with MTs, and Gβγ's ability to stimulate MT assembly, may provide a mechanism by which Gβγ regulates neuronal differentiation.

Overexpression of Gβγ in PC12 cells leads to neurite outgrowth in the absence of NGF, further supporting a key role for Gβγ during neuronal differentiation. Based on our high-resolution image analysis of the neuronal processes induced by overexpression of Gβγ (Fig. 12), it appears that MT filaments and Gβγ interact throughout the neuronal processes, as evidenced by clear yellow labeling. Gβγ labeling (green) was also observed side by side with yellow labeling throughout the neuronal process from all directions. This labeling pattern appears to support our *in vitro* results, which indicates that Gβγ binds laterally on the MT walls (Roychowdhury and Rasenick, 1997). The

decoration of MTs by Gβ appears to be strikingly similar to that observed by MAPs (Murphy and Borisy, 1975). In this context, βγ subunits might represent a new class of microtubule-regulatory molecules similar to MAPs. Like MAPs, Gβγ preferentially associated with microtubules in PC12 cells (Figure 7; Montoya et al., 2007) and MTs assembled *in vitro* in the presence of Gβγ (Roychowdhury and Rasenick, 1997). MAP2, a well-studied MAP, is involved in the initiation of neurite outgrowth and dendrite development. At later developmental stages, MAP2 disappears from axons but is retained in dendrites (Bernhardt and Matus, 1984; Cáceres et al., 1986). Tau regulates MT assembly and neurite outgrowth, and is found only in axons (Binder et al., 1985). It is possible that Gβγ, which is central to G protein-coupled signaling pathways, could mediate the interactions of MAP2/Tau with MTs/actin filaments during neurite outgrowth.

The interdependence between MTs and actin filaments in regulating neurite outgrowth has been previously demonstrated by using pharmacological inhibitors of actin polymerization and MT assembly. The inhibition of actin polymerization resulted in rapid MT advance and axon growth. Conversely, MT dynamics are required for directed growth-cone motility. MT-actin interactions also occur in the central domain of the growth cone, where actin filaments facilitate MT bundling, which is a requirement for axon formation (Bentley and Torojan-Raymond, 1986; Witte and Bradke, 2008; Geraldo and Gordon-Weeks, 2009). The distinctive co-localization pattern of Gβγ with actin filaments at the tip of the neurites and with MTs at the growth cones of PC12 cells (Figure 14) supports the idea that Gβγ functions to mediate the interactions between

MTs and actin filaments. Moreover, axon branching, which requires interactions between MTs and actin filaments (Griffith and Pollard, 1982), was observed in Gβγ-overexpressing PC12 cells (Figure 9), further suggesting the involvement of Gβγ in MT-actin filaments coupling. More recently using CHO cell lines, it has been shown that MTs play an important role in restraining cell movement and establishing directionality (Ganguly et al., 2012). Gβγ, which is found in the leading edge of PC12 cells could be involved in regulating this process by interacting with MTs.

Previously, by using a prenylation-deficient mutant of β1γ2, β1γ2 (C68S), we have shown that prenylation and further carboxy-terminal processing (methylation) of the γ subunit of Gβγ are important for interaction with MTs and stimulation of MT assembly *in vitro* (Roychowdhury et al., 1997). We decided to target the post-prenylation processing enzyme PMPMEase in this study for two reasons. First, although prenylation has been studied extensively because of the prevalence of prenylated proteins in cancer biology, and the prenyl transferase enzyme has been targeted for clinical trials, the results so far have not been promising; therefore, attention has recently been diverted to post-prenylation pathways. The enzyme involved in methylation of the prenylated protein, isoprenylcysteine carboxyl methyltransferase (ICMT), is now being studied for cancer metastasis, and results appear to be promising (Lamango, 2005; Winter-Vann and Casey, 2005; Gelb et al., 2006; Cushman and Casey, 2011). Recent studies have indicated that targeting ICMT might be useful in treating the rare genetic disease progeria (Ibrahim et al., 2013). Second, inhibitors for PMPMEase have recently been synthesized, and they have been shown to induce degeneration of human

neuroblastoma SHSY5Y cells (Aguilar et al., 2011). Although the γ subunit of Gβγ may not be the only target of PMPMEase (the Rho and Ras families of GTPases also undergo prenylation and subsequent methylation/demethylation), based on previous findings that the major protein that undergoes *in vivo* methylation in rat brains in response to injection of endogenous methyl donor S-adenosyl methionine is a molecule with a molecular weight comparable to that of the γ subunit of G proteins (Lamango and Charlton, 2000; Lamango et al., 2003). Therefore, it is likely that the γ subunit of the G protein was a major target of PMPMEase inhibition in our experiment. In addition, the tested PMPMEase inhibitors were proved to cause neuronal damage, alterations in the MT cytoskeleton, and changes in Gβγ organization in three different neuronal cell model systems: NGF-differentiated PC12 cells, SH-SY5Y neuroblastoma cells, and primary neurons from rat cerebellum. These findings support the notion that PMPMEase could be a key regulator of the Gβγ-MT interaction, and makes it an attractive candidate for future therapeutic targeting in neurodegenerative diseases.

Accumulating evidence suggests that PI3K-mediated signaling plays a critical role in the regulation of neuronal outgrowth and differentiation. PI3K is an enzyme that belongs to a family of lipid kinases that phosphorylate phosphoinositides. One of these products, phosphotidylinositol 3,4,5-triphosphate (PIP_3), serves as a second messenger to trigger a variety of cellular responses, including proliferation, differentiation, survival, and metabolism (Whitman et al., 1988; Shepherd et al., 1998; Kong and Yamori, 2008; Knight, 2010). Two downstream effectors of PI3K that have been shown to participate in the regulation of neurite outgrowth and are particularly associated with cytoskeletal

remodeling, are Akt and the glycogen synthase kinase 3β (GSK3β). The PI3K/Akt pathway has been shown to be responsible for mediating neurotrophin responses, which are critical for neuronal outgrowth (Wu and Wong, 2005a and 2005b; Wu and Wong, 2006). In addition, it has been demonstrated that Akt signaling is involved in axonal regeneration (Verma et al., 2005). In the case of GSK3β, this kinase is known to work in concert with PI3K in order to regulate the differentiation of hippocampal neurons (Jiang et al., 2005; Yoshimura et al., 2005). Our results clearly suggest that PI3K signaling and Gβγ coordinate to regulate MT assembly and neurite outgrowth as demonstrated in the proposed model (Figure 30). In this model, NGF-induced activation of TrkA and subsequent activation of PI3K/Akt/pAkt is shown in left panel. Promotion of MT-Gβγ interaction and subsequent alteration of MT assembly and neurite outgrowth (as demonstrated in the current research) is shown in the central panel. Inhibitors of PI3K (wortmannin and LY294002) block the PI3K/Akt/pAkt pathway (left panel, Figure 30) as shown by inhibition of the association of pAkt with cytoskeletal fraction (Figure 29). As indicated in the model (Figure 30), blocking this pathway upregulates Gβγ-MT mediated pathway (central panel) and neurite outgrowth. A similar effect on Gβγ-MT mediated pathway was observed in the presence of gallein, which is known to bind to Gβγ and activate PI3Kγ. However, gallein did not affect Akt/pAkt pathway (Figure 29) suggesting that unlike PI3K inhibitors, which affected Gβγ-MT dependent neurite outgrowth, gallein may not alter PI3K/Akt/pAkt pathway. Our results clearly indicate that PI3K and its downstream effectors are important regulators of Gβγ-MT mediated pathway, and cross-talk between these two pathways is important for neurite outgrowth.

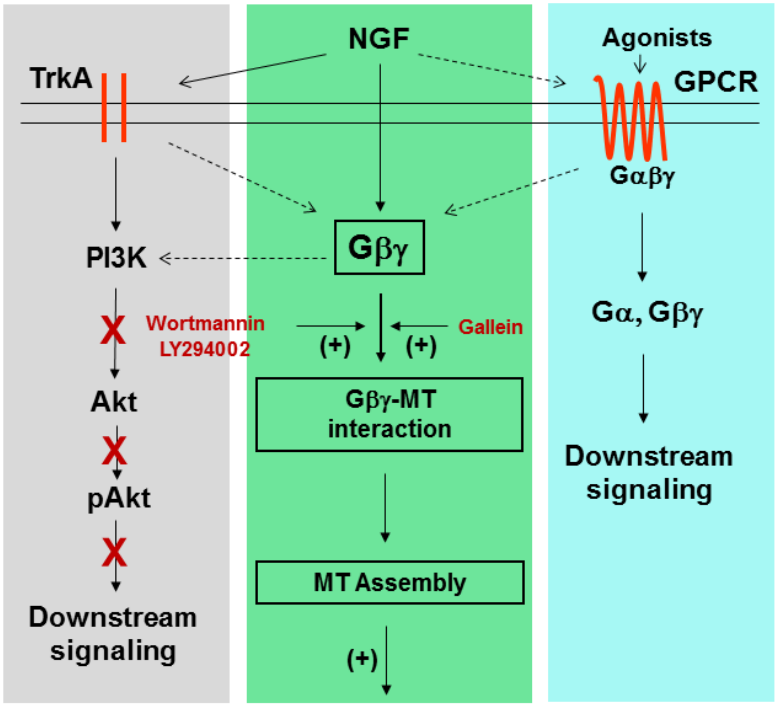

Figure 30. Gβγ-MT mediated pathway and PI3K signaling coordinate to regulate MT assembly and neurite outgrowth. The proposed model shows that NGF acts through TrkA receptors to activate PI3K and its downstream effectors (left panel). The results presented here demonstrate that NGF utilizes Gβγ, a key component of the GPCR pathway (right panel), to alter MT assembly by means of its interaction with MTs, ultimately leading to neurite outgrowth and differentiation (central panel). Inhibition of PI3K blocks downstream effector Akt/pAkt, which seems to positively influence the Gβγ-MT mediated mechanism of neurite outgrowth. Blocking of Gβγ-mediated activation of PI3Kγ by gallein does not affect the PI3K pathway, but it does favor the Gβγ-MT mediated pathway.

It has been shown earlier that in contrast to Gβγ, which promotes MT assembly, Gα inhibits MT assembly and stimulates MT dynamics by activating the intrinsic GTPase activity of tubulin (Roychowdhury et al., 1999). In addition, evidence from several laboratories indicates that Gα-dependent signaling pathways are involved in regulating neurite outgrowth (Strittmatter et al., 1994; Chen et al., 1999; He et al., 2005; Jordan et al., 2005; Bromberg et al., 2011). More recently, it has been shown that overexpression of activated, GTP-bound Gsα (Q204L Gsα), but not wild-type Gsα, in PC12 cells increases MT dynamics and induces neurite formation (Yu et al., 2009). It was suggested that activated Gsα promotes neurite outgrowth by increasing MT dynamics. However, neurite outgrowth involves a dramatic reorganization of MTs, and therefore requires precise control of disassembly and assembly of MTs. It is known that rapid polymerization of MTs is essential for neurite (axon and dendrite) formation, and Gβγ could play an important role in this process. We have shown earlier that G protein activation and subsequent dissociation of α (GTP-bound active form) and βγ subunits are necessary for modulation of MT assembly by G proteins (Roychowdhury et al., 2006). Since activated Gsα (GTP-bound) does not bind to Gβγ, it is possible that while activated Gsα can increase MT dynamics, it is the free Gβγ (not bound to Gsα) that stimulated MT assembly and participated in inducing neurite outgrowth, as observed by Yu et.al (2009). This is further supported by our observation that the overexpression of Gβγ induces neurite outgrowth in the absence of NGF. Clearly, further investigation will be required to understand the in-depth mechanisms by which Gβγ induces neurite outgrowth and the molecules that are involved in this process.

One of the unique features of Gβγ is its ability to interact with a large number of structurally and functionally diverse binding partners (Ford et al., 1998; Smrcka, 2008). Crystal structure and biochemical studies identified a region in Gβγ as a "hot spot," where multiple effectors interact in such a way that they partially overlap one another (Scott et al., 2001; Davis et al., 2005; Lehmann et al., 2008; Mathews et al., 2008), and NMR analysis reveals that Gβγ adopts a range of conformations that can be exploited during molecular recognition by diverse binding partners (Bonacci et al., 2006). Although direct interaction between Gβγ with tubulin has been demonstrated (Roychowdhury et al., 2006), Gβγ-tubulin interacting domain(s) have not been explored yet. Based on the literature, it is likely that tubulin binds to the "hot spot" region of Gβγ, since the majority of Gβγ effectors bind to this region. Moreover, the results presented here identify the MT cytoskeleton as a new class of effector of Gβγ signaling during neurite outgrowth.

The dramatic rearrangement of MTs during neuronal differentiation is critical for vesicular transport, neurotransmitter release, and communication at the synapse. Recent results suggest that Gβγ regulates the formation of SNARE complex, an essential step for neurotransmitter release of a synapse (Blackmer et al., 2005; Yoon et al., 2007). More recently, Gβγ has been shown to inhibit dopamine transporter activity (Garcia-Olivares et al., 2013). Although it is not clear whether these events are interlinked, it is tempting to speculate that signals originating from cell-surface receptors utilize Gβγ to induce specific changes in MT assembly and organization in axons, which may in turn contribute to the Gβγ-dependent transport and neurotransmitter release of a

synapse. Gβγ is known to activate a diverse array of effector molecules, including adenylate cyclases, phospholipases, PI3K, and ion channels. Future investigation will be important to understand how these effector systems influence Gβγ-dependent regulation of MTs and neuronal differentiation.

Recent results have indicated that MT assembly is severely compromised in the early stages of Alzheimer's and Parkinson's diseases (Cash et al., 2003; Buxton et al., 2010; Cartelli et al., 2010; Cartelli et al., 2013). Defects in MT-based transport are thought to be associated with many neurological disorders, including Alzheimer's disease, Huntington's disease, and ALS (De Vos et al., 2008; Millecamps and Julien, 2013; Franker and Hoogenraad, 2013), and disruption of the underlying microtubule network could be one way the transport is impaired (Franker and Hoogenraad, 2013). The data presented here support the notion that the altered interaction of Gβγ with MTs may cause disruption of MTs and may trigger an early stage of neurodegeneration. Therefore, our results identify Gβγ as a potential key molecule for future therapeutic development for the treatment of neurodegenerative diseases.

REFERENCES

Aguilar, B., Amissah, F., Duverna, R., Lamango, N.S. (2011). Polyisoprenylation potentiates the inhibition of polyisoprenylated methylated protein methyl esterase and the cell degenerative effects of sulfonyl fluorides. Curr. Cancer Drug Targets. 11, 752-762.

Al-Chalabi, A., Miller, C.C.J. (2003). Neurofilaments and neurological disease. Bioessays. 25, 346-365.

Alonso, A.C., Li, B., Grundke-Iqbal, I., Iqbal, K. (2008). Mechanism of tau-induced neurodegeneration in Alzheimer disease and related tauopathies. Curr. Alzheimer Res. 5, 375-384.

Amissah, F., Taylor, S., Duverna, R., Ayuk-Takem, L.T., Lamango, N.S. (2011). Regulation of polyisoprenylated methylated protein methyl esterase by polyunsaturated fatty acids and prostaglandins. Eur. J. Lipid Sci. Technol. 113, 1321-1331.

Amniai, L., Barbier, P., Sillen, A., Wieruszeski, J.M., Peyrot, V., Lippens, G., Landrieu, I. (2008). Alzheimer disease specific phosphoepitopes of Tau interfere with assembly of tubulin but not binding to microtubules. FASEB J. 23, 1146-11452.

Argarana, C.E., Barra, H.S., Caputto, R. (1978). Release of [14C]tyrosine from tubulinyl-[14C]tyrosine by brain extract. Separation of a carboxypeptidase from tubulin-tyrosine ligase. Mol Cell. Biochem. 19, 17-21.

Arnold, S.E., Lee, V.M., Gur, R.E., Trojanowski, J.Q. (1991). Abnormal expression of two microtubule-associated proteins (MAP2 and MAP5) in specific subfields of the hippocampal formation in schizophrenia. Proc. Natl. Acad. Sci. 88, 10850-10854.

Bailly, M., Condeelis, J. (2002). Cell motility: insights from the backstage. Nat. Cell Biol. 4, E292-E294.

Barra, H.S., Rodriguez, J.A., Arce, C.A., Caputto, R. (1973). A soluble preparation from rat brain that incorporates into its own proteins (14 C)arginine by a ribonuclease-sensitive system and (14C)tyrosine by a ribonuclease-insensitive system. J. Neurochem. 20, 97-108.

Belmont, L., Mitchison, T.J. (1996) Identification of a protein that interacts with tubulin dimers and increases the catastrophe rate of microtubules. Cell. 84, 623-631.

Bentley, D., Torojan-Raymond, A. (1986). Disoriented pathfinding by pioneer neuron growth cones deprived of filopodia by cytochalasin treatment. Nature. 323, 712-715.

Bernhardt, R., Matus, A. (1984). Light and electron microscopic studies of the distribution of microtubule-associated protein 2 in rat brain: a difference between dendritic and axonal cytoskeletons. J. Comp. Neurol. 226, 203-221.

Binder, L.I., Frankfurter, A., Rebhun, L.I. (1985). The distribution of tau in the mammalian central nervous system. J. Cell Biol. 101, 1371-1378.

Blackmer, T., Larsen, E.C., Bartleson, C., Kowalchyk, J.A., Yoon, E.J., Preininger, A.M., Alford, S., Hamm, H.E., Martin, T.F. (2005). G protein betagamma directly regulates SNARE protein fusion machinery for secretory granule exocytosis. Nat. Neurosci. 8, 421-425.

Bonacci, T.M., Mathews, J.L., Yuan, C., Lehmann, D.M., Malik, S., Wu, D., Font, J.L., Bidlack, J.M., Smrcka A.V. (2006). Differential targeting of Gbetagamma-subunit signaling with small molecules. Science. 312, 443-446.

Bradford, M.M. (1976). A rapid and sensitive method for the quantitation of microgram quantities of protein utilizing the principle of protein-dye binding. Anal. Biochem. 72, 248-54.

Bromberg, K.D., Iyengar, R., He, J.C. (2011). Regulation of neurite outgrowth by Gi/o signaling pathways. Front. Biosci. 13, 4544-4557.

Brunden, K.R., Trojanowski, J.Q., Lee, V.M. (2009). Advances in tau-focused drug discovery for Alzheimer's disease and related tauopathies. Nat. Rev. Drug Discov. 8, 783-793.

Bulinski, J.C., Gundersen, G.G. (1991). Stabilization of post-translational modification of microtubules during cellular morphogenesis. Bioessays. 13, 285-293.

Buxton, G.A., Siedlak, S.L., Perry, G., Smith, M.A. (2010). Mathematical modeling of microtubule dynamics: Insights into physiology and disease. Prog. Neurobiol. 92, 478–483.

Cáceres, A., Banker, G.A., Binder, L. (1986). Immunocytochemical localization of tubulin and microtubule-associated protein 2 during the development of hippocampal neurons in culture. J. Neurosci. 6, 714-722.

Cairns, N.J., Lee, V.M., Trojanowski, J.Q. (2004). The cytoskeleton in neurodegenerative diseases. J. Pathol. 204, 438-449.

Cantley, L.C. (2002). The phosphoinositide 3-kinase pathway. Science. 296, 1655-1657.

Cardoso, S.M., Esteves, A.R., Arduíno, D.M. (2012). Mitochondrial metabolic control of microtubule dynamics impairs the autophagic pathway in Parkinson's disease. Neurodegener. Dis. 10, 38-40.

Carlier, M.F., Didry, D., Simon, C., Pantaloni, D. (1989). Mechanism of GTP hydrolysis in tubulin polymerization: characterization of the kinetic intermediate microtubule-GDP-Pi using phosphate analogues. Biochemistry. 28, 1783-1791.

Cartelli, D., Ronchi, C., Maggioni, M.G., Rodighiero, S., Giavini, E., Cappelletti, G. (2010). Microtubule dysfunction precedes transport impairment and mitochondria damage in MPP+ -induced neurodegeneration. J. Neurochem. 115, 247-258.

Cartelli, D., Casagrande, F., Busceti, C.L., Bucci, D., Molinaro, G., Traficante, A., Passarella, D., Giavini, E., Pezzoli, G., Battaglia, G., Cappelletti, G. (2013). Microtubule alterations occur early in experimental parkinsonism and the microtubule stabilizer epothilone D is neuroprotective. Sci. Rep. 3:1837.

Cash, A.D., Aliev, G., Siedlak, S.L., Nunomura, A., Fujioka, H.. Zhu, X., Raina, A., Vinters, H.V., Tabaton, M., Johnson, A.B., Paula-Barbosa, M., Avila, J., Jones, P.K., Castellani, R.J., Smith, M.A., Perry, G. (2003). Microtubule reduction in Alzheimer's disease and aging is independent of tau filament formation. Am. J. Pathol. 162, 1623-1627.

Chen, L.T., Gilman, A.G., Kozasa, T. (1999). A candidate target for G protein action in brain. J. Biol. Chem. 274, 26931-26938.

Cingolani, L.A., Goda, Y. (2008). Actin in action: the interplay between the actin cytoskeleton and synaptic efficacy. Nat. Rev. Neurosci. 9, 344-356.

Claing, A., Laporte, S.A., Caron, M.G., Lefkowitz, R.J. (2002). Endocytosis of G protein-coupled receptors: roles of G protein coupled receptor kinases and beta-arrestin proteins. Prog. Neurobiol. 66, 61-79.

Conde, C., Cáceres, A. (2009). Microtubule assembly, organization and dynamics in axons and dendrites. Nat. Rev. Neurosci. 10, 319-332.

Cote, M., Payet. M.D., Gallo-Payet, N. (1997). Association of alpha S-subunit of the GS protein with microfilaments and microtubules: implication during adrenocorticotropin stimulation in rat adrenal glomerulosa cells. Endocrinology. 138, 69-78.

Crespo, P., Xu, N., Simonds, W.F., Gutkind, J.S. (1994). Ras-dependent activation of MAP kinase pathway mediated by G-protein beta gamma subunits. Nature. 369, 418-420.

Crouch, M.F., Simon, L. (1997). The G-protein G(i) regulates mitosis but not DNA synthesis in growth factor-activated fibroblasts: a role for the nuclear translocation of G(i). FASEB J. 11, 189-198.

Cushman, I., Casey, P.J. (2011). RHO methylation matters: a role for isoprenylcysteine carboxylmethyltransferase in cell migration and adhesion. Cell Adh. Migr. 5, 11-15.

David-Pfeuty, T., Erickson, H.P., Pantaloni, D. (1977). Guanosinetriphosphatase activity of tubulin associated with microtubule assembly. Proc. Natl. Acad. Sci. 74, 5372-5376.

Davis, T.L., Bonacci, T.M., Sprang, S.R., Smrcka, A.V. (2005). Structural and molecular characterization of a preferred protein interaction surface on G protein beta gamma subunits. Biochemistry. 44, 10593-10604.

Desai, A., Mitchison, T.J. (1997). Microtubule polymerization dynamics. Ann. Rev. Cell Dev. Biol. 13, 83-117.

De Vos, K.J., Grierson, A.J., Ackerley, S., Miller, C.C., (2008). Role of axonal transport in neurodegenerative diseases. Annu. Rev. Neurosci. 31, 151-173.

Dohlman, H.G, Thorner, J., Caron, M.J. Lefkowitz R.J. (1991). Model systems for the study of seven transmembrane-segment receptors. Ann. Rev. Biochem. 60, 653-688.

Dos Remedios, C.G., Chhabra, D., Kekik, M., Dedova, I.V., Tsubakihara, M., Berry, D.A., Nosworthy, M.J. (2003). Actin binding proteins: regulation of cytoskeletal microfilaments. Physiol. Rev. 83, 433-473.

Dotti, C.G., Sullivan, C.A., Banker, G.A. (1988). The establishment of polarity by hippocampal neurons in culture. J. Neurosci. 8, 1454-1468.

Downes, G.B., Gautam, N. (1999). The G protein subunit gene families. Genomics. 62, 554-552.

Drechsel, D.N., Hyman, A.A., Cobb, M.H., Kirschner, M.W. (1992). Modulation of the dynamic instability of tubulin assembly by the microtubule-associated protein tau. Mol. Biol. Cell. 3, 1141-1154.

Du, Q., Macara, I.G. (2004). Mammalian Pins is a conformational switch that links NuMA to heterotrimeric G proteins. Cells. 119, 503-516.

Ebneth, A., Drewes, G., Mandelkow, E.M., Mandelkow, E. (1999). Phosphorylation of MAP2c and MAP4 by MARK kinases leads to the destabilization of microtubules in cells. Cell Motil. Cytoskeleton. 44, 209-224.

Ersfeld, K., Wehland, J., Plessmann, U., Dodemont, H., Gerke, V., Weber, K. (1993). Characterization of the tubulin-tyrosine ligase. J. Cell Biol. 120, 725-732.

Etienne-Manneville, S., Hall, A. (2002). Rho GTPases in cell biology. Nature. 420, 619-635.

Faure, M., Voyno-Yasenetskaya, T.A., Bourne, H.R. (1994). cAMP and beta gamma subunits of heterotrimeric G proteins stimulate the mitogen-activated protein kinase pathway in COS-7 cells. J. Biol. Chem. 269, 7851-7854.

Ford, C.E., Skiba, N.P., Bae, H., Daaka, Y., Reuveny, E., Shekter, L.R., Rosal, R., Weng, G., Yang, C.S., Iyengar, R., Miller, R.J., Jan, L.Y., Lefkowitz, R.J., Hamm, H.E. (1998). Molecular basis for interactions of G protein betagamma subunits with effectors. Science. 280, 1271-1274.

Franker, M.A., Hoogenraad, C.C., (2013). Microtubule-based transport - basic mechanisms, traffic rules and role in neurological pathogenesis. J. Cell Sci. 126, 2319-2329.

Fredriksson, R., Lagerström, M.C., Lundin, L.G., Schiöth, H.B. (2003). The G-protein-coupled receptors in the human genome form five main families. Phylogenetic analysis, paralogon groups, and fingerprints. Mol. Pharmacol. 63, 1256-1272.

Fung, B.K., Yamane, H.K., Ota, I.M., Clarke, S. (2003). The gamma subunits of brain G-proteins is methyl esterified at a C-terminal cysteine. FEBS Lett. 260, 313-317.

Fuse, N., Hisata, K., Katzen, A.L., Matsuzaki, F. (2003). Heterotrimeric G proteins regulate daughter cell size asymmetry in Drosophila neuroblast divisions. Curr. Biol. 13, 947-954.

Fushman, D., Najmabadi-Haske, T., Cahill, S., Zheng, J., Levine, H. 3rd, Cowburn, D. (1998). The solution structure and dynamics of the pleckstrin homology domain of the G protein-coupled receptor kinase 2 (beta-adrenergic receptor kinase 1). A partner of Gbetagamma subunits. J. Biol. Chem. 273, 2845-2873.

Gamblin, T.C., Nachmanoff, K., Halpain, S., Williams, Jr R.C. (1996) Recombinant Microtubule Associated Protein 2C Reduces the Dynamic Instability of Individual Microtubules. Biochemistry. 35, 12575-12586.

Gan, X.Q., Wang, J.Y., Yang, Q.H., Li, Z., Liu, F., Pei, G., Li, L. (2000). Interaction between the conserved region in the C-terminal domain of GRK2 and rhodopsin is necessary for GRK2 to catalyze receptor phosphorylation. J. Biol. Chem. 275, 8469-8474.

Ganguly, A., Yang, H., Sharma, R., Patel, K.D., Cabral, F. (2012). The role of microtubules and their dynamics in cell migration. J. Biol. Chem. 287, 43359-43369.

Garcia-Olivares, J., Torres-Salazar, D., Owens, W.A., Baust, T., Siderovski, D.P., Amara, S.G., Zhu, J., Daws, L.C., Torres, G.E. (2013). Inhibition of dopamine transporter activity by G protein βγ subunits. PLoS One. 8(3):e59788.

Gelb, M.H., Brunsveld, L., Hrycyna, C.A., Michaelis, S., Tamanoi, F., Van Voorhis, W.C., Waldmann, H. (2006). Therapeutic intervention based on protein prenylation and associated modifications. Nat. Chem. Biol. 2, 518-528.

Gelfand, V.I.,Berchadsky, A.D. (1991). Microtubule dynamics: mechanism, regulation, and function. Annu. Rev. Cell Biol. 7, 93-116.

Geraldo, S., Gordon-Weeks, P.R. (2009). Cytoskeletal dynamics in growth-cone steering. J. Cell. Sci. 122, 3595-3604.

Ghobrial, I.M., Adjei, A.A. (2002). Inhibitors of the ras oncogene as therapeutic targets. Hematol. Oncol. Clin. North Am. 16, 1085-1088.

Gilman, A.G. (1987). G proteins: transducers of receptor-generated signals. Ann. Rev. Biochem. 56, 615-649.

Goedert, M., Spillantini, M.G., Serpell, L.C., Berriman, J., Smith, M.J., Jakes, R., Crowther, R.A. (2001). From genetics to pathology: tau and alpha-synuclein assemblies in neurodegenerative diseases. Philos. Trans. R. Soc. Lond. B. Biol. Sci. 356, 213-227.

Goldstein, L.S., Yang, Z. (2000). Microtubule-based transports systems in neurons: the role of kinesins and dyneins. Annu. Rev. Neurosci. 23, 39-71.

Gomez, L. L., Alam, S., Smith, K. E., Horne, E., Dell'Acqua, M. L. (2002). Regulation of A-kinase anchoring protein 79/150-cAMP-dependent protein kinase postsynaptic targeting by NMDA receptor activation of calcineurin and remodeling of dendritic actin. J. Neurosci. 22: 7027-7044.

Goslin, K., Asmussen, H., Banker, G. (1998). Culturing nerve cells. 2nd edition. Cambridge, MA, USA.

Gotta, M., Ahringer, J. (2001). Distinct roles for Galpha and Gbetagamma in regulating spindle position and orientation in Caenorhabditis elegans embryos. Nat. Cell Biol. 3, 297-301.

Govek, E.E., Newey, S.E., Van Aelst, L. (2005). The role of the Rho GTPases in neuronal development. Genes. Dev. 19, 1-49.

Gozes, I. (2011). Microtubules, schizophrenia and cognitive behavior: preclinical development of davunetide (NAP) as a peptide-drug candidate. Peptides. 32, 428-431.

Grazi, E., Trombetta, G. (1985). Effects of temperature on actin polymerized by Ca2+. Direct evidence of fragmentation. Biochem J. 232, 297-300.

Greene, L.A. and Tischler A.S. (1976). Establishment of a noradrenergic clonal line of rat adrenal pheochromocytoma cells which respond to nerve growth factor. Proc. Natl. Acad. Sci. 73, 2424-2428.

Griffith, L.M., Pollard, T.D. (1982). The interaction of actin filaments with microtubules and microtubule-associated proteins. J. Biol. Chem. 257, 9143-9151.

Gundersen, G.G., Gomes, E.R., Wen, Y. (2004). Cortical control of microtubule stability and polarization. Curr. Opin. Cell Biol. 16, 106-112.

Hall, A., Lalli, G. (2010). Rho and Ras GTPases in axon growth, guidance, and branching. Cold Spring Harb. Perspect. Biol. 2: a001818.

Hammond, J.W., Cai, D., Verhey, K.J. (2008). Tubulin modifications and their cellular functions. Curr. Opin. Cell Biol. 20, 71-76.

Harrill, J.A., Mundy, W.R. (2011). Quantitative assessment of neurite outgrowth in PC12 cells. Methods Mol. Biol. 758, 331-348.

He, J.C., Gomes, I., Nguyen, T., Jayaram, G., Ram, P.T., Devi, L.A., and Iyengar, R. (2005). The G alpha(o/i)-coupled cannabinoid receptor-mediated neurite outgrowth involves Rap regulation of Src and Stat3. J. Biol. Chem. 280, 33426-33434.

Ibrahim, M.X., Sayin, V.I., Akula, M.K., Liu, M., Fong, L.G., Young, S.G., Bergo, M.O. (2013). Targeting isoprenylcysteine methylation ameliorates disease in a mouse model of progeria. Science. 340, 1330-1333.

Igarashi, M., Strittmatter, S., Vartanian, T., Fishman, M.C. (1993). Mediation by G proteins of signals that cause collapse of growth cones. Science. 259, 77-84.

Inglese, J., Luttrell, L.M., Iñiguez-Lluhi, J.A., Touhara, K., Koch, W.J., Lefkowitz, R.J. (1994). Functionally active targeting domain of the beta-adrenergic receptor kinase: an inhibitor of G beta gamma-mediated stimulation of type II adenylyl cyclase. Proc. Natl. Acad. Sci. 91, 3637-3641.

Ittner, L.M., Götz, J. (2011). Amyloid-β and tau--a toxic pas de deux in Alzheimer's disease. Nat. Rev. Neurosci. 12, 65-72.

Janke, C., Kneussel, M. (2010). Tubulin post-translational modifications: encoding functions on the neuronal microtubule cytoskeleton. Trends Neurosci. 33, 362-372.

Jellinger, K.A. (2009). Recent advances in our understanding of neurodegeneration. J. Neural Transm. 116, 1111-1166.

Jellinger, K.A. (2010). Basic mechanisms of neurodegeneration: a critical update. J. Cell. Mol. Med. 14, 457-487.

Jiang, H., Guo, W., Liang, X., Rao, Y. (2005). Both the establishment and the maintenance of neuronal polarity require active mechanisms: critical roles of GSK-3beta and its upstream regulators. Cell. 120, 123-135.

Jiang, K., Akhmanova, A. (2011). Microtubule tip-interacting proteins: a view from both ends. Curr. Opin. Cell Biol. 23, 94-101.

Jordan, J.D., He, J.C., Eungdamrong, N.J., Gomes, I., Ali, W., Nguyen, T., Bivona, T.G., Philips, M.R., Devi, L.A., Iyengar, R. (2005). Cannabinoid receptor induced neurite outgrowth is mediated by Rap1 activation through Galphao/I-triggered proteasomal degradation of Rap1GAPII. J. Biol. Chem. 280, 11413-11421.

Kamal, F.A., Smrcka, A.V., Blaxall, B.C. (2011). Taking the heart failure battle inside the cell: small molecule targeting of Gbetagamma subunits. J. Mol. Cell. Cardiol. 51, 462-467.

Kamal, F.A., Travers, J.G., Blaxall, B.C. (2012). G protein-coupled receptor kinases in cardiovascular disease: why “where” matters. Trends Cardiovasc. Med. 22, 213-219.

Kimple, R.J., Willard, F.S. Siderovski, D.P. (2002). The GoLoco Motif: Heralding a new tango between G protein signaling and cell division. Mol. Interv. 2, 88-100.

Kline-Smith, S.L., Walczak, C.E. (2002) The microtubule-destabilizing kinesin XKCM1 regulates microtubule dynamic instability in cells. Mol. Bio. Cell. 13, 2718-31.

Knight, Z.A. (2010). Small molecule inhibitors of the PI3-kinase family. Curr. Top. Microbiol. Immunol. 347, 263-278.

Koch, W.J., Hawes, B.E., Inglese, J., Lutrell, L.M., Lefkowitz, R.J. (1994a). Cellular expression of the carboxyl terminus of a G protein-coupled receptor kinase attenuates G beta gamma-mediated signaling. J. Biol. Chem. 269, 9163-9167.

Koch, W.J., Hawes, B.E., Allen, L.F., Lefkowitz, R.J. (1994b). Direct evidence that Gi-coupled receptor stimulation of mitogen-activated protein kinase is mediated by G beta gamma activation of p21ras. Proc. Natl. Acad. Sci. 91, 12706-12710.

Koch, W.J., Inglese, J., Stone, W.C., Lefkowitz, R.J. (1993). The binding site for the beta gamma subunits of heterotrimeric G proteins on the beta-adrenergic receptor kinase. J. Biol. Chem. 268, 8256-8260.

Koehl, M., Abrous, D.N. (2011). A new chapter in the field of memory: adult hippocampal neurogenesis. Eur. J. Neurosci. 33, 1101-1114.

Kong, D., Yamori, T. (2008). Phosphatidylinositol 3-kinase inhibitors: promising drug candidates for cancer therapy. Cancer Sci. 99, 1734-1740.

Kowalski, R.J., Williams, R.C. Jr. (1993). Microtubule-associated protein 2 alters the dynamic properties of microtubule assembly and disassembly. J. Biol. Chem. 268, 9847-9855.

Kwon, J.H., Vogt Weisenhorn, D.M., Downen, M., Roback, L., Joshi, H., and Wainer B. H. (1998). Beta-adrenergic and fibroblast growth factor receptors induce neuronal process outgrowth through different mechanisms. Eur. J. Neurosci. 10, 2776-2789.

Laemmli, U.K. (1970). Cleavage of structural proteins during the assembly of the head of bacteriophage T4. Nature. 15, 680-685.

Lamango, N.S. (2005). Liver prenylated methylated protein methyl esterase is an organophosphate-sensitive enzyme. J. Biochem. Mol. Toxicol. 19, 347-357.

Lamango, N.S., Ayuk-Takem, L.T., Nesby, R., Zhao, W.Q., Charlton, C.G. (2003). Inhibition mechanism of S-adenosylmethionine-induced movements deficits by prenylcysteine analogs. Pharmacol. Biochem. Behav. 76, 433-442.

Lamango, N.S., Charlton, C.G. (2000). Farnesyl-L-cysteine analogs block SAM-induced Parkinson's disease-like symptoms in rats. Pharmacol. Biochem. Behav. 66, 841-849.

Latek, D., Modzelewska, A., Trzaskowski, B., Palczewski, K., Filipek, S. (2012). G protein-coupled receptors--recent advances. Acta Biochim. Pol. 59, 515-529.

Lee, S.H., Dominguez, R. (2010). Regulation of actin cytoskeleton dynamics in cells. Mol. Cells. 29, 311-325.

Lehmann, D.M., Seneviratne, A.M., Smrcka, A.V. (2008). Small molecule disruption of G protein beta gamma subunit signaling inhibits neutrophil chemotaxis and inflammation. Mol. Pharmacol. 73, 410-418.

Lema, C., Varela-Ramirez, A., and Aguilera R.J. (2011). Differential nuclear staining assay for high-throughput screening to identify cytotoxic compounds. Curr. Cell. Biochem. 1, 1-14.

Li, R., Gundersen, G.G. (2008). Beyond polymer polarity: how the cytoskeleton builds a polarized cell. Nat. Rev. Mol. Cell Biol. 9, 860-873.

Lodowski, D.T., Pitcher, J.A., Capel, W.D., Lefkowitz, R.J., Tesmer, J.J. (2003). Keeping G proteins at bay: a complex between G protein-coupled receptor kinase 2 and Gbetagamma. Science. 300, 1256-1262.

Lotto, B., Upton, L., Price, D.J., and Gaspar, P. (1999). Serotonin receptor activation enhances neurite outgrowth of thalamic neurones in rodents. Neurosci. Lett. 269, 87-90.

Manders, E.M.M., Verbeek, F. J., Aten, J.A. (1993). Measurement of co-localization of objects in dual-colour confocal images. J. Microsc. 169, 375-382.

Margolis, R.L., Rauch, C.T., Job, D. (1986) Purification and assay of a 145-kDa protein (STOP145) with microtubule-stabilizing and motility behavior. Proc. Natl. Acad. Sci. USA. 83, 639-643.

Marklund, U., Larsson, N., Gradin, H.M., Brattsand, G., Gullberg, M. (1996). Oncoprotein 18 is a phosphorylation-responsive regulator of microtubule dynamics. EMBO J. 15, 5290-5298.

Marrari, Y., Crouthamel, M., Irannejad, R., Wedegaertner, P.B. (2007). Assembly and trafficking of heterotrimeric G proteins. Biochemistry. 46, 7665-7677.

Mathews, J.L., Smrcka, A.V., Bidlack, J.M. (2008). A novel Gbetagamma-subunit inhibitor selectively modulates mu-opioid-dependent antinociception and attenuates acute morphine-induced antinociceptive tolerance and dependence. J. Neurosci. 28, 12183-12189.

McCudden, C.R., Hains, M.D., Kimple, R.J., Siderovski, D.P., and Willard, F.S. (2005). G-protein signaling: back to the future. Cell. Mol. Life Sci. 62, 551-577.

McGuire, W.P., Rowinsky, E.K., Rosenshein, N.B., Grumbine, F.C., Ettinger, D.S., Armstrong, D.K., Donehower, R.C. (1988). Taxol: a unique antineoplastic agent with significant activity in advanced ovarian epithelial neoplasms. Ann. Intern. Med. 111, 273-279.

McNally, F.J. (1996). Modulation of microtubule dynamics during the cell cycle. Curr. Opin. Cell Biol. 8, 23-29.

Millecamps, S., Julien, J.P. (2013). Axonal transport deficits and neurodegenerative diseases. Nat. Rev. Neurosci. 14, 161-176.

Mitchison, T., Kirschner, M. (1984). Dynamic instability of microtubule growth. Nature. 312, 237-242.

Montoya, V., Gutierrez, C., Najera, O., Leony, D., Varela, A., Popova, J., Rasenick, M., Das, S., and Roychowdhury, S. (2007). G Protein βγ Subunits Interact with αβ and γ Tubulin and Play a Role in Microtubule Assembly in PC12 Cells. Cell Motil. Cytoskeleton. 64, 936-950.

Murphy, D.B., Borisy. G.G. (1975) Association of high-molecular weight proteins with microtubules and their role in microtubule assembly. Proc. Natl. Acad. Sci. USA. 72, 2696-2700.

Nalivaeva, N.N., Turner, A.J. (2001). Post-translational modifications of proteins: acetylcholinesterase as a model system. Proteomics. 1, 735-747.

Neves, S.R., Ram, P.T., Iyengar, R. (2002). G protein pathways. Science. 296, 1636-1639.

Nogales, E., Wolf, S.G., and Downing, K.H. (1998). Structure of the alpha beta tubulin dimer by electron crystallography. Nature. 391, 199-203.

Okae, H., Iwakura, Y. (2010). Neural tube defects and impaired neural progenitor cell proliferation in Gbeta1-deficient mice. Dev. Dyn. 239, 1089-1101.

Pak, C.W., Flynn, K.C., Bamburg, J.R. (2008). Actin-binding proteins take the reins in growth cones. Nat. Rev. Neurosci. 9, 136-147.

Patapoutian, A., Reichardt, L.F. (2001). Trk receptors: mediators of neurotrophin action. Curr. Opin. Neurobiol. 11, 272-280.

Paturle, L., Wehland, J., Margolis, R.L., Job, D. (1989). Complete separation of tyrosinated, detyrosinated, and nontyrosinatable brain tubulin subpopulations using affinity chromatography. Biochemistry. 28, 2698-2704.

Paturle-Lafanechère, L., Manier, M., Trigault, N., Pirollet, F., Mazarguil, H., Job, D. (1994). Accumulation of delta 2-tubulin, a major tubulin variant that cannot be tyrosinated, in neuronal tissues and in stable microtubule assemblies. J. Cell. Sci. 107, 1529-1543.

Plassman, B.L., Langa, K.M., Fisher, G.G., Heeringa, S.G., Weir, D.R., Ofstedal, M.B., Burke, J.R., Hurd, M.D., Potter, G.G., Rodgers, W.L., Steffens, D.C., Willis, R.J.,

Wallace, R.B. (2007). Prevalence of dementia in the United States: the aging, demographics, and memory study. Neuroepidemiology. 29, 125-132.

Pereira-Leal, J.B., Hume, A.N., Seabra, M.C. (2001). Prenylation of Rab GTPases: molecular mechanisms and involvement in genetic disease. FEBS Lett. 498, 197-200.

Perrino, C., Naga Prasad, S.V., Patel, M., Wolf, M.J., Rockman, H.A. (2005). Targeted inhibition of beta-adrenergic receptor kinase-1-associated phosphoinositide-3 kinase activity preserves beta-adrenergic receptor signaling and prolongs survival in heart failure induced by calsequestrin overexpression. J. Am. Coll. Cardiol. 45, 1862-1870.

Powell, S.K., Rivas, R.J., Rodriguez-Boulan, E., Hatten, M.E. Development of polarity in cerebellar granule neurons. J. Neurobiol. 32, 223-236.

Purves, D., Augustine, G.J., Fitzpatrick, D., Hall, W.C., LaMantia, A.S., McNamara, J.O., White, L.E. (2008). Neuroscience. 4th edition. Sunderland, MA, USA.

Raybin, D., Flavin. M. (1977). Enzyme which specifically adds tyrosine to the alpha chain of tubulin. Biochemistry. 17, 2189-2194.

Reinoso, B.S., Undie, A.S., and Levitt, P. (1996). Dopamine receptors mediate differential morphological effects on cerebral cortical neurons in vitro. J. Neurosci. Res. 43, 439-453.

Roychowdhury, S., Martinez, L., Salgado, L., Das, S., and Rasenick, M.M. (2006). G protein activation is prerequisite for functional coupling between Gα/Gβγ and tubulin/microtubules. Biochem. Biophys. Res. Commun. 340, 441-448.

Roychowdhury, S., Panda, D., Wilson, L. and Rasenick, M.M. (1999). G protein alpha subunits activate tubulin GTPase and modulate microtubule polymerization dynamics. J. Biol. Chem. 274, 13485-13490.

Roychowdhury, S., Rasenick, M.M. (1997). G protein beta1gamma2 subunits promote microtubule assembly, J. Biol. Chem. 272, 31476-31581.

Roychowdhury, S., Rasenick, M.M. (2008). Submembranous microtubule cytoskeleton: regulation of microtubule assembly by heterotrimeric G proteins. FEBS J. 275, 4654-4663.

Sachdev, P., Menon, S., Kastner, D.B., Chuang, J.Z., Yeh, T.Y., Conde, C., Caceres, A., Sung, C.H., Sakmar, T.P. (2007). G protein beta gamma subunit interaction with the dynein light-chain component Tctex-1 regulates neurite outgrowth. EMBO J. 26, 2621-32.

Sakakibara, A., Ando, R., Sapir, T., Tanaka, T. Microtubule dynamics in neuronal morphogenesis. Open Biol. 3:130061.

Salon, J.A., Lodowski, D.T., Palczewski, K. (2011). The significance of G protein-coupled receptor crystallography for drug discovery. Pharmacol. Rev. 63, 901-937.

Sanada, K., Tsai, T.H. (2005). G protein betagamma subunits and AGS3 control spindle orientation and asymmetric cell fate of cerebral cortical progenitors. Cell. 122, 119-131.

Sarma, T., Voyno-Yasenetskaya, T., Hope, T.J., and Rasenick, M.M. (2003). Heterotrimeric G-proteins associate with microtubules during differentiation in PC12 pheochromocytoma cells. FASEB J. 17, 848-859.

Sekino, Y., Kojima, N., Shirao, T. (2007). Role of actin cytoskeleton in dendritic spine morphogenesis. Neurochem. Int. 51, 92-104.

Schaefer, M., Petronczki, M., Dorner, D., Forte, M., Knoblich, J. (2001). Heterotrimeric G proteins direct two modes of asymmetric cell division in the Drosophila nervous system. Cell. 107, 183-194.

Schröder, H.C., Wehland, J., Weber, K. (1985). Purification of brain tubulin-tyrosine ligase by biochemical and immunological methods. J. Cell Biol. 100, 276-281.

Schulze, E., Asai, D.J., Bulinski, J.C., Kirschner, M. (1987). Posttranslational modification and microtubule stability. J. Cell. Biol. 105, 2167-2177.

Scott, J.K., Huang, S.F., Gangadhar, B.P., Samoriski, G.M., Clapp, P., Gross, R.A., Taussig, R., Smrcka, A.V. (2001). Evidence that a protein-protein interaction 'hot spot' on heterotrimeric G protein betagamma subunits is used for recognition of a subclass of effectors. EMBO J. 20, 767-776.

Seabra, M.C., Ho, Y.K., Anant, J.S. (1995). Deficient geranylgeranylation of Ram/Rab27 in choroideremia. J. Biol. Chem. 270, 24420-24427.

Simon, M.I., Strathmann, M.P., Gautam, N. (1991). Diversity of G proteins in signal transduction. Science. 252, 802-808.

Shepherd, P.R., Withers, D.J., Siddle, K. (1998). Phosphoinositide 3-kinase: the key switch mechanism in insulin signalling. Biochem. J. 333, 471-490.

Shi, C.S., Lee, S.B., Sinnarajah, S., Dessauer, C.W., Rhee, S.G., Kehrl, J.H. (2001). Regulator of G-protein signaling 3 (RGS3) inhibits Gbeta1gamma 2-induced inositol phosphate production, mitogen-activated protein kinase activation, and Akt activation. J. Biol. Chem. 276, 24293-24300.

Singh, P., Rathinasamy, K., Mohan, R., and Panda, D. (2008). Microtubule assembly dynamics: an attractive target for anticancer drugs. IUBMB Life. 60, 368-375.

Skovronsky, D.M., Lee, V.M., Trojanowski, J.Q. (2006). Neurodegenerative diseases: new concepts of pathogenesis and their therapeutic implications. Annu. Rev. Pathol. Mech. Dis. 1, 151-170.

Smith, S. (1988) Neuronal cytomechanics: the actin based motility of growth cones. Science. 242, 708-715.

Smrcka, A.V. (2008). G protein beta gamma subunits: central mediators of G protein-coupled receptor signaling. Cell. Mol. Life Sci. 65, 2191-2214.

Smrcka, A.V., Lehmann, D.M., Dessal, A.L. (2008). G protein betagamma subunits as targets for small molecule therapeutic development. Comb. Chem. High Throughput Screen. 11, 382-395.

Stephens, L.R., Eguinoa, A., Erdjument-Bromage, H., Lui, M., Cooke, F., Coadwell, J., Smrcka, A. S., Thelen, M., Cadwallader, K., Tempst, P., Hawkins, P.T. (1997). The G beta gamma sensitivity of a PI3K is dependent upon a tightly associated adaptor, p101. Cell. 89, 105-114.

Sternweis, P.C. (1994). The active role of beta gamma in signal transduction. Curr. Opin. Cell Biol. 6, 198-203.

Stiess, M., Bradke, F. (2010). Neuronal polarization: the cytoskeleton leads the way. Dev. Neurobiol. 71, 430-444.

Stoyanov, B., Volinia, S., Hanck, T., Rubio, I., Loubtchenkov, M, Malek, D., Stoyanova, S., Vanhaesebroeck, B., Dhand, R., Nurnberg, B., et al. (1995). Cloning and characterization of a G protein-activated human phosphoinositide-3 kinase. Science. 269, 690-693.

Strittmatter, S.M., Fishman, M.C., Zhu, X.P. (1994). Activated mutants of the alpha subunit of G(o) promote an increased number of neurites per cell. J. Neurosci. 14, 2327-2338.

Tahirovic, S., Bradke, F. (2009). Neuronal polarity. Cold Spring Harb. Perspect. Biol. 1a001644.

Takenawa, T., Suetsugu, S. (2007). The WASP-WAVE protein network: connecting the membrane to the cytoskeleton. Nat. Rev. Mol. Cell. Biol. 8, 37-48.

Takida, S., Wedegaertner, P.B. (1991). Heterotrimer formation, together with isoprenylation, is required for plasma membrane targeting of Gbetagamma. J. Biol. Chem. 278, 17284-17290.

Towbin, H., Staehelin, T., and Gordon, J. (1970). Electrophoretic transfer of proteins from polyacrylamide gels to nitrocellulose sheets: procedure and some applications. Proc. Natl. Acad. Sci. 76, 4350-4354.

Ueda, N., Iñiguez-Lluhi, J.A., Lee, E., Smrcka, A.V., Robishaw, J.D., Gilman, A.G. (1994). G protein beta gamma subunits. Simplified purification and properties of novel isoforms. J. Biol. Chem. 269, 4388-4395.

van der Vaart, B., Akhmanova, A., Straube, A. (2009). Regulation of microtubule dynamic instability. Biochem. Soc. Trans. 37, 1007-1013.

Vasquez, R.J., Howell, B., Yvon, A.M., Wadsworth, P., Cassimeris, L. (1997). Nanomolar concentrations of nocodazole alter microtubule dynamic instability in vivo and in vitro. Mol. Biol. Cell. 8, 973-985.

Verma, P., Chierzi, S., Codd, A.M., Campbell, D.S., Meyer, R.L., Holt, C.E., Fawcett, J.W. (2005). Axonal protein synthesis and degradation are necessary for efficient growth cone regeneration. J. Neurosci. 25, 331-342.

Wang, D., Li, Y., Zhang, Y., Liu, Y., Shi, G. (2012). High throughput screening (HTS) in identification new ligands and drugable targets of G protein-coupled receptors (GPCRs). Comb. Chem. High Throughput Screen. 15, 232-241.

Wang, F., Sampogna, R.V., Ware, B.R. (1989). pH dependence of actin self-assembly. Biophys J. 55, 293-298.

Wang, K., Wong, Y.H. (2009). G protein signaling controls the differentiation of multiple cell lineages. Biofactors. 35, 232-238.

Wang, N., Yan, K. Rasenick, M.M. (1990). Tubulin binds specifically to the signal-transducing proteins, Gs alpha and Gi alpha 1. J. Biol. Chem. 265, 1239-1242.

Whitman, M., Downes, C.P., Keeler, M., Keller, T., Cantley, L. (1988). Type I phosphatidylinositol kinase makes a novel inositol phospholipid, phosphatidylinositol-3-phosphate. Nature. 332, 644-646.

Wickman, K.D., Iñiguez-Lluhl, J.A., Davenport, P.A., Taussig, R., Krapivinsky, G.B., Linder, M.E., Gilman, A.G., Clapham, D.E. (1994). Recombinant G-protein beta gamma-subunits activate the muscarinic-gated atrial potassium channel. Nature. 368, 255-257.

Willard, F.S., Crouch, M.F. (2000). Nuclear and cytoskeletal translocation and localization of heterotrimeric G-proteins. Immunol. Cell Biol. 78, 387-394.

Winter-Vann, A.M., Casey, P.J. (2005). Post-prenylation-processing enzymes as new targets in oncogenesis. Nat. Rev. Cancer. 5, 405-412.

Witte, H., Bradke, F. (2008). The role of the cytoskeleton during neuronal polarization. Curr. Opin. Neurobiol. 18, 479–487.

Wloga, D., Gaertig, J. (2010). Post-translational modifications of microtubules. J. Cell Sci. 123, 3447-3455.

Wolfgang, W.J., Clay, C., Parker, J., Delgado, R., Labarca, P., Kidokoro, Y., Forte, M. (2004) Signaling through Gs alpha is required for the growth and function of neuromuscular synapses in Drosophila. Dev. Biol. 268, 295-311.

Wong, G.T., Chang, R.C., Law, A.C. (2013). A breach in the scaffold: the possible role of cytoskeleton dysfunction in the pathogenesis of major depression. Ageing Res. Rev. 12, 67-75.

Wu, E.H., Wong, Y.H. (2005a). Involvement of G i/o proteins in nerve growth factor-stimulated phosphorylation and degradation of tuberin in PC-12 cells and cortical neurons. Mol. Pharmacol. 67, 1195-1205.

Wu, E.H., Wong, Y.H. (2005b). Pertussis toxin-sensitive Gi/o proteins are involved in nerve growth factor-induced pro-survival Akt signaling cascade in PC12 cells. Cell Signal. 17, 881-890.

Wu, E.H., Wong, Y.H. (2006). Activation of muscarinic M4 receptor augments NGF-induced pro-survival Akt signaling in PC12 cells. Cell Signal. 18, 285-293.

Wu, H.C., Huang, P.H. Lin, C.T. (2001). G protein beta2 subunit antisense oligonucleotides inhibit cell proliferation and disorganize microtubule and mitotic spindle organization. J. Cell. Biochem. 83, 136-146.

Xie, H.R., Hu, L.S., Li, G.Y. (2010). SH-SY5Y human neuroblastoma cell line: in vitro cell model of dopaminergic neurons in Parkinson's disease. Chin. Med. J. 123, 1086-1092.

Yoon, E.J., Gerachshenko, T., Spiegelberg, B.D., Alford, S., and Hamm, H.E. (2007). G betagamma interferes with Ca2-dependent binding of synaptotagmin to the soluble N-ethylmaleimide sensitive factor attachment protein receptor (SNARE) complex. Mol. Pharmacol 72, 1210-1219.

Yoshimura, T., Kawano, Y., Arimura, N., Kawabata, S., Kikuchi, A., Kaibuchi, K. (2005). GSK-3beta regulates phosphorylation of CRMP-2 and neuronal polarity. Cell. 120, 137-149.

Yu, J.Z., Dave, R.H., Allen, J.A., Sarma, T., Rasenick, M.M. (2009). Cytosolic G{alpha}s acts as an intracellular messenger to increase microtubule dynamics and promote neurite outgrowth. J. Biol. Chem. 284, 10462-10472.

Zhang, J.H., Pandey, M., Seigneur, E.M., Panicker, L.M., Koo, L., Schwartz, O.M., Chen, W., Chen, C.K., Simonds, W.F. (2011). Knockout of G protein β5 impairs brain development and causes multiple neurologic abnormalities in mice. J. Neurochem. 119, 544-554.

Zhou, F.Q., Zhou, J., Dedhar, S., Wu, Y.H., Snider, W.D. (2004). NGF-induced axon growth is mediated by localized inactivation of GSK-3beta and functions of the microtubule plus end binding protein APC. Neuron. 42, 897-912.

CURRICULUM VITA

Jorge. A. Sierra-Fonseca was born in Ciudad Juarez, Chihuahua, Mexico. The second son of Cosme Sierra and Celia Fonseca, he graduated from El Chamizal High School, Ciudad Juarez, in 2002, after which he entered the Autonomous University of Ciudad Juarez, earning a Bachelor of Science degree in Biology in 2007. While pursuing his bachelor's degree, he joined the Biochemistry and Molecular Biology Laboratory, where he conducted research in the areas of Biochemistry and Cell Biology for three years under the guidance of Dr. Fernando Plenge. He entered the doctoral program in Biological Sciences at the University of Texas at El Paso in 2008, joining the Cytoskeleton and Cell Signaling laboratory. Here, he developed a research project under the supervision of Dr. Sukla Roychowdhury, studying the intracellular signals that regulate the cytoskeleton during neuronal differentiation and neurodegeneration. He presented the results of his research in prestigious scientific meetings, such as the annual meeting of the American Society for Cell Biology, and the RCMI symposium. He was also a recipient of the Pan American Round Table of El Paso Scholarship for three consecutive years. In addition, he trained several undergraduate and graduate students in the laboratory, and worked as an Assistant Instructor at the University, teaching undergraduate-level courses for 5 years.

Permanent address: 946 Cerrada Basalto

Ciudad Juarez, Chihuahua, Mexico 32540

This dissertation was typed by Jorge A. Sierra Fonseca